

On the self-consistency of off-shell Slavnov-Taylor identities in QCD

J.A. Gracey

Theoretical Physics Division, Department of Mathematical Sciences, University of Liverpool,
P.O. Box 147, Liverpool, L69 3BX, United Kingdom

H. Kißler & D. Kreimer

Department of Mathematics, Humboldt-Universität zu Berlin, Rudower Chaussee 25, D-12489
Berlin, Germany

August, 2019.

Abstract. Using Hopf-algebraic structures as well as diagrammatic techniques for determining the Slavnov-Taylor identities for QCD we construct the relations for the triple and quartic gluon vertices at one loop. By making the longitudinal projection on an external gluon of a Green's function we show that the gluon self-energy of that leg is consistently replaced by a ghost self-energy. The resulting identities are then studied by evaluating all the graphs for an off-shell non-exceptional momentum configuration. In the case of the 3-point function this is for the most general momentum case and for the 4-point function we consider the fully symmetric point.

1 Introduction

One of the cornerstones of quantum field theory is the accommodation of spin-1 gauge fields in the Lagrangian of a theory in such a way that the core properties of the gauge field are retained. For instance, a gauge field A_μ^a will describe a photon or gluon in the respective abelian or non-abelian cases where the Lagrangian will be built from gauge invariant operators of A_μ^a . However, such an object has too many degrees of freedom and to properly describe physical phenomena the gauge field needs to satisfy constraints known as gauge conditions. The inclusion of such a condition in the Lagrangian breaks gauge invariance which is one guiding principle behind physical predictions. In the classical theory such gauge fixings do not lead to insurmountable problems. For instance, performing computations in different gauges will give the same physical outcome. In the quantum theory this is not as straightforward since in covariant gauges, as an example, the choice of gauge can change due to quantum corrections. Therefore it is not clear if the remnant of the gauge symmetry, evident in the classical case, is also preserved quantum mechanically. The development of the Becchi-Rouet-Stora-Tyutin (BRST) transformation put this problem on a firm footing in that a symmetry of the gauge fixed and hence gauge variant Lagrangian was constructed. One benefit was that it provided the machinery to confirm that the physical state space of the gauge field was positive definite ensuring that the Lagrangian satisfies unitarity. As equally as important as this is that the formalism reproduced the non-abelian extension of the Ward-Takahashi identities which are termed the Slavnov-Taylor identities, [1, 2]. Briefly these are relations between different n -point functions of the *quantum* theory and such relations have to hold in the bare and renormalized cases. In the latter situation this means that constraints on the renormalization constants implied by the identities have to be satisfied in each choice of renormalization scheme, [1, 2, 3, 4]. It is widely known that in Quantum Chromodynamics (QCD) that the coupling renormalization constant derived from one of the 3- or 4-point vertices in the modified minimal subtraction ($\overline{\text{MS}}$) scheme is automatically consistent with that derived from the remaining ones, [3, 5]. In other schemes this may not be the case. So fixing the coupling constant renormalization from one vertex means that the structure of the other vertex functions is determined *using* the restrictions from the Slavnov-Taylor identities. This has been studied in depth in QCD in a variety of early articles such as [3, 6, 7, 8, 9, 10, 11]. More recently Slavnov-Taylor identities have been used to analyse the structure of n -point functions in order to probe the infrared dynamics of QCD. Various review articles, for instance, give a flavour of developments over the last decade, [12, 13, 14, 15]. More recently, progress in understanding the non-perturbative structure of the triple gluon vertex has been made through Dyson-Schwinger, functional renormalization group and lattice methods, [16, 17, 18, 19, 20]. For example, a comprehensive study of the non-perturbative longitudinal part of the triple gluon vertex was provided in [21]. Although 3-point QCD vertex studies have been the main focus, a similar level of non-perturbative analysis is becoming available for 4-point vertices primarily through the Dyson-Schwinger technique, [22, 23, 24, 25, 26, 27].

Diagrammatic techniques for the construction of QCD Slavnov-Taylor identities have been provided in [1, 3, 28, 29, 30]. More recently these ideas have been used in several articles, [31, 32]. For instance, in [31] the Hopf-algebraic structure of Slavnov-Taylor identities was examined with the ghost sector being shown to have a connection with the Corolla polynomial. In [28, 33] the diagrammatic approach was used to reorganize Feynman diagrams contributing to Dyson-Schwinger equations in Quantum Electrodynamics (QED). An important result was that the gauge parameter dependence of the electron propagator in a linear covariant gauge was reconstructed from a pure Feynman gauge analysis. The formalism was shown to be correct to *four* loops. While the diagrammatic approach of [1, 3, 28, 29, 30] is perhaps not a mainstream method since it does not use path integral methods or the technique of algebraic renormaliza-

tion, [34], importantly it does preserve the distinction between the transverse and longitudinal components of the gauge field within Green's functions and allows one to follow their individual routes through a graph. One useful aspect of diagrammatic techniques is that Slavnov-Taylor identity-like relations between one-particle irreducible (1PI) Green's functions can be derived without explicitly studying connected Green's functions. Such 1PI Green's functions have been checked calculationally in several articles, [10, 11]. In [10] the triple gluon vertex was studied in QCD in the linear covariant gauge and axial gauge at one loop. While the identity for the gluon 4-point was discussed in [3, 10] it was not checked but one loop calculations were carried out in [11]. In that latter article the quartic vertex was examined at the completely symmetric point which is a non-exceptional momentum configuration. Moreover the consequences of the Slavnov-Taylor identity for the renormalization constants were studied in the Weinberg scheme, [4]. More recently the analysis of [11] was extended in [35] where the full decomposition of the quartic vertex into all the Lorentz tensor and colour channels was given. Aside from a few minor typographical errors the expression found in [11] for the Lorentz tensors purely corresponding to the quartic gluon Feynman rule was effectively correct. However one observation of [11] was that the relations between renormalization constants were not satisfied as they ought to have been due to the Slavnov-Taylor implications. Choices of the gauge parameter were found to ameliorate the situation.

Therefore to study the Slavnov-Taylor identities afresh we return to basics and apply modern algebraic and diagrammatic methods to construct the identities of the various relevant 3- and 4-point functions. These will involve the triple gluon and ghost-gluon vertices and both the pure gluon and ghost-gluon 4-point functions. The latter was studied in [36] together with the other possible 4-point functions of QCD at one loop at the symmetric point. While the 3- and 4-point ghost-gluon vertex functions have been studied in earlier work we have to carry out a new evaluation here. This is because in the standard construction of the Slavnov-Taylor identity the vertex connecting to one of the external ghost fields is not the standard one derived using the Faddeev-Popov method, [1, 2, 3]. Instead for that specific vertex the momentum appearing in the Feynman rule is stripped off to produce a vertex rule with two Lorentz indices. Since the vertex function of this modified vertex is required for our computations we have to evaluate it for a completely off-shell momentum configuration. We will also provide a general derivation of the identities using Hopf-algebraic arguments based on [37] valid at all orders in perturbation theory. In addition to this we will carry out explicit one loop calculations for each Slavnov-Taylor identity for an off-shell setup. In the case of the 3-point identity this will be in the fully off-shell case while for the 4-point one we will focus on the same fully symmetric point as [11]. In both cases we will show that the identities are fully satisfied in all colour and Lorentz channels. While this appears to contradict the observation of [11], in our derivation using combinatorial Dyson-Schwinger equations, [37], and the diagrammatic approach following [1, 3, 28, 29, 30, 40], additional graphs arise which appear to be absent or implicit in earlier work for 1PI Green's functions. Their presence is crucial to reconciling the identities. At this juncture our primary concern is to demonstrate the consistency of the 1PI Slavnov-Taylor identities. What the implications of the results are for other work still has to be followed through.

The paper is organized as follows. We devote Section 2 to the description of the Hopf-algebraic and diagrammatic constructions of the 3- and 4-point identities which we will study using explicit computations. The identity relating the triple gluon vertex to ghost-gluon 3-point functions is studied in depth at one loop in the off-shell case in Section 3. A similar analysis but for the 4-point identity at the fully symmetric point is carried out in the next section with conclusions given in Section 5. Several appendices are provided. These give the details of the projection matrices and tensor basis, the core colour group theory needed for the 4-point function calculation with the final appendix giving explicit expressions for the purely gluonic 3-

and 4-point functions.

2 Construction of identities.

We devote this section to the derivation of the identities by exploiting algebraic structures which originate due to combinatorial insertions of Green's functions [37] and studying diagrammatic techniques following [1, 3, 28, 29, 30]. In particular we will offer two different derivations of the desired identities. The main goal is to clarify how gauge symmetry can be expressed on the level of renormalized 1PI Green's functions and the resulting implications in the corresponding algebra of structure functions.

2.1 Hopf-algebra derivation.

Our first starting point is to consider the Dyson-Schwinger equations for the 1PI Green's functions. The demand that QCD can be renormalized by the unique renormalization of a single coupling constant g delivers a set of identities for the renormalization factor Z_g of the coupling constant

$$Z_g = \frac{Z_{\Gamma ggg}}{(Z_{\Gamma gg})^{\frac{3}{2}}} = \frac{Z_{\Gamma g\bar{q}q}}{Z_{\Gamma \bar{q}q}\sqrt{Z_{\Gamma gg}}} = \frac{Z_{\Gamma g\bar{c}c}}{Z_{\Gamma \bar{c}c}\sqrt{Z_{\Gamma gg}}} = \frac{\sqrt{Z_{\Gamma gggg}}}{Z_{\Gamma gg}}. \quad (2.1)$$

We note that at the outset our notation is that when we label the renormalization constants or Green's function to distinguish which n -point function they relate to we use the letters g , c and q to indicate gluons, Faddeev-Popov ghosts and quarks respectively as well as the associated antiparticles in the latter two instances. So, for example, the label $gggg$ indicates the gluon 4-point function or quartic gluon vertex function. A derivation of these identities (2.1) can be achieved using the locality of counterterms in a renormalizable field theory which implies that the all orders counterterms can be obtained from a solution of a fixed point equation in Hochschild cohomology [37] and we refer readers to that article for background to the notation used for the derivation by this method.

As a consequence the relations (2.1) are obtained by applying the counterterm map S_R^Φ to combinatorial Green's functions. They themselves obey a similar formal identity

$$\frac{\Gamma ggg}{(\Gamma gg)^{\frac{3}{2}}} = \frac{\Gamma g\bar{q}q}{\Gamma \bar{q}q\sqrt{\Gamma gg}} = \frac{\Gamma g\bar{c}c}{\Gamma \bar{c}c\sqrt{\Gamma gg}} = \frac{\sqrt{\Gamma gggg}}{\Gamma gg}. \quad (2.2)$$

Let us define 1PI combinatorial Green's functions

$$\Gamma^r(g^2) := t_r \pm \sum_{\text{res}(\Gamma)=r} g^{2|\Gamma|} \frac{\Gamma}{|\text{Aut}(\Gamma)|} = t_r \pm \sum_{k=1}^{\infty} g^{2k} B_+^{k;r}(\Gamma^r Q^{2k}), \quad (2.3)$$

where $r \in \mathcal{R}$ specifies the 1PI amplitude under consideration. For us it suffices to consider

$$\mathcal{R} = \{\bar{c}c, gg, ggg, gggg, g\bar{c}c, \bar{c}cgg\}$$

the inverse ghost and gluon propagators, the 3- and 4-gluon vertex functions, and the coupling of one or two gluons with a ghost pair. We take $t_r = \Gamma_{(0)}^r$ to be the tree-level contribution for such an amplitude. It can vanish as it does in $t_{\bar{c}cgg} = 0$, as there is no quartic gluon-ghost interaction in the linear covariant gauge fixed Lagrangian. Indeed there is no need for such a term as it does not have to be renormalized as an overall convergent contribution. Furthermore, $\text{res}(\Gamma)$ is obtained by shrinking internal edges in 1PI graphs to zero length. The fact that the

$B_+^{k;r}$ act as Hochschild 1-cocycles ensures the desired renormalization by local counterterms. For the maps $B_+^{k;r}$ to be indeed closed in Hochschild cohomology the identities (2.2) are necessary and sufficient [37]. Note that the 1PI 2-point functions are inverse propagators, in particular

$$\Gamma^{gg}(g^2) = 1 - \tilde{\Gamma}^{gg}(g^2) \quad , \quad \Gamma^{\bar{c}c}(g^2) = 1 - \tilde{\Gamma}^{\bar{c}c}(g^2) \quad (2.4)$$

where $\tilde{\Gamma}$ indicates self-energies.

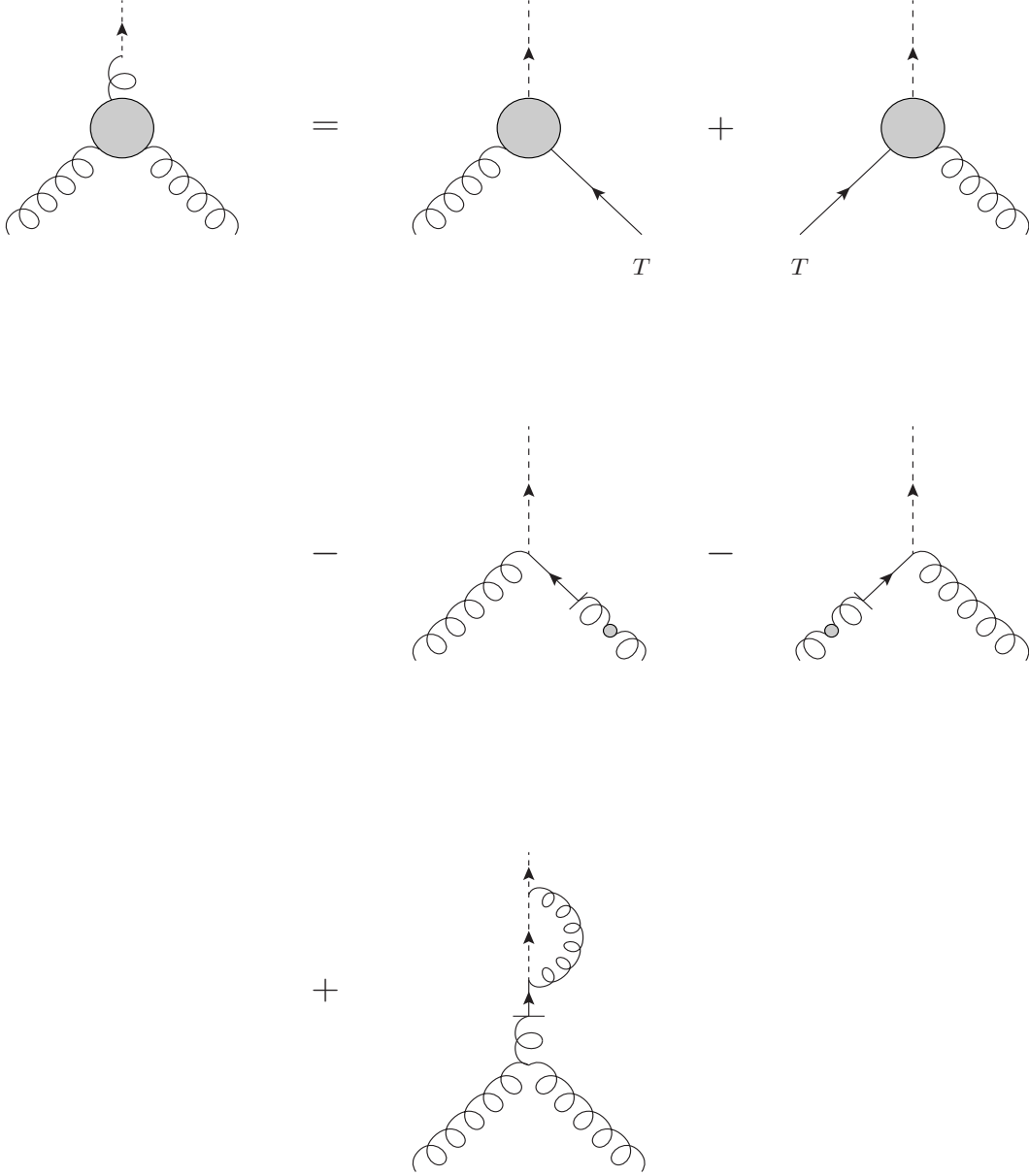


Figure 1: Slavnov-Taylor identity for 3-point function.

Two further remarks are in order. The product of combinatorial Green's functions always implies a product as connected diagrams with a sum over all orientations understood. This is required by Hochschild cohomology where products of combinatorial Green's functions appear in arguments of the 1-cocycles $B_+^{k;r}$, and closedness can only be achieved when the correct sum

over all orientations is taken into account [37, 38]. As an example,

$$\frac{\Gamma^{gggg}}{\Gamma^{ggg}} = \frac{\Gamma^{ggg}}{\Gamma^{gg}} \Leftrightarrow \Gamma^{gggg} = \Gamma^{ggg} \cdot \frac{1}{\Gamma^{gg}} \cdot \Gamma^{ggg}$$

where the propagator $\frac{1}{\Gamma^{gg}}$ is sandwiched between two 3-gluon vertex functions in the three s , t and u topologies, with respect to the Mandelstam variables, as indicated by the \cdot notation. Also understood is a form factor decomposition whenever appropriate. To allow for a projection onto chosen form factors, we extend the notion of a graph Γ to a pair (Γ, σ) where $\sigma \in \{\varsigma\}$, with $\{\varsigma\}$ a complete basis for the form factor decomposition of the evaluation of Γ under renormalized Feynman rules. The graph insertion is stable under projection onto a chosen form factor σ upon summing over the complete basis for the inserted graphs γ

$$\sum_{\tilde{\sigma}} (\bar{\Gamma}, \sigma) * (\gamma, \tilde{\sigma}) = \sum_{\Gamma} \frac{n(\bar{\Gamma}, \gamma, \Gamma)}{|\gamma|_{\wedge}} (\Gamma, \sigma) \quad (2.5)$$

in the notation of [37]. This ensures that projection onto a desired form factor commutes with replacing an edge or vertex by a full propagator or vertex Green's function.

The identities (2.2) above constitute several co-ideals in accordance with Hochschild cohomology

$$\frac{\Gamma^{ggg}}{\Gamma^{gg}} = \frac{\Gamma^{g\bar{c}c}}{\Gamma^{\bar{c}c}} = \frac{\Gamma^{g\bar{q}q}}{\Gamma^{\bar{q}q}} = \frac{\Gamma^{gggg}}{\Gamma^{ggg}}. \quad (2.6)$$

Of particular interest is the equation constituted by the first equality

$$\Gamma^{\bar{c}c} \cdot \Gamma^{ggg} = \Gamma^{g\bar{c}c} \cdot \Gamma^{gg} \quad (2.7)$$

which implies

$$\Gamma^{\bar{c}c} \cdot \Gamma^{gggg} = \underbrace{\Gamma^{\bar{c}cgg} + \Gamma^{g\bar{c}c} \cdot \Gamma^{ggg}}_{=\Gamma_c^{\bar{c}cgg}} \quad (2.8)$$

where $\Gamma_c^{\bar{c}cgg}$ is a connected combinatorial Green's function from

$$\Gamma^{\bar{c}c} \cdot \Gamma^{ggg} \cdot \frac{1}{\Gamma^{gg}} \cdot \Gamma^{ggg} = \Gamma^{g\bar{c}c} \cdot \frac{\Gamma^{gg}}{\Gamma^{gg}} \cdot \Gamma^{ggg} = \Gamma^{g\bar{c}c} \cdot \Gamma^{ggg} \quad (2.9)$$

using (2.7). The Green's function $\Gamma_c^{\bar{c}cgg}$ as a 1PI Green's function contributing to the same amplitude as the connected Green's function is (2.9). It hence must be included.

Upon using (2.4) and expanding in g^2 , (2.7) formally becomes

$$\Gamma_{(1)}^{ggg} = \tilde{\Gamma}_{(1)}^{\bar{c}c} \cdot \Gamma_{(0)}^{ggg} + \Gamma_{(1)}^{g\bar{c}c} \cdot \underbrace{P}_{\equiv \Gamma_{(0)}^{gg}} - \Gamma_{(0)}^{g\bar{c}c} \cdot \tilde{\Gamma}_{(1)}^{gg} \quad (2.10)$$

where

$$P_{\mu\nu}(p) = \eta_{\mu\nu} - \frac{p_{\mu}p_{\nu}}{p^2} \quad (2.11)$$

is the transverse projector and this is the first desired identity. It is illustrated in Figure 1 and given in more explicit detail in (3.10), where a projection onto a longitudinal component p_{σ} for a fixed chosen external leg is automatic on both sides above. We note that in Figure 1 a blob at a vertex represents all 1PI one loop contributions and a gluon leg with a blob indicates the one loop corrections to the 2-point function. Similarly, using (2.4) again and expanding in g^2 , (2.8) becomes

$$\Gamma_{(1)}^{gggg} = \tilde{\Gamma}_{(1)}^{\bar{c}c} \cdot \Gamma_{(0)}^{gggg} + \Gamma_{(1)}^{\bar{c}cgg} + \Gamma_{(1)}^{g\bar{c}c} \cdot P \cdot \Gamma_{(0)}^{ggg} + \Gamma_{(0)}^{g\bar{c}c} \cdot P \cdot \Gamma_{(1)}^{ggg} \quad (2.12)$$

which is the second desired identity. A sum over orientations is understood in both equations so that they are indeed in complete agreement with Figures 1 and 2. Again, a projection onto the longitudinal component p_σ on a chosen external leg is automatic. We have illustrated our notation for the various edges in Figure 3 together with their various Feynman rules. In each rule the through momentum is p and we have omitted the unit matrix in the colour indices.

The same result can be obtained by studying the contraction of a connected Green's function with n external gluons at a fixed external gluon leg i with its momentum p_i . The Slavnov–Taylor identity is

$$p_i \cdot G^n(p_1, \dots, p_n) = 0. \quad (2.13)$$

From [31] we know that all graphs contributing to such a connected amplitude can be obtained by applying the Corolla polynomial [39] to a corresponding sum of 3-regular scalar graphs. Underlying this is a bi-complex in graph and cycle homology studied in [31] which puts the approach of [28, 29, 30] on a firm mathematical footing. A careful rederivation of the Slavnov-Taylor identities using this approach is given in [40]. In particular see Lemma 5.9 there which allows one to follow the resulting propagation of the corresponding longitudinal momenta through the graphs. If we dress an external gluon leg of a 1PI vertex function in QCD by a gluon self-energy and contract with the gluon momentum, properties of the Corolla polynomial, discussed in Sections 6.1 and 6.9 of [31], ensure that this results in a 1PI vertex function where that external leg is longitudinal and dressed by a ghost self-energy. Indeed the Feynman graphs for the latter pair off with the sum of all paths through a gluon self-energy. This again leads to the desired identities.

2.2 Diagrammatic derivation.

Our first derivation of the Slavnov-Taylor identities clearly shows how the underlying algebra implies restrictions on the renormalization of Green's functions to all loop orders. In order to provide an illustration of the derived identities as well as a practical alternative to complement the general argument, and which in fact was the original way we discovered the relations (2.10) and (2.12), we now examine one loop diagrams and discuss the diagrammatic approach following [1, 3, 28, 29, 30].

For the concrete evaluation of the diagrams below, we are mainly concerned with two basic identities that either link the 3-gluon 1PI Green's function Γ^{ggg} or the 4-gluon 1PI Green's functions Γ^{gggg} to a linear combination of certain connected Green's functions. The procedure for achieving this for one loop diagrams begins with contracting one of the external gluon legs with its in-going momentum. We will refer to this here as the longitudinal contraction which corresponds to the final rule in Figure 3. The next stage is to examine the effect this contraction has on each individual graphs of the Green's function. As each contributing diagram is 1PI and has amputated external propagators, the longitudinal contraction of the external gluon leg is always incident to a vertex. At this stage we need to distinguish the effect the contraction has on each of the possible vertices of the linear covariant gauge fixed QCD Lagrangian we focus on in this article.

First, if the incident vertex is of quark-gluon type then the diagrammatic cancellations which are applied are very similar to the abelian case that was discussed in [33, 41]. However, due to the presence of the non-abelian group generator in the quark-gluon vertex we need to consider gauge invariant sets of graphs as discussed in [42]. This includes diagrams which are no longer 1PI. They will feature connected diagrams with a bridge corresponding to the contracted propagator of the final two terms of (2.12) or the third and fourth graphs on the right hand

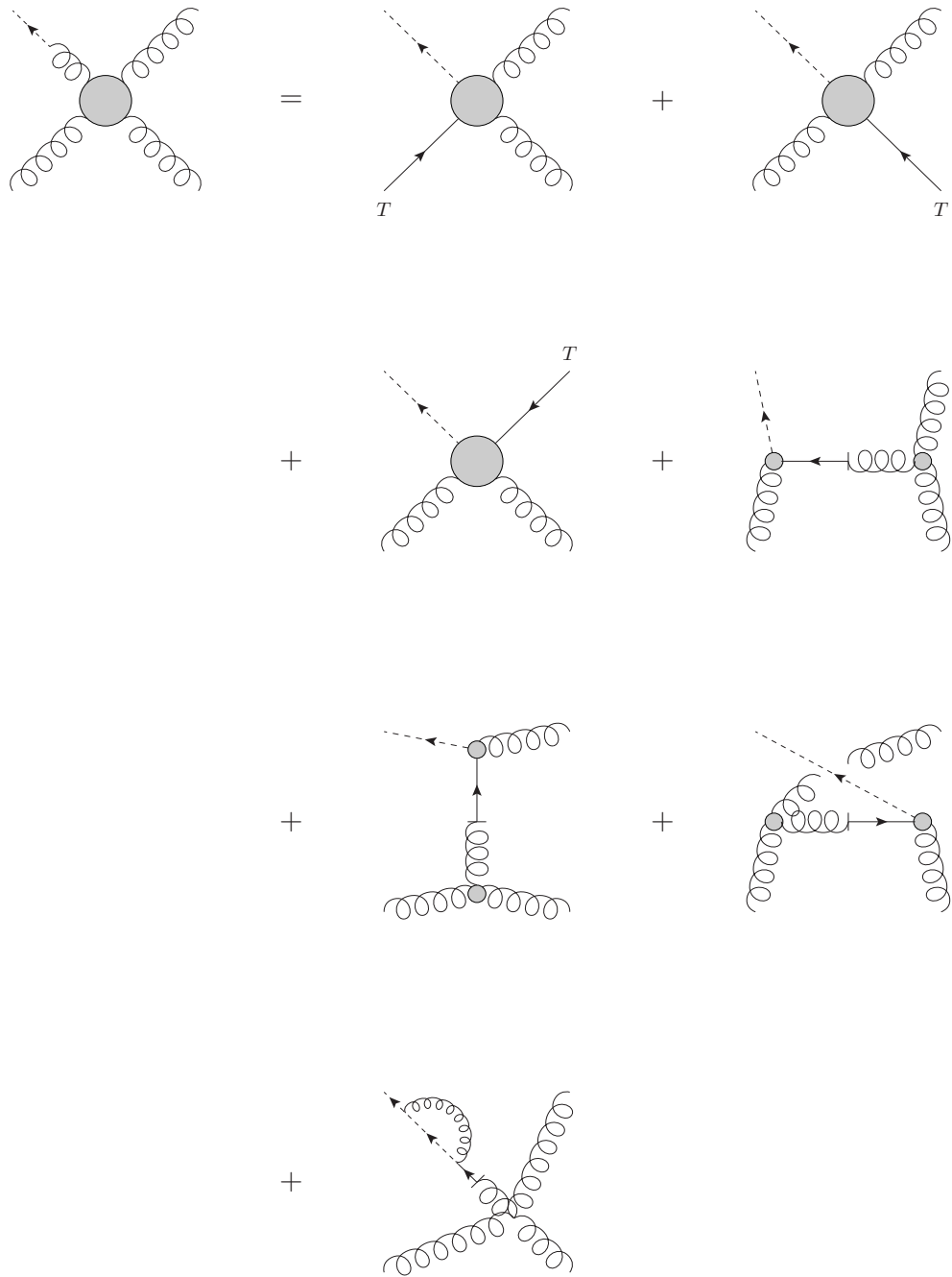


Figure 2: Slavnov-Taylor identity for 4-point function.

side of Figure 1 for instance. Next if the incident vertex is a triple gluon vertex then it is straightforward to see that using the rules given in [28, 29, 30, 40] the contracted vertex can be rewritten in terms of an auxiliary ghost vertex allowing us to recognize that the longitudinal gluon momentum propagates to the next adjacent vertex or contracts the propagator adjacent to both of these vertices. Repeating the application of the rules means that the longitudinal gluon momentum propagates through a diagram until it hits a vertex which is not a triple gluon vertex or eventually reaches an external leg. The former diagram can be shown to cancel 1PI diagrams with a contracted propagator that emerges from longitudinal contractions of a 4-gluon vertex which is discussed below. The latter diagrams constitute a new type of Green's function where the external leg that has been reached equals an in-going ghost leg of an incident vertex which has a purely transverse component as derived in [1]. The corresponding fixed longitudinal gluon leg is then identified with an out-going ghost leg. An illustration of this is given, for example, in the first and second Green's functions on the right hand side of Figure 1. In terms of (2.10) and (2.12) this is consistent with the transverse projection there.

Next for the case when the incident vertex involves a ghost vertex then it is possible to show that a certain linear combination of diagrams with internal ghost loops together with diagrams which have an external ghost line that originated from the longitudinal contraction of the fixed gluon vanishes. The essence of this cancellation of the ghost loops and longitudinal lines resides in the Jacobi identity for the structure constants. The final situation we have to consider is that where the incident vertex involves the quartic gluon vertex. Then the 4-valent vertex gets replaced by two 3-valent vertices that are connected by a contracted propagator edge, [29, 30, 31]. To be more precise, all (2|2) partitions of the four edges of the 4-gluon vertex to the two emerging vertices need to be considered. From graph homology these partitions are well known and termed IHX terms and more familiarly correspond to the s , t and u channels in the Mandelstam variable notation. For full details on the quartic gluon vertex identity, we refer the reader to [31] which also includes a detailed account of graph homology in QCD that underlies these identities. As discussed in the case of the gluon 3-point case, the contracted propagator edge that connected the new 3-valent vertices can be arranged to cancel contributions from other diagrams as long it is not a bridge. By contrast if it is a bridge then the contracted propagator edge contributes a new type of connected Green's function to the identity. Examples of this are evident in either the third, fourth or fifth graph on the right hand side of Figure 1 or the third, fourth or fifth graphs on the right hand side of Figure 2. This explains the extra diagram of the gluon 3-point function Γ^{ggg} in Figure 1. A separate case that we need to consider is the circumstance that occurs when an edge that is incident to a 4-gluon vertex is contracted. This can be resolved since there is a simple cancellation rule that follows from the Jacobi identity

$$\begin{array}{ccc}
 \begin{array}{c} \xrightarrow{\mu} \\ \nu \end{array} & \frac{T}{\nu} & [\eta^{\mu\nu} p^2 - p^\mu p^\nu] \\
 \\
 \begin{array}{c} \text{---} \\ \mu \end{array} & \begin{array}{c} \text{---} \\ \nu \end{array} & \eta^{\mu\nu} \\
 \\
 \begin{array}{c} \text{---} \\ \mu \end{array} & \text{---} & \frac{p^\mu}{p^2}
 \end{array}$$

Figure 3: Notation for graph representation of Slavnov-Taylor identities.

as demonstrated in [31, 40]. As a result the sum over all ways to contract one of the edges of the 4-gluon vertex vanishes. Therefore, all 1PI diagrams with a contracted edge incident to a 4-gluon vertex vanish on the right hand side of the Slavnov-Taylor identity in Figure 2. However, a single diagram remains since the contracted edge is a bridge. Therefore this explains the appearance of the last diagram of Figure 2 in full accord with a similar origin in the previous Hochschild construction.

3 Triple gluon vertex.

In deriving both Slavnov-Taylor identities by algebraic and diagrammatic methods we have arrived at the same relations. However in comparing our expressions with relations between similar Green's functions provided in, say, [10] we note that for both cases we have an additional graph which is not 1PI but involves self-energy corrections to the ghost on the same external leg corresponding to the longitudinal projection. In other words this Faddeev-Popov ghost is intimately tied to the longitudinal gluon. This is already well known in the 2-point context since the ghost is necessary to cancel unphysical degrees of freedom in the longitudinal sector and ensure the gluon 2-point function is transverse. Therefore we now turn to explicit computations to demonstrate how important this extra graph is to ensuring our relations are consistent. We will carry this out for the cases where the momentum of none of the external legs is set to zero and focus on general non-exceptional momentum configurations. In the case of the 3-point relation we will do so for the completely off-shell configuration. This will build on earlier work of [7, 8, 43, 44, 45, 46] where in the latter the two loop off-shell QCD 3-point vertex functions were computed. However it is not possible to immediately lift even the one loop vertex functions from [46] to effect an immediate check on our 3-point identity. This is because like [1, 2, 10] the ghost-gluon vertex function of the identity is a modification of the corresponding vertex function of the Lagrangian. We note that the Feynman rule for the canonical ghost-gluon vertex for the linear covariant gauge we use involves the momentum of one of the ghost fields. The associated connected vertex function would then be denoted by $\Gamma_{\mu}^{g\bar{c}c}(p, q, r)$ where the Lorentz index matches that of the gluon field and p, q and r are the external momenta. However as we have noted in the derivation of the identities an adjusted ghost-gluon vertex plays the major role. It is related to the canonical ghost-gluon vertex Feynman rule but with the external ghost momentum dropped. In general this vertex function is denoted by $\Gamma_{\mu\nu}^{g\bar{c}c}(p, q, r)$ and is graphically defined in Figure 4. The second Lorentz index is the place where the external ghost momentum would be attached to produce the canonical vertex present in the Lagrangian. Therefore the Feynman rule for $\Gamma_{\mu\nu}^{g\bar{c}c}(p, q, r)$ is proportional to $\eta_{\mu\nu}$ with the colour group and other factors remaining unchanged. In Figure 4 we have included two ghost-gluon Green's functions labelled separately by A and B . This is because both orientations appear in the identity and we need to be careful in computing both off-shell. The other Green's function of Figure 4 defines the triple gluon vertex function of the identity which was computed in [43, 46]. We refer the reader to [46] for the result with the same conventions used here.

While the ghost-gluon vertex function itself was also computed in [43, 46] we will need the off-shell result for $\Gamma_{\mu\nu}^{g\bar{c}c}(p, q, r)$ for both orientations. We briefly summarize the computation of [46] here first noting that we used the same projection principle to decompose the vertex function into a basis of Lorentz tensors. Using r in each instance of a 3-point function as the dependent external momentum then there are now five possible tensors for both versions of $\Gamma_{\mu\nu}^{g\bar{c}c}(p, q, r)$, rather than two for the conventional vertex function, which are

$$\mathcal{P}_{(1)\mu\nu}^{g\bar{c}c}(p, q) = \eta_{\mu\nu} \quad , \quad \mathcal{P}_{(2)\mu\nu}^{g\bar{c}c}(p, q) = \frac{p_{\mu}p_{\nu}}{\mu^2} \quad , \quad \mathcal{P}_{(3)\mu\nu}^{g\bar{c}c}(p, q) = \frac{p_{\mu}q_{\nu}}{\mu^2}$$

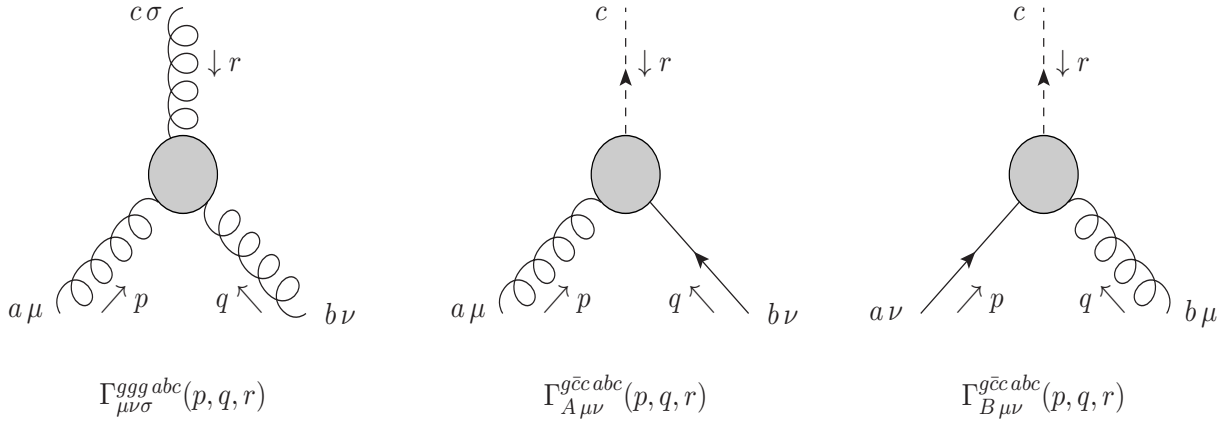


Figure 4: Basic one particle irreducible Green's functions for 3-point identity.

$$\mathcal{P}_{(4)\mu\nu}^{g\bar{c}c}(p, q) = \frac{q_\mu q_\nu}{\mu^2} \quad , \quad \mathcal{P}_{(5)\mu\nu}^{g\bar{c}c}(p, q) = \frac{q_\mu q_\nu}{\mu^2} \quad (3.1)$$

for the orientations of Figure 4. The kinematic variables for our off-shell analysis are the same as [47] and we note that

$$x = \frac{p^2}{r^2} \quad , \quad y = \frac{q^2}{r^2} \quad , \quad r^2 = -\mu^2 \quad (3.2)$$

when we consider 3-point Green's functions. The associated Gram determinant is, [47],

$$\Delta_G(x, y) = x^2 - 2xy + y^2 - 2x - 2y + 1 . \quad (3.3)$$

With this basis then for route A we have

$$\langle A_\mu^a(p) c^b(q) \bar{c}_\nu^c(r) \rangle = f^{abc} \Gamma_{A\mu\nu}^{g\bar{c}c}(p, q, r) = f^{abc} \sum_{k=1}^5 \mathcal{P}_{A(k)\mu\nu}^{g\bar{c}c}(p, q) \Sigma_{A(k)}^{g\bar{c}c}(p, q) \quad (3.4)$$

with

$$p + q + r = 0 \quad (3.5)$$

and we have factored off the common colour group structure constants f^{abc} which play a passive role at one loop. The Lorentz index on the field \bar{c}_μ^a indicates the removal of the external momentum from the associated ghost-gluon vertex. We also define

$$\langle A_\mu^a(p) A_\nu^b(q) A_\sigma^c(r) \rangle = f^{abc} \Gamma_{\mu\nu\sigma}^{ggg}(p, q, r) . \quad (3.6)$$

The associated scalar amplitudes are $\Sigma_{A(k)}^{g\bar{c}c}(p, q)$ and are deduced by multiplying $\Gamma_{A\mu\nu}^{g\bar{c}c}(p, q, r)$ by the projection matrix $\mathcal{M}_{kl}^{g\bar{c}c}$ which is the inverse of the matrix

$$\mathcal{N}_{kl}^{g\bar{c}c} = \mathcal{P}_{(k)\mu\nu}^{g\bar{c}c}(p, q) \mathcal{P}_{(l)}^{g\bar{c}c\mu\nu}(p, q) \quad (3.7)$$

where $1 \leq k \leq 5$. The explicit expressions for the elements of $\mathcal{M}_{kl}^{g\bar{c}c}$ are provided in Appendix A as they are complicated functions of the variables x and y as well as the spacetime dimension d . We note that throughout we use dimensional regularization to carry out all our loop calculations in $d = 4 - 2\epsilon$ dimensions. So we have to carry out the projection in d -dimensions. To evaluate the vertex functions to one loop we use the same method outlined in detail in [46] and refer the

reader to that for more technical details. Though to summarize we note that the integration by parts algorithm devised by Laporta, [48], is the main tool and we used the REDUZE implementation, [49, 50]. The underlying master integrals are imported from [51, 52] to complete the decomposition into scalar amplitudes. All our calculations for both 3- and 4-point functions are carried out automatically with the symbolic manipulation language FORM, [53, 54], used to handle the algebraic manipulations after the contributing Feynman graphs are generated using the QGRAF package, [55].

To get a flavour of the consequences of our computations we record the expressions for both orientations of $\Gamma_{\mu\nu}^{g\bar{c}c}(p, q, r)$ in Figure 4. However given that the completely off-shell results involve polylogarithms we provide the versions at the completely symmetric point defined by $x = y = 1$ for illustration. We have

$$\begin{aligned}
-i \Gamma_{A\mu\nu}^{g\bar{c}c}(p, q, r) \Big|_{x=y=1} &= -\eta_{\mu\nu}g \\
&+ \left[\left[\left[\frac{\xi}{2} - \frac{1}{2} \right] \frac{1}{\epsilon} - 1 - \frac{\pi^2}{9} + \frac{\xi}{2} + \frac{7\pi^2}{54}\xi + \frac{\xi^2}{8} \right. \right. \\
&\quad \left. \left. + \frac{1}{6}\psi'(\tfrac{1}{3}) - \frac{7}{36}\psi'(\tfrac{1}{3})\xi \right] \eta_{\mu\nu} \right. \\
&\quad \left. + \left[\frac{4\pi^2}{27} - \frac{\xi}{6} + \frac{\pi^2}{27}\xi - \frac{\pi^2}{54}\xi^2 - \frac{2}{9}\psi'(\tfrac{1}{3}) - \frac{\xi}{18}\psi'(\tfrac{1}{3}) \right. \right. \\
&\quad \left. \left. + \frac{\xi^2}{36}\psi'(\tfrac{1}{3}) \right] \frac{p_\mu p_\nu}{\mu^2} + \left[\frac{\xi}{6} + \frac{\pi^2}{27}\xi - \frac{\xi}{18}\psi'(\tfrac{1}{3}) \right] \frac{p_\mu q_\nu}{\mu^2} \right. \\
&\quad \left. + \left[\frac{4\pi^2}{27} + \frac{\xi}{6} - \frac{\pi^2}{27}\xi - \frac{\xi^2}{4} - \frac{\pi^2}{27}\xi^2 - \frac{2}{9}\psi'(\tfrac{1}{3}) + \frac{\xi}{18}\psi'(\tfrac{1}{3}) \right. \right. \\
&\quad \left. \left. + \frac{1}{18}\psi'(\tfrac{1}{3})\xi^2 \right] \frac{p_\nu q_\mu}{\mu^2} \right. \\
&\quad \left. + \left[\frac{1}{3}\xi - \frac{2}{27}\pi^2 + \frac{1}{27}\pi^2\xi + \frac{1}{9}\psi'(\tfrac{1}{3}) - \frac{1}{18}\psi'(\tfrac{1}{3})\xi \right] \frac{q_\mu q_\nu}{\mu^2} \right] C_A g^3 \\
&+ O(g^5) \tag{3.8}
\end{aligned}$$

and

$$\begin{aligned}
-i \Gamma_{B\mu\nu}^{g\bar{c}c}(p, q, r) \Big|_{x=y=1} &= \eta_{\mu\nu}g \\
&+ \left[\left[\left[\frac{1}{2} - \frac{\xi}{2} \right] \frac{1}{\epsilon} + 1 + \frac{\pi^2}{9} - \frac{\xi}{2} - \frac{7\xi}{54}\pi^2 - \frac{\xi^2}{8} \right. \right. \\
&\quad \left. \left. - \frac{1}{6}\psi'(\tfrac{1}{3}) + \frac{7\xi}{36}\psi'(\tfrac{1}{3}) \right] \eta_{\mu\nu} \right. \\
&\quad \left. + \left[\frac{2\pi^2}{27} - \frac{1}{3}\xi - \frac{1}{27}\pi^2\xi - \frac{1}{9}\psi'(\tfrac{1}{3}) + \frac{1}{18}\psi'(\tfrac{1}{3})\xi \right] \frac{p_\mu p_\nu}{\mu^2} \right. \\
&\quad \left. + \left[-\frac{4\pi^2}{27} - \frac{\xi}{6} + \frac{\pi^2}{27}\xi + \frac{1}{4}\xi^2 + \frac{\pi^2}{27}\xi^2 + \frac{2}{9}\psi'(\tfrac{1}{3}) - \frac{\xi}{18}\psi'(\tfrac{1}{3}) \right. \right. \\
&\quad \left. \left. - \frac{1}{18}\psi'(\tfrac{1}{3})\xi^2 \right] \frac{p_\mu q_\nu}{\mu^2} + \left[-\frac{1}{6}\xi - \frac{1}{27}\pi^2\xi + \frac{1}{18}\psi'(\tfrac{1}{3})\xi \right] \frac{p_\nu q_\mu}{\mu^2} \right. \\
&\quad \left. + \left[-\frac{4}{27}\pi^2 + \frac{1}{6}\xi - \frac{1}{27}\pi^2\xi + \frac{1}{54}\pi^2\xi^2 + \frac{2}{9}\psi'(\tfrac{1}{3}) + \frac{1}{18}\psi'(\tfrac{1}{3})\xi \right. \right. \\
&\quad \left. \left. - \frac{1}{36}\psi'(\tfrac{1}{3})\xi^2 \right] \frac{q_\mu q_\nu}{\mu^2} \right] C_A g^3 + O(g^5) \tag{3.9}
\end{aligned}$$

where $\alpha = 1 - \xi$ is the gauge parameter with $\alpha = 0$ corresponding to the Landau gauge, $\psi(z)$ is the derivative of the logarithm of Euler Γ -function*, C_A is the usual colour group Casimir and g is the gauge coupling constant. We do not carry out any renormalization at any instance since the identities hold in the bare case. So the parameters ξ , α and g are bare. We have provided the expressions for these off-shell vertex functions in the attached data file.

At this point it is worth recording the 3-point Slavnov-Taylor identity for the triple gluon vertex, illustrated in Figure 1, as an equation with the Lorentz indices explicit, now that we have introduced the modified ghost-gluon vertex $\Gamma_{\mu\nu}^{g\bar{c}c}(p, q, r)$. We have

$$\begin{aligned} r^\sigma \Gamma_{\mu\nu\sigma}^{ggg}(p, q, r) &= \Gamma_{A\mu\rho}^{g\bar{c}c}(p, q, r) P_\nu^\rho(q) q^2 + \Gamma_{B\nu\rho}^{g\bar{c}c}(p, q, r) P_\mu^\rho(p) p^2 \\ &\quad - \Gamma_{(0)A\mu\rho}^{g\bar{c}c}(p, q, r) P_\nu^\rho(p) \Gamma_{(1)}^{gg}(p) p^2 x^{-\epsilon} - \Gamma_{(0)B\nu\rho}^{g\bar{c}c}(p, q, r) P_\mu^\rho(q) \Gamma_{(1)}^{gg}(q) q^2 y^{-\epsilon} \\ &\quad + r^\sigma \Gamma_{(0)\mu\nu\sigma}^{ggg}(p, q, r) \Gamma_{(1)}^{\bar{c}c}(r) \end{aligned} \quad (3.10)$$

where we recall a subscript 0 on a Green's function means the tree contribution only. We note that we have set

$$\Gamma_{\mu\nu}^g(p) = P_{\mu\nu}(p) + \Gamma_{(1)}^{gg}(p) P_{\mu\nu}(p) \quad (3.11)$$

for the inverse propagator to one loop with $\Gamma_{(1)}^{\bar{c}c}$ indicating the one loop correction of the ghost leg of the final graph of Figure 1. For reference we note

$$\begin{aligned} \Gamma_{(1)}^{gg}(p) &= \left[\left[\frac{5}{3} C_A - \frac{4}{3} N_f T_F + \frac{1}{2} \xi C_A \right] \frac{1}{\epsilon} + \frac{31}{9} C_A - \frac{20}{9} N_f T_F - \xi C_A + \frac{1}{4} \xi^2 C_A \right. \\ &\quad \left. + \left[\frac{188}{27} C_A - \frac{112}{27} N_f T_F - 2\xi C_A + \frac{1}{2} \xi^2 C_A \right] \epsilon + O(\epsilon^2) \right] g^2 \end{aligned} \quad (3.12)$$

and

$$\Gamma_{(1)}^{\bar{c}c}(p) = \left[\frac{1}{2\epsilon} C_A + \frac{1}{4\epsilon} \xi C_A + C_A + 2C_A \epsilon + O(\epsilon^2) \right] g^2 \quad (3.13)$$

as well as

$$\Gamma_{(0)\mu\nu\rho}^{ggg}(p, q, r) = i [\eta_{\mu\nu} q_\sigma - \eta_{\mu\nu} p_\sigma + 2\eta_{\mu\sigma} p_\nu + \eta_{\mu\sigma} q_\nu - \eta_{\nu\sigma} p_\mu - 2\eta_{\nu\sigma} q_\mu] g \quad (3.14)$$

for the tree term of the 3-point gluon vertex. We have included diagrams with quarks in all our computations and their contributions are associated with the number of flavours N_f and Dynkin index T_F . However for the 3-point identity (3.10) they primarily play a passive role in the verification by calculation.

To illustrate how each of the various terms of (3.10) conspire together to satisfy the identity we have provided the values for each of the terms on the right hand side of (3.10) in Table 1. We do this for the completely symmetric point for simplicity here purely due to the cumbersome expressions for the fully off-shell case. In Table 1 there are five separate sections which correspond to the respective terms of (3.10) in order. Within each graph we have divided the contributions by the respective structures which can appear in the expression. These correspond respectively to the residue of the simple pole in ϵ , the rational finite part and the coefficients of π^2 and $\psi'(\frac{1}{3})$. As each graph was decomposed into the Lorentz basis there are five columns corresponding to the basis of the factored ghost-gluon vertex. Therefore Table 1 compactly summarizes all contributions to the right hand side of (3.10). The corresponding coefficients of the left hand side of the identity are given in Table 2 in the same notation. Therefore it is a straightforward exercise to sum the respective coefficients for each structure and tensor in Table 1 and see that they completely tally with the corresponding entries in Table 2. It is worth noting that this

*The presence of $\psi(\frac{1}{3})$ is not unrelated to the cyclotomic polynomials of [56].

| Entity | $\mathcal{P}_{(1)}^{g\bar{c}c}$ | $\mathcal{P}_{(2)}^{g\bar{c}c}$ | $\mathcal{P}_{(3)}^{g\bar{c}c}$ | $\mathcal{P}_{(4)}^{g\bar{c}c}$ | $\mathcal{P}_{(5)}^{g\bar{c}c}$ |
|----------------------|---|--|---------------------------------|---------------------------------|---|
| $\frac{1}{\epsilon}$ | 0 | 0 | 0 | 0 | 0 |
| Q | $-\frac{3}{8}C_A$ | $-\frac{1}{6}C_A$ | $-\frac{1}{12}C_A$ | $-\frac{1}{12}C_A$ | $-\frac{5}{12}C_A$ |
| π^2 | $\frac{1}{54}C_A$ | $\frac{1}{6}C_A$ | $\frac{1}{16}C_A$ | $\frac{2}{27}C_A$ | $\frac{1}{18}C_A$ |
| $\psi'(\frac{1}{3})$ | $-\frac{1}{36}C_A$ | $-\frac{1}{4}C_A$ | $-\frac{1}{8}C_A$ | $-\frac{1}{12}C_A$ | $-\frac{1}{36}C_A$ |
| $\frac{1}{\epsilon}$ | 0 | 0 | 0 | 0 | 0 |
| Q | $\frac{3}{8}C_A$ | $\frac{5}{12}C_A$ | $\frac{1}{12}C_A$ | $\frac{1}{12}C_A$ | $\frac{1}{6}C_A$ |
| π^2 | $-\frac{1}{54}C_A$ | $-\frac{1}{18}C_A$ | $-\frac{1}{12}C_A$ | $-\frac{2}{27}C_A$ | $-\frac{1}{6}C_A$ |
| $\psi'(\frac{1}{3})$ | $\frac{1}{36}C_A$ | $\frac{1}{12}C_A$ | $\frac{1}{8}C_A$ | $\frac{1}{9}C_A$ | $\frac{1}{4}C_A$ |
| $\frac{1}{\epsilon}$ | $\frac{4}{3}T_F N_f - \frac{13}{6}C_A$ | $\frac{4}{3}T_F N_f - \frac{13}{6}C_A$ | 0 | 0 | 0 |
| Q | $\frac{20}{9}T_F N_f - \frac{97}{36}C_A$ | $\frac{20}{9}T_F N_f - \frac{97}{36}C_A$ | 0 | 0 | 0 |
| π^2 | 0 | 0 | 0 | 0 | 0 |
| $\psi'(\frac{1}{3})$ | 0 | 0 | 0 | 0 | 0 |
| $\frac{1}{\epsilon}$ | $-\frac{4}{3}T_F N_f + \frac{13}{6}C_A$ | 0 | 0 | 0 | $-\frac{4}{3}T_F N_f + \frac{13}{6}C_A$ |
| Q | $-\frac{20}{9}T_F N_f + \frac{97}{36}C_A$ | 0 | 0 | 0 | $-\frac{20}{9}T_F N_f + \frac{97}{36}C_A$ |
| π^2 | 0 | 0 | 0 | 0 | 0 |
| $\psi'(\frac{1}{3})$ | 0 | 0 | 0 | 0 | 0 |
| $\frac{1}{\epsilon}$ | 0 | $\frac{3}{4}C_A$ | 0 | 0 | $-\frac{3}{4}C_A$ |
| Q | 0 | C_A | 0 | 0 | $-C_A$ |
| π^2 | 0 | 0 | 0 | 0 | 0 |
| $\psi'(\frac{1}{3})$ | 0 | 0 | 0 | 0 | 0 |

Table 1. Coefficients of each of the tensors and different structures for each of the five terms on the right hand side of (3.10) in the Landau gauge.

represents a check of the Slavnov-Taylor identity derived using the methods of [28, 29, 30] for a non-exceptional momentum configuration. No external momenta have been nullified. We have repeated the same check for the completely off-shell case for x and y not restricted to unity and found the same total consistency of (3.10). This is non-trivial and to give an indication of the nature of the functions involved in this case we note that the coefficient of $\mathcal{P}_{(1)}^{g\bar{c}c}$ for the first term on the right hand side of (3.10) is

$$\begin{aligned}
& \left[\frac{1}{4}y \ln(x) - \frac{3}{8}y - \frac{1}{2}y \ln(y) + \left[\frac{1}{2}y^2 - \frac{3}{8}y - \frac{1}{4}xy \right] \Phi_1(x, y) \right. \\
& + \left[\left[\frac{1}{8}y - \frac{1}{4}y^2 + \frac{1}{8}y^3 + \frac{3}{8}xy - \frac{1}{8}xy^2 \right] \ln(x) + \left[\frac{1}{4}y - \frac{1}{8}y^2 - \frac{1}{8}y^3 - \frac{1}{4}xy + \frac{1}{8}xy^2 \right] \ln(y) \right. \\
& \left. \left. + \left[\frac{1}{4}y - \frac{1}{2}y^2 + \frac{1}{4}y^3 - \frac{1}{4}xy \right] \Phi_1(x, y) \right] \frac{1}{\Delta_G} \right] C_A \tag{3.15}
\end{aligned}$$

which is considerably more involved than the three coefficients in the first column of Table 1 corresponding to this graph. At the symmetric point (3.15) reduces to the corresponding entry where the function $\Phi_1(x, y)$ contains the polylogarithm function $\text{Li}_n(z)$ and is defined by, [52],

$$\Phi_1(x, y) = \frac{1}{\lambda} \left[2\text{Li}_2(-\rho x) + 2\text{Li}_2(-\rho y) + \ln\left(\frac{y}{x}\right) \ln\left(\frac{(1+\rho y)}{(1+\rho x)}\right) + \ln(\rho x) \ln(\rho y) + \frac{\pi^2}{3} \right] \tag{3.16}$$

where

$$\rho(x, y) = \frac{2}{[1 - x - y + \lambda(x, y)]} \quad , \quad \lambda(x, y) = \sqrt{\Delta_G} . \quad (3.17)$$

The more involved x and y dependence would make the extension of Table 1 to the off-shell case large but the data file contains the details of the full off-shell case for arbitrary gauge. However we confirm that the sum of the graphs on the right side of (3.10) fully agree with the expression for $\frac{r^\sigma}{r^2} \Gamma_{\mu\nu\sigma}^{ggg}(p, q, r)$ for non-unit x and y . We note that in addition to $\Phi_1(x, y)$ the $O(\epsilon)$ correction to one loop master triangle graph is required for several Green's function contributing to the 4-point identity. Therefore as this is the appropriate place to note this we record that the $O(\epsilon)$ term of the triangle master is

$$\begin{aligned} \Psi_1(x, y) = & -\frac{1}{\lambda} \left[4\text{Li}_3 \left(-\frac{\rho x(1 + \rho y)}{(1 - \rho^2 xy)} \right) + 4\text{Li}_3 \left(-\frac{\rho y(1 + \rho x)}{(1 - \rho^2 xy)} \right) - 4\text{Li}_3 \left(-\frac{xy\rho^2}{(1 - \rho^2 xy)} \right) \right. \\ & + 2\text{Li}_3 \left(\frac{x\rho(1 + \rho y)}{(1 + \rho x)} \right) + 2\text{Li}_3 \left(\frac{y\rho(1 + \rho x)}{(1 + \rho y)} \right) - 2\text{Li}_3(\rho^2 xy) - 2\zeta_3 \\ & - 2\ln(y)\text{Li}_2 \left(\frac{x\rho(1 + \rho y)}{(1 + \rho x)} \right) - 2\ln(x)\text{Li}_2 \left(\frac{y\rho(1 + \rho x)}{(1 + \rho y)} \right) - \frac{2}{3}\ln^3(1 - \rho^2 xy) \\ & + \frac{2}{3}\ln^3(1 + \rho x) + \frac{2}{3}\ln^3(1 + \rho y) + 2\ln(\rho)\ln^2(1 - \rho^2 xy) \\ & - 2\ln(1 - \rho^2 xy) \left[\ln(\rho x)\ln(\rho y) + \ln\left(\frac{y}{x}\right)\ln\left(\frac{(1 + \rho y)}{(1 + \rho x)}\right) \right. \\ & \quad \left. + 2\ln(1 + \rho x)\ln(1 + \rho y) + \frac{\pi^2}{3} \right] \\ & + \frac{1}{2}\ln(xy\rho^2) \left[\ln(\rho x)\ln(\rho y) + \ln\left(\frac{y}{x}\right)\ln\left(\frac{(1 + \rho y)}{(1 + \rho x)}\right) - \ln^2\left(\frac{(1 + \rho x)}{(1 + \rho y)}\right) \right. \\ & \quad \left. + \frac{2\pi^2}{3} \right] \Bigg] . \quad (3.18) \end{aligned}$$

| Entity | $\mathcal{P}_{(1)}^{g\bar{c}c}$ | $\mathcal{P}_{(2)}^{g\bar{c}c}$ | $\mathcal{P}_{(3)}^{g\bar{c}c}$ | $\mathcal{P}_{(4)}^{g\bar{c}c}$ | $\mathcal{P}_{(5)}^{g\bar{c}c}$ |
|----------------------|---------------------------------|---|---------------------------------|---------------------------------|--|
| $\frac{1}{\epsilon}$ | 0 | $\frac{4}{3}T_F N_f - \frac{13}{6}C_A$ | 0 | 0 | $-\frac{4}{3}T_F N_f + \frac{13}{6}C_A$ |
| Q | 0 | $\frac{20}{9}T_F N_f - \frac{13}{9}C_A$ | 0 | 0 | $-\frac{20}{9}T_F N_f + \frac{13}{9}C_A$ |
| π^2 | 0 | $\frac{1}{9}C_A$ | 0 | 0 | $-\frac{1}{9}C_A$ |
| $\psi'(\frac{1}{3})$ | 0 | $-\frac{1}{6}C_A$ | 0 | 0 | $\frac{1}{6}C_A$ |

Table 2. Coefficients of each of the tensors and different structures for the left hand side of (3.10) in the Landau gauge.

4 Quartic gluon vertex.

We now turn to the examination of the 4-point identity which was considered in [3, 5, 11] and that derived using algebraic and diagrammatic methods which is illustrated in Figure 2. It relates the purely gluonic 4-point vertex function to three ghost-gluon boxes as well as the 4-point functions built from reduced 3-point ghost-gluon functions. We have labelled the respective orientations with C and D as they differ from the previous ones and illustrated their definitions in Figure 5 for clarity. The graphical definitions of the 4-point terms are provided in Figure 6 which includes

the three orientations of the reduced 4-point ghost-gluon functions where one external ghost leg corresponds to the reduced 3-point ghost-gluon vertex. For reference we note that the quartic gluon vertex is defined by

$$\langle A_\mu^a(p) A_\nu^b(q) A_\sigma^c(r) A_\rho^d(s) \rangle = \Gamma_{\mu\nu\sigma\rho}^{gggg\,abcd}(p, q, r, s). \quad (4.1)$$

Unlike its 3-point counterpart we cannot factor off a common group theory structure. This is because even at one loop there are a large number of different combinations of the structure constants and unit matrix in colour space to produce symmetric rank 4 colour tensors. This was also apparent in the early work of [11] and had to be taken into account in [35] as well. In Appendix B we have summarized our algorithm for dealing with aspects of the group theory issues which is based on [35]. Though we note that throughout this section alone we restrict ourselves to the $SU(N_c)$ group rather than the general Lie group considered previously. The 4-point identity of Figure 6 corresponds to

$$\begin{aligned} \Gamma_{\mu\nu\sigma\rho}^{gggg\,abcd}(p, q, r, s) s^\rho &= \Gamma_{A\nu\sigma\lambda}^{c\bar{c}gg\,abcd}(p, q, r, s) P_\mu^\lambda(p) + \Gamma_{B\mu\sigma\lambda}^{c\bar{c}gg\,abcd}(p, q, r, s) P_\nu^\lambda(q) \\ &+ \Gamma_{C\mu\nu\lambda}^{c\bar{c}gg\,abcd}(p, q, r, s) P_\sigma^\lambda(r) \\ &+ \Gamma_{D\nu\lambda}^{g\bar{c}c\,dbe}(s, q, -s - q) \Gamma_{\mu\sigma\lambda}^{ggg\,ace}(p, r, -p - r) ((p + r)^2)^{-\epsilon} \\ &+ \Gamma_{C\sigma\lambda}^{g\bar{c}c\,cde}(r, s, -r - s) \Gamma_{\mu\nu\lambda}^{ggg\,abe}(p, q, -p - q) ((p + q)^2)^{-\epsilon} \\ &+ \Gamma_{D\mu\lambda}^{g\bar{c}c\,dae}(s, p, -s - p) \Gamma_{\nu\sigma\lambda}^{ggg\,bce}(q, r, -q - r) ((q + r)^2)^{-\epsilon} \\ &+ \Gamma_{(0)\mu\nu\sigma\rho}^{gggg\,abcd}(p, q, r, s) s^\rho \Gamma_{(1)}^{\bar{c}c}(s) \end{aligned} \quad (4.2)$$

or to (2.12) with the Lorentz and colour indices included for the practical task of its evaluation. Due to the presence of two 3-point vertices appearing in graphs with a bridge we have temporarily reintroduced the colour indices in those vertex functions to assist with the placement of the structure constants in an evaluation.

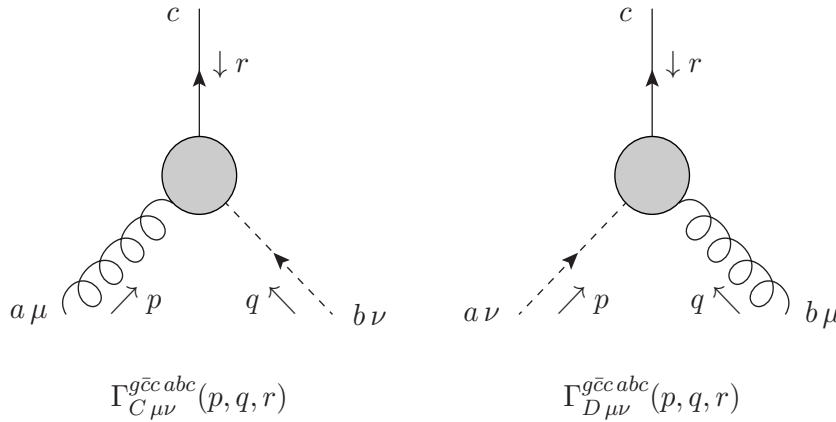


Figure 5: Extra ghost-gluon 3-point function configurations for 4-point identity.

To study (4.2) we will restrict to the fully symmetric point setup of [11] but using the notation of [35]. For a 4-point function the symmetric point is defined by the following relations between the external momenta

$$p^2 = q^2 = r^2 = -\mu^2, \quad pq = pr = qr = \frac{1}{3}\mu^2 \quad (4.3)$$

where we take s as the dependent momentum since

$$p + q + r + s = 0. \quad (4.4)$$

The Mandelstam variables are explicitly defined by

$$\bar{s} = \frac{1}{2}(p+q)^2, \quad \bar{t} = \frac{1}{2}(q+r)^2, \quad \bar{u} = \frac{1}{2}(p+r)^2 \quad (4.5)$$

then take the values

$$\bar{s} = \bar{t} = \bar{u} = -\frac{4}{3}\mu^2. \quad (4.6)$$

Here μ is the overall mass scale to which all the external momenta relate to. In the previous section we considered the completely off-shell 3-point identity and it is apparent in Figure 6 that these functions play a role. However at the 4-point symmetric point it is important to realise that in bolting two 3-point functions together each of these functions are *not* at the 3-point symmetric point. With (4.3) the bridging momentum corresponds to one of the Mandelstam variables (4.5).

Aside from the various different colour channels which are present in the 4-point functions there is a larger number of Lorentz tensors for each of the Green's functions of Figure 6. For instance $\Gamma_{\mu\nu\sigma\rho}^{gggg\,abcd}(p, q, r, s)$ has 138 such tensors, [35], which reduces to 36 when contracted with s^ρ . These match the same 36 possibilities for the decomposition of $\Gamma_{\nu\sigma\lambda}^{c\bar{c}gg\,abcd}(p, q, r, s)$ into its tensor basis. As this Green's function was not computed in [36] we need to evaluate it here for the three different routings. To do so we follow the same procedure as (3.4). The tensor basis for each case is structurally the same differing only in the rotation of the Lorentz indices with respect to the various external legs. In Appendix A we have given the tensor basis as well as the projection matrix for the 4-point ghost-gluon function at the symmetric point. For a more general off-shell setup the projection matrix method is not appropriate to use given the large dependence on the kinematic variables which would be present. Aside from the Mandelstam variables the other variables in that instance would be the ratios of the three dependent external momenta, akin to x and y of (3.2), as well as one overall mass scale which would be μ^2 . To be clear we decompose the ghost-gluon 4-point function of the identity via

$$\left\langle A_\mu^a(p) A_\nu^b(q) c^c(r) \bar{c}_\sigma^d(s) \right\rangle = \Gamma_{\mu\nu\sigma}^{c\bar{c}gg\,abcd}(p, q, r, s) = \sum_{k=1}^{36} \mathcal{P}_{(k)\mu\nu\sigma}^{c\bar{c}gg}(p, q, r) \Sigma_{(k)}^{c\bar{c}gg\,abcd}(p, q, r) \quad (4.7)$$

using the same basic notation as earlier. The full Lorentz tensor basis is given in Appendix A together with the elements of the projection matrix $\mathcal{M}^{c\bar{c}gg}$ at the symmetric point (4.3). For each of the three orientations there are 7 Feynman graphs at one loop none of which involve quarks. Again the method we employ to evaluate the scalar amplitudes of $\Gamma_{\mu\nu\sigma}^{c\bar{c}gg\,abcd}(p, q, r, s)$ is the same as that for the 3-point case in that we use the Laporta algorithm after the scalar amplitudes have been isolated by the projection method. One of the main differences in computing $\Gamma_{\mu\nu\sigma\rho}^{gggg\,abcd}(p, q, r, s)$ and the various orientations of $\Gamma_{\mu\nu\sigma}^{c\bar{c}gg\,abcd}(p, q, r, s)$ is that there is more than one possible rank 4 colour group tensor which can appear at one loop. For a 3-point function involving only ghosts and gluons there is only one possible rank 3 colour tensor. For the 4-point functions we have to be careful in our colour tensor basis choice and have retained that which was used in [35, 36]. The technical details of this have been relegated to Appendix B but we note that we do not use a method of projection similar to that for the Lorentz structure. Instead we map the colour combinations into our choice of basis tensors. For completeness this is

$$\left\{ \delta^{ab}\delta^{cd}, \delta^{ac}\delta^{bd}, \delta^{ad}\delta^{bc}, f^{abe}f^{cde}, f^{ace}f^{bde}, d_A^{abcd}, d_F^{abcd} \right\} \quad (4.8)$$

where the fully symmetric rank 4 tensors d_A^{abcd} and d_F^{abcd} are defined in (B.1) and their properties discussed at length in [57]. We have used the Jacobi identity to ensure there are only two independent rank 4 combinations of the product of two structure constants. For illustration we have provided the expressions for $\Gamma_{\mu\nu\sigma\rho}^{gggg\,abcd}(p, q, r, s)$ and $\Gamma_{A\mu\nu\sigma}^{c\bar{e}gg\,abcd}(p, q, r, s)$ in the Landau gauge at the fully symmetric point in Appendix C. Full explicit expressions for each of the graphs in Figure 2 in an arbitrary linear covariant gauge are given in the attached data file.

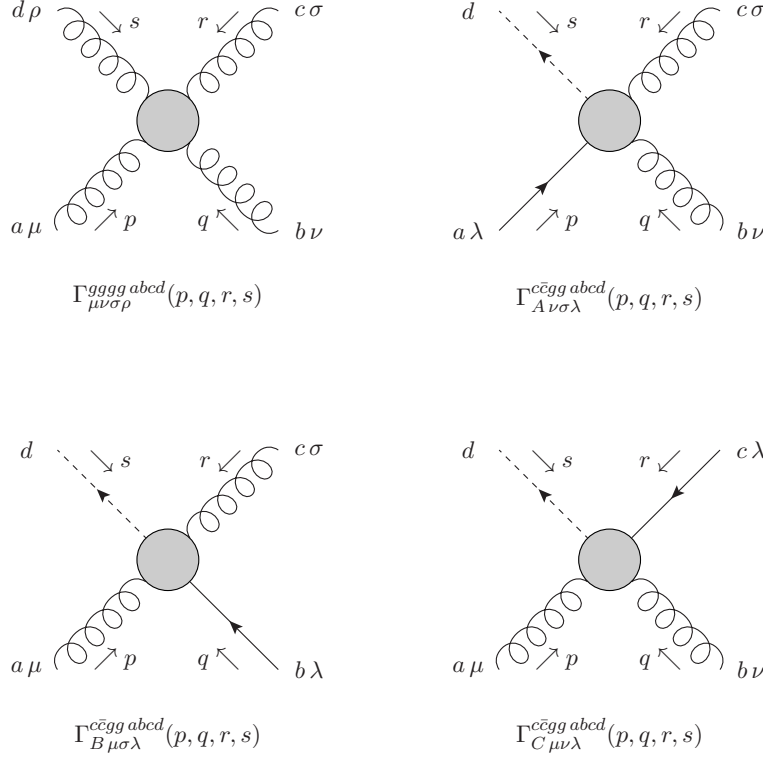


Figure 6: Basic one particle irreducible Green's functions for 4-point function.

Having discussed the technical issues around computing the individual graphs contributing to (4.2) we now turn to demonstrating that the identity is satisfied at the symmetric point (4.3). Compared to the 3-point case this is much more involved because of the structure of the Green's function. First there are three colour and 36 Lorentz tensors in the basis for each graph. On top of this there are four different numerical structures in each tensor coefficient aside from the pole term in ϵ . These structures are the pure rational piece, $\ln(\frac{4}{3})$ and two specific functions involving dilogarithms. These are $\Phi_1(\frac{3}{4}, \frac{3}{4})$ and $\Phi_1(\frac{9}{16}, \frac{9}{16})$. This gives a large number of overall terms which have to sum to match both sides of (4.2) exactly. If we dissect the origin of $\Phi_1(\frac{3}{4}, \frac{3}{4})$ and $\Phi_1(\frac{9}{16}, \frac{9}{16})$ more carefully we can understand how part of this cancellation proceeds. The arguments of both functions reflect the kinematics of the underlying master integral deriving from the application of the Laporta algorithm. For instance the completely off-shell box fully symmetric point master integral of Figure 7 is given by, [58, 59],

$$\Phi_1\left(\frac{p^2 r^2}{(p+q)^2 (q+r)^2}, \frac{q^2 s^2}{(p+q)^2 (q+r)^2}\right) \quad (4.9)$$

which depend on the Mandelstam variables. Using their values at the symmetric point, (4.6), determines the origin of $\Phi_1(\frac{9}{16}, \frac{9}{16})$. Therefore in (4.2) the only terms where such a function can

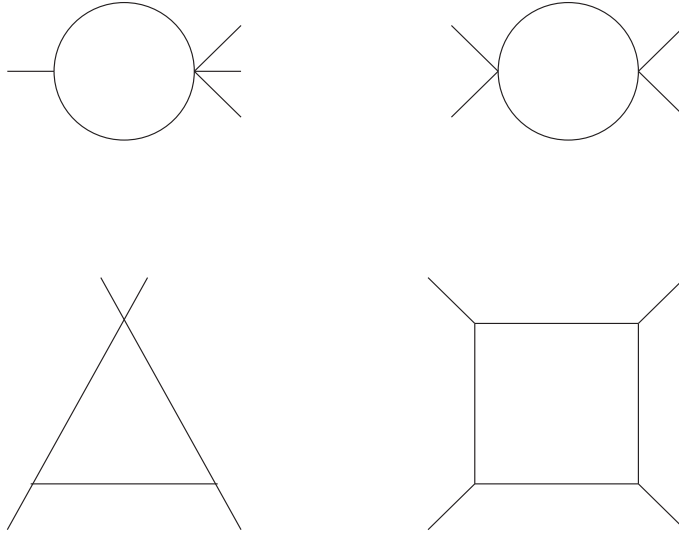


Figure 7: Master integrals for reduction of 4-point function.

arise is in 1PI 4-point functions which is the first three terms of the right hand side as well as the left side. The other structure $\Phi_1(\frac{3}{4}, \frac{3}{4})$ occurs in all but the last term on the right hand side of (4.2). However it has different origins in the three 4-point functions and the three graphs of Figure 2 where there is a bridging propagator between two 3-point functions. For instance the box graph of Figure 7 is also one of the three box topologies in the integral family which is the starting point of the Laporta algorithm. Within the integration by parts routine various masters can be deduced by taking one of the integral family topologies and removing lines or propagators in such a way as not to produce a zero sector integral. Doing this for the box graph of Figure 7 produces the three remaining graphs of that Figure. Given this $\Phi_1(\frac{3}{4}, \frac{3}{4})$ corresponds to the triangle graph. We have deliberately retained the two external lines of the top apex to indicate the origin of this master. However both lines reflect that the momentum flowing out of that point is the sum of the two incoming momenta. Therefore from (4.3) one does not have a triangle master at the fully symmetric point of the 3-point functions of the previous section. Instead the variable for the top apex momentum is one of the three Mandelstam variables of (4.6). For the connected graphs of Figure 2 each 3-point vertex function is likewise evaluated with the connecting vertex momentum taking the same Mandelstam variable to produce terms involving $\Phi_1(\frac{3}{4}, \frac{3}{4})$. Finally the remaining two bubble topologies of Figure 7 give different values for similar reasons. This is because upon reduction from the box the momentum flow across the left bubble graph is p for instance but $(p + q)$ say for the second. The latter involves a Mandelstam variable and also is one source of the $\ln(\frac{4}{3})$ structure in the final expressions.

In order to give a flavour of how these different structures are assembled to ensure the Slavnov-Taylor identity is satisfied at the fully symmetric point we have repeated the approach used for the 3-point case. In other words we have provided a breakdown of the terms contributing to graphs in (4.2) in Tables 3 to 6. However given the large number of different tensor structures, both colour and Lorentz, we focus on a representative selection of each. In each of these tables the coefficients of the various structures are given for each graph. We note not every graph has simple poles in ϵ and only record data for them where they occur. In each of the Tables 3 to 6 we focus on 5 of the 36 different Lorentz tensors noting for instance in Table 3 only 5 graphs on the right side of (4.2) have contributions for these tensors. For a different choice of Lorentz tensors other graphs would contribute. To differentiate between the colour structures Tables 3 and 4 correspond to the colour tensor f_4^{abcd} while Tables 5 and 6 relate to the symmetric tensor

d_A^{abcd} where both these tensors are defined in (B.4). Similar to before the respective terms in Table 3 sum to the values give in Table 4 which are the calculated values of the left side of (4.2). For the case of d_A^{abcd} the respective Tables are 5 and 6 and we note that for the former table only the first three terms on the right hand side of (4.2) can have terms involving this colour tensor. As before we confirm that adding all the contributions from the right hand side of (4.2) gives precisely the same expression for fully agree with the expression for $s^\rho \Gamma_{\mu\nu\sigma\rho}^{gggg\,abcd}(p, q, r, s)$ for the configuration (4.3) in all Lorentz and colour channels.

| Entity | $\mathcal{P}_{(1)}^{c\bar{c}gg}$ | $\mathcal{P}_{(10)}^{c\bar{c}gg}$ | $\mathcal{P}_{(11)}^{c\bar{c}gg}$ | $\mathcal{P}_{(16)}^{c\bar{c}gg}$ | $\mathcal{P}_{(31)}^{c\bar{c}gg}$ |
|--------------------------------|---|---|--|--|--|
| \mathbb{Q} | $-\frac{63}{1280}N_c$ | $-\frac{1609}{30720}N_c$ | $-\frac{4151}{15360}N_c$ | $\frac{37}{360}N_c$ | $-\frac{453}{1280}N_c$ |
| $\ln(\frac{4}{3})$ | $\frac{2821}{25600}N_c$ | $-\frac{183663}{204800}N_c$ | $-\frac{931}{1600}N_c$ | $\frac{113231}{307200}N_c$ | $-\frac{36063}{102400}N_c$ |
| $\tilde{\Phi}_1(\frac{9}{16})$ | $\frac{33}{25600}N_c$ | $\frac{18211}{204800}N_c$ | $\frac{35329}{819200}N_c$ | $-\frac{16307}{819200}N_c$ | $-\frac{17427}{819200}N_c$ |
| $\tilde{\Phi}_1(\frac{3}{4})$ | $\frac{101}{4096}N_c$ | $-\frac{3983}{32768}N_c$ | $-\frac{129}{4096}N_c$ | $-\frac{111}{16384}N_c$ | $\frac{2925}{16384}N_c$ |
| \mathbb{Q} | $\frac{23}{160}N_c$ | 0 | $-\frac{867}{5120}N_c$ | $-\frac{257}{5760}N_c$ | $-\frac{221}{5120}N_c$ |
| $\ln(\frac{4}{3})$ | $\frac{13}{25}N_c$ | 0 | $\frac{4791}{51200}N_c$ | $-\frac{17929}{76800}N_c$ | $\frac{37989}{51200}N_c$ |
| $\tilde{\Phi}_1(\frac{9}{16})$ | $-\frac{1649}{25600}N_c$ | 0 | $\frac{8253}{819200}N_c$ | $-\frac{9137}{204800}N_c$ | $\frac{103707}{819200}N_c$ |
| $\tilde{\Phi}_1(\frac{3}{4})$ | $\frac{1}{128}N_c$ | 0 | $\frac{477}{8192}N_c$ | $-\frac{63}{4096}N_c$ | $-\frac{1521}{8192}N_c$ |
| \mathbb{Q} | $-\frac{263}{3840}N_c$ | $\frac{1609}{30720}N_c$ | $\frac{9331}{30720}N_c$ | $-\frac{59}{9216}N_c$ | $-\frac{1009}{5120}N_c$ |
| $\ln(\frac{4}{3})$ | $\frac{15661}{76800}N_c$ | $\frac{183663}{204800}N_c$ | $\frac{154731}{204800}N_c$ | $\frac{6341}{30720}N_c$ | $-\frac{1101}{102400}N_c$ |
| $\tilde{\Phi}_1(\frac{9}{16})$ | $\frac{3503}{76800}N_c$ | $-\frac{18211}{204800}N_c$ | $-\frac{69073}{819200}N_c$ | $-\frac{17859}{163840}N_c$ | $\frac{7331}{51200}N_c$ |
| $\tilde{\Phi}_1(\frac{3}{4})$ | $-\frac{337}{4096}N_c$ | $\frac{3983}{32768}N_c$ | $\frac{563}{32768}N_c$ | $\frac{945}{8192}N_c$ | $\frac{1715}{16384}N_c$ |
| $\frac{1}{\epsilon}$ | $\frac{17N_c}{12} - \frac{2N_f}{3}$ | 0 | 0 | 0 | 0 |
| \mathbb{Q} | $-\frac{N_c}{72} - \frac{37N_f}{36}$ | $\frac{63N_c}{64} + \frac{3N_f}{32}$ | $\frac{73N_c}{64} - \frac{11N_f}{32}$ | 0 | $-\frac{N_c}{4}$ |
| $\ln(\frac{4}{3})$ | $\frac{95N_c}{96} - \frac{7N_f}{48}$ | $\frac{191N_c}{256} - \frac{5N_f}{128}$ | $-\frac{847N_c}{256} + \frac{93N_f}{128}$ | 0 | $-\frac{25N_c}{16}$ |
| $\tilde{\Phi}_1(\frac{9}{16})$ | 0 | 0 | 0 | 0 | 0 |
| $\tilde{\Phi}_1(\frac{3}{4})$ | $-\frac{43N_c}{128} + \frac{27N_f}{64}$ | $\frac{327N_c}{1024} - \frac{189N_f}{512}$ | $\frac{681N_c}{1024} - \frac{171N_f}{512}$ | 0 | $-\frac{9N_c}{64}$ |
| $\frac{1}{\epsilon}$ | $-\frac{17N_c}{12} + \frac{2N_f}{3}$ | 0 | 0 | 0 | 0 |
| \mathbb{Q} | $-\frac{23N_c}{72} + \frac{37N_f}{36}$ | $-\frac{63N_c}{64} - \frac{3N_f}{32}$ | $-\frac{83N_c}{64} + \frac{11N_f}{32}$ | $-\frac{91N_c}{192} - \frac{N_f}{16}$ | $-\frac{15N_c}{32} + \frac{9N_f}{8}$ |
| $\ln(\frac{4}{3})$ | $\frac{455N_c}{96} - \frac{53N_f}{48}$ | $-\frac{191N_c}{256} + \frac{5N_f}{128}$ | $-\frac{203N_c}{256} + \frac{19N_f}{64}$ | $\frac{847N_c}{256} - \frac{41N_f}{64}$ | $-\frac{531N_c}{128} + \frac{41N_f}{32}$ |
| $\tilde{\Phi}_1(\frac{9}{16})$ | 0 | 0 | 0 | 0 | 0 |
| $\tilde{\Phi}_1(\frac{3}{4})$ | $-\frac{15N_c}{128} + \frac{15N_f}{64}$ | $-\frac{327N_c}{1024} + \frac{189N_f}{512}$ | $-\frac{243N_c}{1024} + \frac{27N_f}{256}$ | $-\frac{297N_c}{1024} + \frac{63N_f}{256}$ | $\frac{261N_c}{512} - \frac{63N_f}{128}$ |

Table 3. Coefficients of selected tensors and different structures for the first three, fifth and sixth terms on the right hand side of (4.2) for the f_4^{abcd} sector in the Landau gauge.

5 Discussion.

The main aim of our analysis was to first generate relations between various 3- and 4-point 1PI Green's functions in QCD when the gauge fixing was the canonical linear covariant one, and then to check that they were identically satisfied by explicit one loop computations. To derive these identities, we start from the contraction $p_i \cdot \Gamma_c^n = 0$ given by gauge invariance, which is the basic Slavnov-Taylor identity. Here, Γ_c^n can be any connected Green's function with n external gluons. The connected Green's function Γ_c^n above has the structure of an amputated connected

| Entity | $\mathcal{P}_{(1)}^{c\bar{c}gg}$ | $\mathcal{P}_{(10)}^{c\bar{c}gg}$ | $\mathcal{P}_{(11)}^{c\bar{c}gg}$ | $\mathcal{P}_{(16)}^{c\bar{c}gg}$ | $\mathcal{P}_{(31)}^{c\bar{c}gg}$ |
|--------------------------------|--|-----------------------------------|--|--|---|
| \mathbb{Q} | $-\frac{59N_c}{72} - \frac{5N_f}{4}$ | 0 | $-\frac{2991N_c}{10240} + \frac{11N_f}{32}$ | $-\frac{1297N_c}{3072} - \frac{N_f}{16}$ | $-\frac{3361N_c}{2560} + \frac{9N_f}{8}$ |
| $\ln(\frac{4}{3})$ | $\frac{8401N_c}{1280} - \frac{5N_f}{4}$ | 0 | $-\frac{785273N_c}{204800} + \frac{131N_f}{128}$ | $\frac{14951N_c}{4096} - \frac{41N_f}{64}$ | $-\frac{272993N_c}{51200} + \frac{41N_f}{32}$ |
| $\tilde{\Phi}_1(\frac{9}{16})$ | $-\frac{269N_c}{15360}$ | 0 | $-\frac{25491N_c}{819200}$ | $-\frac{2843N_c}{16384}$ | $\frac{25447N_c}{102400}$ |
| $\tilde{\Phi}_1(\frac{3}{4})$ | $-\frac{515N_c}{1024} + \frac{3N_f}{16}$ | 0 | $\frac{15455N_c}{32768} - \frac{117N_f}{512}$ | $-\frac{3225N_c}{16384} + \frac{63N_f}{256}$ | $\frac{3823N_c}{8192} - \frac{63N_f}{128}$ |

Table 4. Coefficients of selected tensors and different structures for the left hand side of (4.2) for the f_4^{abcd} sector in the Landau gauge.

| Entity | $\mathcal{P}_{(1)}^{c\bar{c}ggg}$ | $\mathcal{P}_{(10)}^{c\bar{c}ggg}$ | $\mathcal{P}_{(11)}^{c\bar{c}ggg}$ | $\mathcal{P}_{(16)}^{c\bar{c}ggg}$ | $\mathcal{P}_{(31)}^{c\bar{c}ggg}$ |
|--------------------------------|-----------------------------------|------------------------------------|------------------------------------|------------------------------------|------------------------------------|
| \mathbb{Q} | $\frac{81}{640}$ | $\frac{2119}{2560}$ | $\frac{1}{256}$ | $\frac{709}{3840}$ | $\frac{207}{640}$ |
| $\ln(\frac{4}{3})$ | $\frac{6909}{6400}$ | $\frac{123771}{51200}$ | $\frac{93951}{51200}$ | $-\frac{15791}{25600}$ | $-\frac{2007}{2048}$ |
| $\tilde{\Phi}_1(\frac{9}{16})$ | $\frac{134337}{102400}$ | $\frac{6603}{3200}$ | $\frac{345189}{409600}$ | $-\frac{14397}{102400}$ | $-\frac{111879}{81920}$ |
| $\tilde{\Phi}_1(\frac{3}{4})$ | $-\frac{285}{1024}$ | $-\frac{23493}{8192}$ | $-\frac{8469}{8192}$ | $-\frac{135}{4096}$ | $\frac{10125}{8192}$ |
| \mathbb{Q} | $-\frac{21}{80}$ | 0 | $\frac{297}{640}$ | $\frac{709}{3840}$ | $\frac{1209}{2560}$ |
| $\ln(\frac{4}{3})$ | $\frac{1437}{1600}$ | 0 | $\frac{64863}{51200}$ | $-\frac{15791}{25600}$ | $\frac{11277}{5120}$ |
| $\tilde{\Phi}_1(\frac{9}{16})$ | $-\frac{2967}{12800}$ | 0 | $\frac{245187}{409600}$ | $-\frac{14397}{102400}$ | $\frac{336609}{81920}$ |
| $\tilde{\Phi}_1(\frac{3}{4})$ | $\frac{57}{256}$ | 0 | $-\frac{5805}{8192}$ | $-\frac{135}{4096}$ | $-\frac{22761}{4096}$ |
| \mathbb{Q} | $\frac{7}{640}$ | $-\frac{2119}{2560}$ | $-\frac{931}{2560}$ | $-\frac{103}{768}$ | $-\frac{453}{640}$ |
| $\ln(\frac{4}{3})$ | $-\frac{1057}{6400}$ | $-\frac{123771}{51200}$ | $-\frac{14727}{12800}$ | $-\frac{1411}{1280}$ | $-\frac{24129}{10240}$ |
| $\tilde{\Phi}_1(\frac{9}{16})$ | $-\frac{79301}{102400}$ | $-\frac{6603}{3200}$ | $-\frac{599997}{409600}$ | $\frac{49509}{40960}$ | $-\frac{44049}{16384}$ |
| $\tilde{\Phi}_1(\frac{3}{4})$ | $\frac{1161}{1024}$ | $\frac{23493}{8192}$ | $\frac{2211}{1024}$ | $-\frac{171}{128}$ | $\frac{24927}{8192}$ |

Table 5. Coefficients of selected tensors and different structures for the first three terms on the right hand side of (4.2) for the d_A^{abcd} sector in the Landau gauge.

n -point vertex function where each of the external legs is then dressed by a propagator function. Contraction of leg i with its external momentum p_i kills the transverse degrees of freedom in leg i . Remaining is a longitudinal ghost self-energy which dresses leg i in a connected Green's function as a through-going longitudinal degree of freedom exiting at any leg j transversally. Hence the structure of the dressed Green's function is consistently maintained when replacing an external gluon leg by a longitudinal degree of freedom followed through the connected function in all possible ways. See, for example, Figure 8. At one loop for Γ^{ggg} and Γ^{gggg} this resulted in an extra graph in each case and their presence could be deduced by the systematic use of Hopf-algebraic and diagrammatic formalisms of [1, 3, 28, 29, 30, 37]. Indeed the approach in [37] was instrumental in gaining previous insights into the structure of gauge fixed QED and QCD, [31, 32]. The extra graphs in both identities involved the ghost self-energy appended to an external leg as expected and its absence would have invalidated each relation computationally. In the connected Green's function version of the Slavnov-Taylor identities such additional graphs are automatically incorporated. However in certain applications the 1PI version of the identities may be more applicable and our derivations and examples therefore crucially emphasize that one has to be careful in applying the correct relation. The fact that we check both our examples for non-exceptional momenta configurations, rather than nullifying an external leg as is carried out in some verifications, represents a robust check and circumvents any potential infrared issues.

| Entity | $\mathcal{P}_{(1)}^{c\bar{c}gg}$ | $\mathcal{P}_{(10)}^{c\bar{c}gg}$ | $\mathcal{P}_{(11)}^{c\bar{c}gg}$ | $\mathcal{P}_{(16)}^{c\bar{c}gg}$ | $\mathcal{P}_{(31)}^{c\bar{c}gg}$ |
|--------------------------------|----------------------------------|-----------------------------------|-----------------------------------|-----------------------------------|-----------------------------------|
| \mathbb{Q} | $-\frac{1}{8}$ | 0 | $\frac{267}{2560}$ | $\frac{301}{1280}$ | $\frac{45}{512}$ |
| $\ln(\frac{4}{3})$ | $\frac{29}{16}$ | 0 | $\frac{49953}{25600}$ | $-\frac{29901}{12800}$ | $-\frac{1161}{1024}$ |
| $\tilde{\Phi}_1(\frac{9}{16})$ | $-\frac{7}{8}$ | 0 | $-\frac{9621}{409600}$ | $\frac{189957}{204800}$ | $\frac{879}{16384}$ |
| $\tilde{\Phi}_1(\frac{3}{4})$ | $\frac{69}{64}$ | 0 | $\frac{1707}{4096}$ | $-\frac{2871}{2048}$ | $-\frac{5235}{4096}$ |

Table 6. Coefficients of selected tensors and different structures for the left hand side of (4.2) for the d_A^{abcd} sector in the Landau gauge.

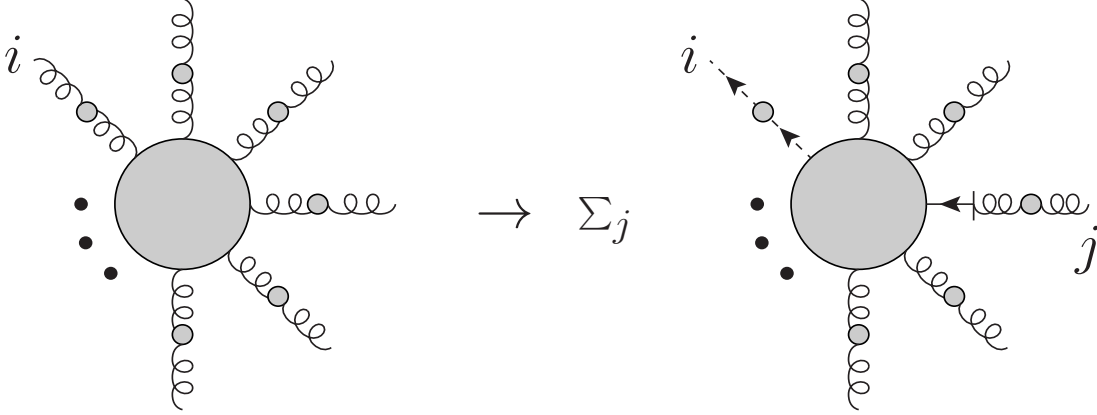


Figure 8: Self-consistent Slavnov-Taylor identity. A connected n -gluon vertex function with n dressed external gluon propagators when contracted at leg i becomes a dressed vertex for a connected vertex function with $n-2$ external gluons and one through-going ghost line, providing one external ghost propagator and one transversal external leg and $n-2$ further external dressed gluon propagators.

This is particularly the case for the 4-point function given the large number of colour and Lorentz tensors that are present in each of the contributing graphs.

In light of these there are several natural avenues to pursue. One obvious one is to first derive general relations for other gluon n -point functions as well as to extend our calculations to the two loop case. For the 3-point identity this would be the first place to start since the full off-shell vertex functions of QCD are known, [46]. So the necessary computational tools are in place to determine the two loop corrections to $\Gamma_{\mu\nu}^{g\bar{c}c}(p, q, r)$ that would be needed. This would also provide the forum to study the effect and relation the identities we have derived have on the renormalization of QCD in kinematical schemes such as the momentum subtraction one of [7, 8]. Equally at a practical level the current use of the Dyson-Schwinger methods to probe the infrared behaviour of 2-point and vertex functions in QCD, [12, 13, 14, 15, 16, 17, 18, 19, 20, 21, 22, 23, 24, 25, 26, 27], relies on relations between different n -point functions. Therefore constructing the identity for the 5-point gluon function, for instance, could provide a useful off-shell consistency check. Another direction that has been followed in recent years is to consider nonlinear gauges such as the Curci-Ferrari, [60], and maximal abelian gauges, [61, 62, 63]. From a structural point of view the former gauge would be the starting place to understand the subtleties of the nonlinear aspect of such gauges. The former gauge differs from the linear covariant gauge only in having an asymmetric ghost-gluon vertex as well as a quartic

ghost interaction. While the latter is a valid term in a renormalizable gauge theory, BRST symmetry excludes it in the linear covariant case. Therefore given the insights we have found here we aim to study some of these potential new directions in future work.

Acknowledgements. This work was carried out with the support of DFG Grant KR1401/5-1. The work of JAG was supported by a DFG Mercator Fellowship and he thanks the Mathematical Physics Group at Humboldt University, Berlin for hospitality. The figures were prepared with AXODRAW [64].

A Projection matrices.

In this appendix we record the projection matrices for the computation of $\Gamma_{\mu\nu}^{g\bar{c}c}(p, q, r)$ and $\Gamma_{\mu\nu\sigma}^{c\bar{c}gg\,abcd}(p, q, r, s)$ where the formalism was introduced earlier. For the former if we define the related projection matrix $\tilde{\mathcal{M}}^{g\bar{c}c}$ with a common factor removed by

$$\mathcal{M}^{g\bar{c}c} = \frac{1}{4[d-2]\Delta_G^2} \tilde{\mathcal{M}}^{g\bar{c}c} \quad (\text{A.1})$$

then the elements are

$$\begin{aligned} \tilde{\mathcal{M}}_{11}^{g\bar{c}c} &= 4[x^2 - 2xy - 2x + y^2 - 2y + 1]^2, & \tilde{\mathcal{M}}_{12}^{g\bar{c}c} &= -16[[y-1]^2 + x^2 - 2[y+1]x]y \\ \tilde{\mathcal{M}}_{13}^{g\bar{c}c} &= \tilde{\mathcal{M}}_{14}^{g\bar{c}c} = -8[x^2 - 2xy - 2x + y^2 - 2y + 1][x+y-1] \\ \tilde{\mathcal{M}}_{15}^{g\bar{c}c} &= -16[[y-1]^2 + x^2 - 2[y+1]x]x, & \tilde{\mathcal{M}}_{22}^{g\bar{c}c} &= 64[d-1]y^2 \\ \tilde{\mathcal{M}}_{23}^{g\bar{c}c} &= \tilde{\mathcal{M}}_{24}^{g\bar{c}c} = 32[d-1][x+y-1]y \\ \tilde{\mathcal{M}}_{25}^{g\bar{c}c} &= -16[2[x^2 - 2x + y^2 - 2y + 1] - [x+y-1]^2]d \\ \tilde{\mathcal{M}}_{33}^{g\bar{c}c} &= 16[[y-1]^2 + x^2 + 4dxy - 2[3y+1]x], & \tilde{\mathcal{M}}_{34}^{g\bar{c}c} &= 16[d-1][x+y-1]^2 \\ \tilde{\mathcal{M}}_{35}^{g\bar{c}c} &= 32[y-1+x][d-1]x, & \tilde{\mathcal{M}}_{44}^{g\bar{c}c} &= 16[[y-1]^2 + x^2 + 4dxy - 2[3y+1]x] \\ \tilde{\mathcal{M}}_{45}^{g\bar{c}c} &= 32[y-1+x][d-1]x, & \tilde{\mathcal{M}}_{55}^{g\bar{c}c} &= 64[d-1]x^2. \end{aligned} \quad (\text{A.2})$$

As $\mathcal{M}^{g\bar{c}c}$ is by construction a symmetric matrix we have only provided the upper triangle entries.

For the 4-point ghost-gluon function there are 36 Lorentz tensors in the projection basis for each orientation. They are

$$\begin{aligned} \mathcal{P}_{(1)\mu\nu\sigma}^{c\bar{c}gg} &= \eta_{\mu\nu}p_\sigma, & \mathcal{P}_{(2)\mu\nu\sigma}^{c\bar{c}gg} &= \eta_{\mu\nu}q_\sigma, & \mathcal{P}_{(3)\mu\nu\sigma}^{c\bar{c}gg} &= \eta_{\mu\nu}r_\sigma, & \mathcal{P}_{(4)\mu\nu\sigma}^{c\bar{c}gg} &= \eta_{\mu\sigma}p_\nu \\ \mathcal{P}_{(5)\mu\nu\sigma}^{c\bar{c}gg} &= \eta_{\mu\sigma}q_\nu, & \mathcal{P}_{(6)\mu\nu\sigma}^{c\bar{c}gg} &= \eta_{\mu\sigma}r_\nu, & \mathcal{P}_{(7)\mu\nu\sigma}^{c\bar{c}gg} &= \eta_{\nu\sigma}p_\mu, & \mathcal{P}_{(8)\mu\nu\sigma}^{c\bar{c}gg} &= \eta_{\nu\sigma}q_\mu \\ \mathcal{P}_{(9)\mu\nu\sigma}^{c\bar{c}gg} &= \eta_{\nu\sigma}r_\mu, & \mathcal{P}_{(10)\mu\nu\sigma}^{c\bar{c}gg} &= \frac{p_\mu p_\nu p_\sigma}{\mu^2}, & \mathcal{P}_{(11)\mu\nu\sigma}^{c\bar{c}gg} &= \frac{p_\mu p_\nu q_\sigma}{\mu^2}, & \mathcal{P}_{(12)\mu\nu\sigma}^{c\bar{c}gg} &= \frac{p_\mu p_\nu r_\sigma}{\mu^2} \\ \mathcal{P}_{(13)\mu\nu\sigma}^{c\bar{c}gg} &= \frac{p_\mu p_\sigma q_\nu}{\mu^2}, & \mathcal{P}_{(14)\mu\nu\sigma}^{c\bar{c}gg} &= \frac{p_\mu p_\sigma r_\nu}{\mu^2}, & \mathcal{P}_{(15)\mu\nu\sigma}^{c\bar{c}gg} &= \frac{p_\mu q_\nu q_\sigma}{\mu^2}, & \mathcal{P}_{(16)\mu\nu\sigma}^{c\bar{c}gg} &= \frac{p_\mu q_\nu r_\sigma}{\mu^2} \\ \mathcal{P}_{(17)\mu\nu\sigma}^{c\bar{c}gg} &= \frac{p_\mu q_\sigma r_\nu}{\mu^2}, & \mathcal{P}_{(18)\mu\nu\sigma}^{c\bar{c}gg} &= \frac{p_\mu r_\nu r_\sigma}{\mu^2}, & \mathcal{P}_{(19)\mu\nu\sigma}^{c\bar{c}gg} &= \frac{p_\nu p_\sigma q_\mu}{\mu^2}, & \mathcal{P}_{(20)\mu\nu\sigma}^{c\bar{c}gg} &= \frac{p_\nu p_\sigma r_\mu}{\mu^2} \\ \mathcal{P}_{(21)\mu\nu\sigma}^{c\bar{c}gg} &= \frac{p_\nu q_\mu q_\sigma}{\mu^2}, & \mathcal{P}_{(22)\mu\nu\sigma}^{c\bar{c}gg} &= \frac{p_\nu q_\mu r_\sigma}{\mu^2}, & \mathcal{P}_{(23)\mu\nu\sigma}^{c\bar{c}gg} &= \frac{p_\nu q_\sigma r_\mu}{\mu^2}, & \mathcal{P}_{(24)\mu\nu\sigma}^{c\bar{c}gg} &= \frac{p_\nu r_\mu r_\sigma}{\mu^2} \\ \mathcal{P}_{(25)\mu\nu\sigma}^{c\bar{c}gg} &= \frac{p_\sigma q_\mu q_\nu}{\mu^2}, & \mathcal{P}_{(26)\mu\nu\sigma}^{c\bar{c}gg} &= \frac{p_\sigma q_\mu r_\nu}{\mu^2}, & \mathcal{P}_{(27)\mu\nu\sigma}^{c\bar{c}gg} &= \frac{p_\sigma q_\nu r_\mu}{\mu^2}, & \mathcal{P}_{(28)\mu\nu\sigma}^{c\bar{c}gg} &= \frac{p_\sigma r_\mu r_\nu}{\mu^2} \\ \mathcal{P}_{(29)\mu\nu\sigma}^{c\bar{c}gg} &= \frac{q_\mu q_\nu q_\sigma}{\mu^2}, & \mathcal{P}_{(30)\mu\nu\sigma}^{c\bar{c}gg} &= \frac{q_\mu q_\nu r_\sigma}{\mu^2}, & \mathcal{P}_{(31)\mu\nu\sigma}^{c\bar{c}gg} &= \frac{q_\mu q_\sigma r_\nu}{\mu^2}, & \mathcal{P}_{(32)\mu\nu\sigma}^{c\bar{c}gg} &= \frac{q_\mu r_\nu r_\sigma}{\mu^2} \end{aligned}$$

$$\begin{aligned}
\mathcal{P}_{(33)\mu\nu\sigma}^{c\bar{c}gg} &= \frac{q_\nu q_\sigma r_\mu}{\mu^2}, \quad \mathcal{P}_{(34)\mu\nu\sigma}^{c\bar{c}gg} = \frac{q_\nu r_\mu r_\sigma}{\mu^2}, \quad \mathcal{P}_{(35)\mu\nu\sigma}^{c\bar{c}gg} = \frac{q_\sigma r_\mu r_\nu}{\mu^2} \\
\mathcal{P}_{(36)\mu\nu\sigma}^{c\bar{c}gg} &= \frac{r_\mu r_\nu r_\sigma}{\mu^2}
\end{aligned} \tag{A.3}$$

where we have suppressed the argument. The symmetric projection matrix is constructed in the same way as for the 3-point case. First defining the related matrix $\tilde{\mathcal{M}}^{c\bar{c}gg}$ by

$$\mathcal{M}^{c\bar{c}gg} = \frac{1}{64[d-3]} \tilde{\mathcal{M}}^{c\bar{c}gg} \tag{A.4}$$

then the upper triangle elements are

$$\begin{aligned}
\tilde{\mathcal{M}}_{1,1}^{c\bar{c}gg} &= -96, \quad \tilde{\mathcal{M}}_{1,2}^{c\bar{c}gg} = \tilde{\mathcal{M}}_{1,3}^{c\bar{c}gg} = -48 \\
\tilde{\mathcal{M}}_{1,4}^{c\bar{c}gg} &= \tilde{\mathcal{M}}_{1,5}^{c\bar{c}gg} = \tilde{\mathcal{M}}_{1,6}^{c\bar{c}gg} = \tilde{\mathcal{M}}_{1,7}^{c\bar{c}gg} = \tilde{\mathcal{M}}_{1,8}^{c\bar{c}gg} = \tilde{\mathcal{M}}_{1,9}^{c\bar{c}gg} = 0, \quad \tilde{\mathcal{M}}_{1,10}^{c\bar{c}gg} = -144 \\
\tilde{\mathcal{M}}_{1,11}^{c\bar{c}gg} &= \tilde{\mathcal{M}}_{1,12}^{c\bar{c}gg} = \tilde{\mathcal{M}}_{1,13}^{c\bar{c}gg} = \tilde{\mathcal{M}}_{1,14}^{c\bar{c}gg} = -72 \\
\tilde{\mathcal{M}}_{1,15}^{c\bar{c}gg} &= \tilde{\mathcal{M}}_{1,16}^{c\bar{c}gg} = \tilde{\mathcal{M}}_{1,17}^{c\bar{c}gg} = \tilde{\mathcal{M}}_{1,18}^{c\bar{c}gg} = -36, \quad \tilde{\mathcal{M}}_{1,19}^{c\bar{c}gg} = \tilde{\mathcal{M}}_{1,20}^{c\bar{c}gg} = -72 \\
\tilde{\mathcal{M}}_{1,21}^{c\bar{c}gg} &= \tilde{\mathcal{M}}_{1,22}^{c\bar{c}gg} = \tilde{\mathcal{M}}_{1,23}^{c\bar{c}gg} = \tilde{\mathcal{M}}_{1,24}^{c\bar{c}gg} = -36, \quad \tilde{\mathcal{M}}_{1,25}^{c\bar{c}gg} = -144 \\
\tilde{\mathcal{M}}_{1,26}^{c\bar{c}gg} &= \tilde{\mathcal{M}}_{1,27}^{c\bar{c}gg} = -72, \quad \tilde{\mathcal{M}}_{1,28}^{c\bar{c}gg} = -144, \quad \tilde{\mathcal{M}}_{1,29}^{c\bar{c}gg} = \tilde{\mathcal{M}}_{1,30}^{c\bar{c}gg} = -72 \\
\tilde{\mathcal{M}}_{1,31}^{c\bar{c}gg} &= \tilde{\mathcal{M}}_{1,32}^{c\bar{c}gg} = \tilde{\mathcal{M}}_{1,33}^{c\bar{c}gg} = \tilde{\mathcal{M}}_{1,34}^{c\bar{c}gg} = -36, \quad \tilde{\mathcal{M}}_{1,35}^{c\bar{c}gg} = \tilde{\mathcal{M}}_{1,36}^{c\bar{c}gg} = -72 \\
\tilde{\mathcal{M}}_{2,2}^{c\bar{c}gg} &= -96, \quad \tilde{\mathcal{M}}_{2,3}^{c\bar{c}gg} = -48 \\
\tilde{\mathcal{M}}_{2,4}^{c\bar{c}gg} &= \tilde{\mathcal{M}}_{2,5}^{c\bar{c}gg} = \tilde{\mathcal{M}}_{2,6}^{c\bar{c}gg} = \tilde{\mathcal{M}}_{2,7}^{c\bar{c}gg} = \tilde{\mathcal{M}}_{2,8}^{c\bar{c}gg} = \tilde{\mathcal{M}}_{2,9}^{c\bar{c}gg} = 0, \quad \tilde{\mathcal{M}}_{2,10}^{c\bar{c}gg} = -72 \\
\tilde{\mathcal{M}}_{2,11}^{c\bar{c}gg} &= -144, \quad \tilde{\mathcal{M}}_{2,12}^{c\bar{c}gg} = -72, \quad \tilde{\mathcal{M}}_{2,13}^{c\bar{c}gg} = \tilde{\mathcal{M}}_{2,14}^{c\bar{c}gg} = -36, \quad \tilde{\mathcal{M}}_{2,15}^{c\bar{c}gg} = -72 \\
\tilde{\mathcal{M}}_{2,16}^{c\bar{c}gg} &= -36, \quad \tilde{\mathcal{M}}_{2,17}^{c\bar{c}gg} = -72, \quad \tilde{\mathcal{M}}_{2,18}^{c\bar{c}gg} = \tilde{\mathcal{M}}_{2,19}^{c\bar{c}gg} = \tilde{\mathcal{M}}_{2,20}^{c\bar{c}gg} = -36 \\
\tilde{\mathcal{M}}_{2,21}^{c\bar{c}gg} &= -72, \quad \tilde{\mathcal{M}}_{2,22}^{c\bar{c}gg} = -36, \quad \tilde{\mathcal{M}}_{2,23}^{c\bar{c}gg} = -72, \quad \tilde{\mathcal{M}}_{2,24}^{c\bar{c}gg} = -36 \\
\tilde{\mathcal{M}}_{2,25}^{c\bar{c}gg} &= -72, \quad \tilde{\mathcal{M}}_{2,26}^{c\bar{c}gg} = \tilde{\mathcal{M}}_{2,27}^{c\bar{c}gg} = -36, \quad \tilde{\mathcal{M}}_{2,28}^{c\bar{c}gg} = -72 \\
\tilde{\mathcal{M}}_{2,29}^{c\bar{c}gg} &= -144, \quad \tilde{\mathcal{M}}_{2,30}^{c\bar{c}gg} = \tilde{\mathcal{M}}_{2,31}^{c\bar{c}gg} = -72, \quad \tilde{\mathcal{M}}_{2,32}^{c\bar{c}gg} = -36, \quad \tilde{\mathcal{M}}_{2,33}^{c\bar{c}gg} = -72 \\
\tilde{\mathcal{M}}_{2,34}^{c\bar{c}gg} &= -36, \quad \tilde{\mathcal{M}}_{2,35}^{c\bar{c}gg} = -144, \quad \tilde{\mathcal{M}}_{2,36}^{c\bar{c}gg} = -72, \quad \tilde{\mathcal{M}}_{3,3}^{c\bar{c}gg} = -96 \\
\tilde{\mathcal{M}}_{3,4}^{c\bar{c}gg} &= \tilde{\mathcal{M}}_{3,5}^{c\bar{c}gg} = \tilde{\mathcal{M}}_{3,6}^{c\bar{c}gg} = \tilde{\mathcal{M}}_{3,7}^{c\bar{c}gg} = \tilde{\mathcal{M}}_{3,8}^{c\bar{c}gg} = \tilde{\mathcal{M}}_{3,9}^{c\bar{c}gg} = 0 \\
\tilde{\mathcal{M}}_{3,10}^{c\bar{c}gg} &= \tilde{\mathcal{M}}_{3,11}^{c\bar{c}gg} = -72, \quad \tilde{\mathcal{M}}_{3,12}^{c\bar{c}gg} = -144 \\
\tilde{\mathcal{M}}_{3,13}^{c\bar{c}gg} &= \tilde{\mathcal{M}}_{3,14}^{c\bar{c}gg} = \tilde{\mathcal{M}}_{3,15}^{c\bar{c}gg} = -36, \quad \tilde{\mathcal{M}}_{3,16}^{c\bar{c}gg} = -72, \quad \tilde{\mathcal{M}}_{3,17}^{c\bar{c}gg} = -36 \\
\tilde{\mathcal{M}}_{3,18}^{c\bar{c}gg} &= -72, \quad \tilde{\mathcal{M}}_{3,19}^{c\bar{c}gg} = \tilde{\mathcal{M}}_{3,20}^{c\bar{c}gg} = \tilde{\mathcal{M}}_{3,21}^{c\bar{c}gg} = -36, \quad \tilde{\mathcal{M}}_{3,22}^{c\bar{c}gg} = -72 \\
\tilde{\mathcal{M}}_{3,23}^{c\bar{c}gg} &= -36, \quad \tilde{\mathcal{M}}_{3,24}^{c\bar{c}gg} = \tilde{\mathcal{M}}_{3,25}^{c\bar{c}gg} = -72, \quad \tilde{\mathcal{M}}_{3,26}^{c\bar{c}gg} = \tilde{\mathcal{M}}_{3,27}^{c\bar{c}gg} = -36 \\
\tilde{\mathcal{M}}_{3,28}^{c\bar{c}gg} &= \tilde{\mathcal{M}}_{3,29}^{c\bar{c}gg} = -72, \quad \tilde{\mathcal{M}}_{3,30}^{c\bar{c}gg} = -144, \quad \tilde{\mathcal{M}}_{3,31}^{c\bar{c}gg} = -36 \\
\tilde{\mathcal{M}}_{3,32}^{c\bar{c}gg} &= -72, \quad \tilde{\mathcal{M}}_{3,33}^{c\bar{c}gg} = -36, \quad \tilde{\mathcal{M}}_{3,34}^{c\bar{c}gg} = \tilde{\mathcal{M}}_{3,35}^{c\bar{c}gg} = -72 \\
\tilde{\mathcal{M}}_{3,36}^{c\bar{c}gg} &= -144, \quad \tilde{\mathcal{M}}_{4,4}^{c\bar{c}gg} = -96, \quad \tilde{\mathcal{M}}_{4,5}^{c\bar{c}gg} = \tilde{\mathcal{M}}_{4,6}^{c\bar{c}gg} = -48 \\
\tilde{\mathcal{M}}_{4,7}^{c\bar{c}gg} &= \tilde{\mathcal{M}}_{4,8}^{c\bar{c}gg} = \tilde{\mathcal{M}}_{4,9}^{c\bar{c}gg} = 0, \quad \tilde{\mathcal{M}}_{4,10}^{c\bar{c}gg} = -144 \\
\tilde{\mathcal{M}}_{4,11}^{c\bar{c}gg} &= \tilde{\mathcal{M}}_{4,12}^{c\bar{c}gg} = \tilde{\mathcal{M}}_{4,13}^{c\bar{c}gg} = \tilde{\mathcal{M}}_{4,14}^{c\bar{c}gg} = -72 \\
\tilde{\mathcal{M}}_{4,15}^{c\bar{c}gg} &= \tilde{\mathcal{M}}_{4,16}^{c\bar{c}gg} = \tilde{\mathcal{M}}_{4,17}^{c\bar{c}gg} = \tilde{\mathcal{M}}_{4,18}^{c\bar{c}gg} = -36 \\
\tilde{\mathcal{M}}_{4,19}^{c\bar{c}gg} &= \tilde{\mathcal{M}}_{4,20}^{c\bar{c}gg} = -72, \quad \tilde{\mathcal{M}}_{4,21}^{c\bar{c}gg} = -144, \quad \tilde{\mathcal{M}}_{4,22}^{c\bar{c}gg} = \tilde{\mathcal{M}}_{4,23}^{c\bar{c}gg} = -72 \\
\tilde{\mathcal{M}}_{4,24}^{c\bar{c}gg} &= -144, \quad \tilde{\mathcal{M}}_{4,25}^{c\bar{c}gg} = \tilde{\mathcal{M}}_{4,26}^{c\bar{c}gg} = \tilde{\mathcal{M}}_{4,27}^{c\bar{c}gg} = \tilde{\mathcal{M}}_{4,28}^{c\bar{c}gg} = -36, \quad \tilde{\mathcal{M}}_{4,29}^{c\bar{c}gg} = -72 \\
\tilde{\mathcal{M}}_{4,30}^{c\bar{c}gg} &= -36, \quad \tilde{\mathcal{M}}_{4,31}^{c\bar{c}gg} = -72, \quad \tilde{\mathcal{M}}_{4,32}^{c\bar{c}gg} = \tilde{\mathcal{M}}_{4,33}^{c\bar{c}gg} = -36, \quad \tilde{\mathcal{M}}_{4,34}^{c\bar{c}gg} = -72
\end{aligned}$$

$$\begin{aligned}
\tilde{\mathcal{M}}_{15,32}^{\bar{c}cgg} &= -27[d+3] , \tilde{\mathcal{M}}_{15,33}^{\bar{c}cgg} = -108[d-1] , \tilde{\mathcal{M}}_{15,34}^{\bar{c}cgg} = \tilde{\mathcal{M}}_{15,35}^{\bar{c}cgg} = -27[2d+1] \\
\tilde{\mathcal{M}}_{15,36}^{\bar{c}cgg} &= -27[d+5] , \tilde{\mathcal{M}}_{16,16}^{\bar{c}cgg} = -54[4d-9] , \tilde{\mathcal{M}}_{16,17}^{\bar{c}cgg} = -54[d-1] \\
\tilde{\mathcal{M}}_{16,18}^{\bar{c}cgg} &= -27[4d-5] , \tilde{\mathcal{M}}_{16,19}^{\bar{c}cgg} = \tilde{\mathcal{M}}_{16,20}^{\bar{c}cgg} = \tilde{\mathcal{M}}_{16,21}^{\bar{c}cgg} = -27[d+1] \\
\tilde{\mathcal{M}}_{16,22}^{\bar{c}cgg} &= -54[d-1] , \tilde{\mathcal{M}}_{16,23}^{\bar{c}cgg} = -27d , \tilde{\mathcal{M}}_{16,24}^{\bar{c}cgg} = \tilde{\mathcal{M}}_{16,25}^{\bar{c}cgg} = -27[2d-1] \\
\tilde{\mathcal{M}}_{16,26}^{\bar{c}cgg} &= -27d , \tilde{\mathcal{M}}_{16,27}^{\bar{c}cgg} = -54[d-1] , \tilde{\mathcal{M}}_{16,28}^{\bar{c}cgg} = -27[d+1] \\
\tilde{\mathcal{M}}_{16,29}^{\bar{c}cgg} &= -54[d+1] , \tilde{\mathcal{M}}_{16,30}^{\bar{c}cgg} = -27[4d-5] , \tilde{\mathcal{M}}_{16,31}^{\bar{c}cgg} = -27[d+1] \\
\tilde{\mathcal{M}}_{16,32}^{\bar{c}cgg} &= -27[2d-1] , \tilde{\mathcal{M}}_{16,33}^{\bar{c}cgg} = -27[2d-1] , \tilde{\mathcal{M}}_{16,34}^{\bar{c}cgg} = -27[4d-5] \\
\tilde{\mathcal{M}}_{16,35}^{\bar{c}cgg} &= -27[d+1] , \tilde{\mathcal{M}}_{16,36}^{\bar{c}cgg} = -54[d+1] , \tilde{\mathcal{M}}_{17,17}^{\bar{c}cgg} = -54[4d-9] \\
\tilde{\mathcal{M}}_{17,18}^{\bar{c}cgg} &= -27[4d-5] , \tilde{\mathcal{M}}_{17,19}^{\bar{c}cgg} = \tilde{\mathcal{M}}_{17,20}^{\bar{c}cgg} = -27[d+1] , \tilde{\mathcal{M}}_{17,21}^{\bar{c}cgg} = -27[2d-1] \\
\tilde{\mathcal{M}}_{17,22}^{\bar{c}cgg} &= -27d , \tilde{\mathcal{M}}_{17,23}^{\bar{c}cgg} = -54[d-1] , \tilde{\mathcal{M}}_{17,24}^{\bar{c}cgg} = \tilde{\mathcal{M}}_{17,25}^{\bar{c}cgg} = -27[d+1] \\
\tilde{\mathcal{M}}_{17,26}^{\bar{c}cgg} &= -54[d-1] , \tilde{\mathcal{M}}_{17,27}^{\bar{c}cgg} = -27d , \tilde{\mathcal{M}}_{17,28}^{\bar{c}cgg} = -27[2d-1] \\
\tilde{\mathcal{M}}_{17,29}^{\bar{c}cgg} &= -54[d+1] , \tilde{\mathcal{M}}_{17,30}^{\bar{c}cgg} = -27[d+1] , \tilde{\mathcal{M}}_{17,31}^{\bar{c}cgg} = -27[4d-5] \\
\tilde{\mathcal{M}}_{17,32}^{\bar{c}cgg} &= \tilde{\mathcal{M}}_{17,33}^{\bar{c}cgg} = -27[2d-1] , \tilde{\mathcal{M}}_{17,34}^{\bar{c}cgg} = -27[d+1] \\
\tilde{\mathcal{M}}_{17,35}^{\bar{c}cgg} &= -27[4d-5] , \tilde{\mathcal{M}}_{17,36}^{\bar{c}cgg} = -54[d+1] , \tilde{\mathcal{M}}_{18,18}^{\bar{c}cgg} = -108[2d-3] \\
\tilde{\mathcal{M}}_{18,19}^{\bar{c}cgg} &= \tilde{\mathcal{M}}_{18,20}^{\bar{c}cgg} = -27[d+3] , \tilde{\mathcal{M}}_{18,21}^{\bar{c}cgg} = -27[d+2] , \tilde{\mathcal{M}}_{18,22}^{\bar{c}cgg} = -27[2d-1] \\
\tilde{\mathcal{M}}_{18,23}^{\bar{c}cgg} &= -27[d+1] , \tilde{\mathcal{M}}_{18,24}^{\bar{c}cgg} = -54d , \tilde{\mathcal{M}}_{18,25}^{\bar{c}cgg} = -27[d+2] \\
\tilde{\mathcal{M}}_{18,26}^{\bar{c}cgg} &= -27[2d-1] , \tilde{\mathcal{M}}_{18,27}^{\bar{c}cgg} = -27[d+1] , \tilde{\mathcal{M}}_{18,28}^{\bar{c}cgg} = -54d \\
\tilde{\mathcal{M}}_{18,29}^{\bar{c}cgg} &= -27[d+5] , \tilde{\mathcal{M}}_{18,30}^{\bar{c}cgg} = \tilde{\mathcal{M}}_{18,31}^{\bar{c}cgg} = -27[2d+1] , \tilde{\mathcal{M}}_{18,32}^{\bar{c}cgg} = -108[d-1] \\
\tilde{\mathcal{M}}_{18,33}^{\bar{c}cgg} &= -27[d+3] , \tilde{\mathcal{M}}_{18,34}^{\bar{c}cgg} = \tilde{\mathcal{M}}_{18,35}^{\bar{c}cgg} = -54d , \tilde{\mathcal{M}}_{18,36}^{\bar{c}cgg} = -108d \\
\tilde{\mathcal{M}}_{19,19}^{\bar{c}cgg} &= -108[2d-3] , \tilde{\mathcal{M}}_{19,20}^{\bar{c}cgg} = -108[d-1] , \tilde{\mathcal{M}}_{19,21}^{\bar{c}cgg} = -27[4d-3] \\
\tilde{\mathcal{M}}_{19,22}^{\bar{c}cgg} &= -27[4d-5] , \tilde{\mathcal{M}}_{19,23}^{\bar{c}cgg} = -27[2d-1] , \tilde{\mathcal{M}}_{19,24}^{\bar{c}cgg} = -27[2d+1] \\
\tilde{\mathcal{M}}_{19,25}^{\bar{c}cgg} &= -27[4d-3] , \tilde{\mathcal{M}}_{19,26}^{\bar{c}cgg} = -27[4d-5] , \tilde{\mathcal{M}}_{19,27}^{\bar{c}cgg} = -27[2d-1] \\
\tilde{\mathcal{M}}_{19,28}^{\bar{c}cgg} &= -27[2d+1] , \tilde{\mathcal{M}}_{19,29}^{\bar{c}cgg} = -54[d+3] , \tilde{\mathcal{M}}_{19,30}^{\bar{c}cgg} = -27[2d+1] \\
\tilde{\mathcal{M}}_{19,31}^{\bar{c}cgg} &= -27[2d+1] , \tilde{\mathcal{M}}_{19,32}^{\bar{c}cgg} = -54[d+2] , \tilde{\mathcal{M}}_{19,33}^{\bar{c}cgg} = -27[d+3] \\
\tilde{\mathcal{M}}_{19,34}^{\bar{c}cgg} &= \tilde{\mathcal{M}}_{19,35}^{\bar{c}cgg} = -27[d+2] , \tilde{\mathcal{M}}_{19,36}^{\bar{c}cgg} = -27[d+5] , \tilde{\mathcal{M}}_{20,20}^{\bar{c}cgg} = -108[2d-3] \\
\tilde{\mathcal{M}}_{20,21}^{\bar{c}cgg} &= -27[2d+1] , \tilde{\mathcal{M}}_{20,22}^{\bar{c}cgg} = -27[2d-1] , \tilde{\mathcal{M}}_{20,23}^{\bar{c}cgg} = -27[4d-5] \\
\tilde{\mathcal{M}}_{20,24}^{\bar{c}cgg} &= -27[4d-3] , \tilde{\mathcal{M}}_{20,25}^{\bar{c}cgg} = -27[2d+1] , \tilde{\mathcal{M}}_{20,26}^{\bar{c}cgg} = -27[2d-1] \\
\tilde{\mathcal{M}}_{20,27}^{\bar{c}cgg} &= -27[4d-5] , \tilde{\mathcal{M}}_{20,28}^{\bar{c}cgg} = -27[4d-3] , \tilde{\mathcal{M}}_{20,29}^{\bar{c}cgg} = -27[d+5] \\
\tilde{\mathcal{M}}_{20,30}^{\bar{c}cgg} &= \tilde{\mathcal{M}}_{20,31}^{\bar{c}cgg} = -27[d+2] , \tilde{\mathcal{M}}_{20,32}^{\bar{c}cgg} = -27[d+3] , \tilde{\mathcal{M}}_{20,33}^{\bar{c}cgg} = -54[d+2] \\
\tilde{\mathcal{M}}_{20,34}^{\bar{c}cgg} &= \tilde{\mathcal{M}}_{20,35}^{\bar{c}cgg} = -27[2d+1] , \tilde{\mathcal{M}}_{20,36}^{\bar{c}cgg} = -54[d+3] \\
\tilde{\mathcal{M}}_{21,21}^{\bar{c}cgg} &= -108[2d-3] , \tilde{\mathcal{M}}_{21,22}^{\bar{c}cgg} = \tilde{\mathcal{M}}_{21,23}^{\bar{c}cgg} = -27[4d-5] \\
\tilde{\mathcal{M}}_{21,24}^{\bar{c}cgg} &= -54[d+2] , \tilde{\mathcal{M}}_{21,25}^{\bar{c}cgg} = -54d , \tilde{\mathcal{M}}_{21,26}^{\bar{c}cgg} = -27[2d-1] \\
\tilde{\mathcal{M}}_{21,27}^{\bar{c}cgg} &= -27[d+1] , \tilde{\mathcal{M}}_{21,28}^{\bar{c}cgg} = -27[d+2] , \tilde{\mathcal{M}}_{21,29}^{\bar{c}cgg} = -108d \\
\tilde{\mathcal{M}}_{21,30}^{\bar{c}cgg} &= -54d , \tilde{\mathcal{M}}_{21,31}^{\bar{c}cgg} = -108[d-1] , \tilde{\mathcal{M}}_{21,32}^{\bar{c}cgg} = -27[2d+1] \\
\tilde{\mathcal{M}}_{21,33}^{\bar{c}cgg} &= -54d , \tilde{\mathcal{M}}_{21,34}^{\bar{c}cgg} = -27[d+3] , \tilde{\mathcal{M}}_{21,35}^{\bar{c}cgg} = -27[2d+1] \\
\tilde{\mathcal{M}}_{21,36}^{\bar{c}cgg} &= -27[d+5] , \tilde{\mathcal{M}}_{22,22}^{\bar{c}cgg} = -54[4d-9] , \tilde{\mathcal{M}}_{22,23}^{\bar{c}cgg} = -54[d-1]
\end{aligned}$$

$$\begin{aligned}
\tilde{\mathcal{M}}_{22,24}^{\bar{c}cgg} &= -27[4d-5] , \tilde{\mathcal{M}}_{22,25}^{\bar{c}cgg} = -27[2d-1] , \tilde{\mathcal{M}}_{22,26}^{\bar{c}cgg} = -54[d-1] \\
\tilde{\mathcal{M}}_{22,27}^{\bar{c}cgg} &= -27d , \tilde{\mathcal{M}}_{22,28}^{\bar{c}cgg} = -27[d+1] , \tilde{\mathcal{M}}_{22,29}^{\bar{c}cgg} = -54[d+1] \\
\tilde{\mathcal{M}}_{22,30}^{\bar{c}cgg} &= -27[4d-5] , \tilde{\mathcal{M}}_{22,31}^{\bar{c}cgg} = -27[2d-1] , \tilde{\mathcal{M}}_{22,32}^{\bar{c}cgg} = -27[4d-5] \\
\tilde{\mathcal{M}}_{22,33}^{\bar{c}cgg} &= -27[d+1] , \tilde{\mathcal{M}}_{22,34}^{\bar{c}cgg} = -27[2d-1] , \tilde{\mathcal{M}}_{22,35}^{\bar{c}cgg} = -27[d+1] \\
\tilde{\mathcal{M}}_{22,36}^{\bar{c}cgg} &= -54[d+1] , \tilde{\mathcal{M}}_{23,23}^{\bar{c}cgg} = -54[4d-9] , \tilde{\mathcal{M}}_{23,24}^{\bar{c}cgg} = -27[4d-5] \\
\tilde{\mathcal{M}}_{23,25}^{\bar{c}cgg} &= -27[d+1] , \tilde{\mathcal{M}}_{23,26}^{\bar{c}cgg} = -27d , \tilde{\mathcal{M}}_{23,27}^{\bar{c}cgg} = -54[d-1] \\
\tilde{\mathcal{M}}_{23,28}^{\bar{c}cgg} &= -27[2d-1] , \tilde{\mathcal{M}}_{23,29}^{\bar{c}cgg} = -54[d+1] , \tilde{\mathcal{M}}_{23,30}^{\bar{c}cgg} = -27[d+1] \\
\tilde{\mathcal{M}}_{23,31}^{\bar{c}cgg} &= -27[2d-1] , \tilde{\mathcal{M}}_{23,32}^{\bar{c}cgg} = -27[d+1] , \tilde{\mathcal{M}}_{23,33}^{\bar{c}cgg} = -27[4d-5] \\
\tilde{\mathcal{M}}_{23,34}^{\bar{c}cgg} &= -27[2d-1] , \tilde{\mathcal{M}}_{23,35}^{\bar{c}cgg} = -27[4d-5] , \tilde{\mathcal{M}}_{23,36}^{\bar{c}cgg} = -54[d+1] \\
\tilde{\mathcal{M}}_{24,24}^{\bar{c}cgg} &= -108[2d-3] , \tilde{\mathcal{M}}_{24,25}^{\bar{c}cgg} = -27[d+2] , \tilde{\mathcal{M}}_{24,26}^{\bar{c}cgg} = -27[d+1] \\
\tilde{\mathcal{M}}_{24,27}^{\bar{c}cgg} &= -27[2d-1] , \tilde{\mathcal{M}}_{24,28}^{\bar{c}cgg} = -54d , \tilde{\mathcal{M}}_{24,29}^{\bar{c}cgg} = -27[d+5] \\
\tilde{\mathcal{M}}_{24,30}^{\bar{c}cgg} &= -27[2d+1] , \tilde{\mathcal{M}}_{24,31}^{\bar{c}cgg} = -27[d+3] , \tilde{\mathcal{M}}_{24,32}^{\bar{c}cgg} = -54d \\
\tilde{\mathcal{M}}_{24,33}^{\bar{c}cgg} &= -27[2d+1] , \tilde{\mathcal{M}}_{24,34}^{\bar{c}cgg} = -108[d-1] , \tilde{\mathcal{M}}_{24,35}^{\bar{c}cgg} = -54d \\
\tilde{\mathcal{M}}_{24,36}^{\bar{c}cgg} &= -108d , \tilde{\mathcal{M}}_{25,25}^{\bar{c}cgg} = -108[2d-3] , \tilde{\mathcal{M}}_{25,26}^{\bar{c}cgg} = -27[4d-5] \\
\tilde{\mathcal{M}}_{25,27}^{\bar{c}cgg} &= -27[4d-5] , \tilde{\mathcal{M}}_{25,28}^{\bar{c}cgg} = -54[d+2] , \tilde{\mathcal{M}}_{25,29}^{\bar{c}cgg} = -108d \\
\tilde{\mathcal{M}}_{25,30}^{\bar{c}cgg} &= -108[d-1] , \tilde{\mathcal{M}}_{25,31}^{\bar{c}cgg} = -54d , \tilde{\mathcal{M}}_{25,32}^{\bar{c}cgg} = -27[2d+1] \\
\tilde{\mathcal{M}}_{25,33}^{\bar{c}cgg} &= -54d , \tilde{\mathcal{M}}_{25,34}^{\bar{c}cgg} = -27[2d+1] , \tilde{\mathcal{M}}_{25,35}^{\bar{c}cgg} = -27[d+3] \\
\tilde{\mathcal{M}}_{25,36}^{\bar{c}cgg} &= -27[d+5] , \tilde{\mathcal{M}}_{26,26}^{\bar{c}cgg} = -54[4d-9] , \tilde{\mathcal{M}}_{26,27}^{\bar{c}cgg} = -54[d-1] \\
\tilde{\mathcal{M}}_{26,28}^{\bar{c}cgg} &= -27[4d-5] , \tilde{\mathcal{M}}_{26,29}^{\bar{c}cgg} = -54[d+1] , \tilde{\mathcal{M}}_{26,30}^{\bar{c}cgg} = -27[2d-1] \\
\tilde{\mathcal{M}}_{26,31}^{\bar{c}cgg} &= \tilde{\mathcal{M}}_{26,32}^{\bar{c}cgg} = -27[4d-5] , \tilde{\mathcal{M}}_{26,33}^{\bar{c}cgg} = \tilde{\mathcal{M}}_{26,34}^{\bar{c}cgg} = -27[d+1] \\
\tilde{\mathcal{M}}_{26,35}^{\bar{c}cgg} &= -27[2d-1] , \tilde{\mathcal{M}}_{26,36}^{\bar{c}cgg} = -54[d+1] , \tilde{\mathcal{M}}_{27,27}^{\bar{c}cgg} = -54[4d-9] \\
\tilde{\mathcal{M}}_{27,28}^{\bar{c}cgg} &= -27[4d-5] , \tilde{\mathcal{M}}_{27,29}^{\bar{c}cgg} = -54[d+1] , \tilde{\mathcal{M}}_{27,30}^{\bar{c}cgg} = -27[2d-1] \\
\tilde{\mathcal{M}}_{27,31}^{\bar{c}cgg} &= \tilde{\mathcal{M}}_{27,32}^{\bar{c}cgg} = -27[d+1] , \tilde{\mathcal{M}}_{27,33}^{\bar{c}cgg} = \tilde{\mathcal{M}}_{27,34}^{\bar{c}cgg} = -27[4d-5] \\
\tilde{\mathcal{M}}_{27,35}^{\bar{c}cgg} &= -27[2d-1] , \tilde{\mathcal{M}}_{27,36}^{\bar{c}cgg} = -54[d+1] , \tilde{\mathcal{M}}_{28,28}^{\bar{c}cgg} = -108[2d-3] \\
\tilde{\mathcal{M}}_{28,29}^{\bar{c}cgg} &= -27[d+5] , \tilde{\mathcal{M}}_{28,30}^{\bar{c}cgg} = -27[d+3] , \tilde{\mathcal{M}}_{28,31}^{\bar{c}cgg} = -27[2d+1] \\
\tilde{\mathcal{M}}_{28,32}^{\bar{c}cgg} &= -54d , \tilde{\mathcal{M}}_{28,33}^{\bar{c}cgg} = -27[2d+1] , \tilde{\mathcal{M}}_{28,34}^{\bar{c}cgg} = -54d \\
\tilde{\mathcal{M}}_{28,35}^{\bar{c}cgg} &= -108[d-1] , \tilde{\mathcal{M}}_{28,36}^{\bar{c}cgg} = -108d , \tilde{\mathcal{M}}_{29,29}^{\bar{c}cgg} = -216d \\
\tilde{\mathcal{M}}_{29,30}^{\bar{c}cgg} &= \tilde{\mathcal{M}}_{29,31}^{\bar{c}cgg} = -108d , \tilde{\mathcal{M}}_{29,32}^{\bar{c}cgg} = -54[d+3] , \tilde{\mathcal{M}}_{29,33}^{\bar{c}cgg} = -108d \\
\tilde{\mathcal{M}}_{29,34}^{\bar{c}cgg} &= \tilde{\mathcal{M}}_{29,35}^{\bar{c}cgg} = -54[d+3] , \tilde{\mathcal{M}}_{29,36}^{\bar{c}cgg} = -27[d+9] \\
\tilde{\mathcal{M}}_{30,30}^{\bar{c}cgg} &= -108[2d-3] , \tilde{\mathcal{M}}_{30,31}^{\bar{c}cgg} = -54d , \tilde{\mathcal{M}}_{30,32}^{\bar{c}cgg} = -27[4d-3] \\
\tilde{\mathcal{M}}_{30,33}^{\bar{c}cgg} &= -54d , \tilde{\mathcal{M}}_{30,34}^{\bar{c}cgg} = -27[4d-3] , \tilde{\mathcal{M}}_{30,35}^{\bar{c}cgg} = -27[d+3] \\
\tilde{\mathcal{M}}_{30,36}^{\bar{c}cgg} &= -54[d+3] , \tilde{\mathcal{M}}_{31,31}^{\bar{c}cgg} = -108[2d-3] , \tilde{\mathcal{M}}_{31,32}^{\bar{c}cgg} = -27[4d-3] \\
\tilde{\mathcal{M}}_{31,33}^{\bar{c}cgg} &= -54d , \tilde{\mathcal{M}}_{31,34}^{\bar{c}cgg} = -27[d+3] , \tilde{\mathcal{M}}_{31,35}^{\bar{c}cgg} = -27[4d-3] \\
\tilde{\mathcal{M}}_{31,36}^{\bar{c}cgg} &= -54[d+3] , \tilde{\mathcal{M}}_{32,32}^{\bar{c}cgg} = -108[2d-3] , \tilde{\mathcal{M}}_{32,33}^{\bar{c}cgg} = -27[d+3] \\
\tilde{\mathcal{M}}_{32,34}^{\bar{c}cgg} &= \tilde{\mathcal{M}}_{32,35}^{\bar{c}cgg} = -54d , \tilde{\mathcal{M}}_{32,36}^{\bar{c}cgg} = -108d , \tilde{\mathcal{M}}_{33,33}^{\bar{c}cgg} = -108[2d-3] \\
\tilde{\mathcal{M}}_{33,34}^{\bar{c}cgg} &= \tilde{\mathcal{M}}_{33,35}^{\bar{c}cgg} = -27[4d-3] , \tilde{\mathcal{M}}_{33,36}^{\bar{c}cgg} = -54[d+3]
\end{aligned}$$

$$\begin{aligned}
\tilde{\mathcal{M}}_{34,34}^{c\bar{c}gg} &= -108[2d-3] \ , \ \tilde{\mathcal{M}}_{34,35}^{c\bar{c}gg} = -54d \ , \ \tilde{\mathcal{M}}_{34,36}^{c\bar{c}gg} = -108d \\
\tilde{\mathcal{M}}_{35,35}^{c\bar{c}gg} &= -108[2d-3] \ , \ \tilde{\mathcal{M}}_{35,36}^{c\bar{c}gg} = -108d \ , \ \tilde{\mathcal{M}}_{36,36}^{c\bar{c}gg} = -216d
\end{aligned}
\tag{A.5}$$

in d -dimensions. Useful in deriving these was the symbolic manipulation language REDUCE, [65].

B Group theory.

In this Appendix we summarize aspects of the colour group theory used in examining the 4-point identity. For that example we have concentrated exclusively on the $SU(N_c)$ case due to the presence of rank 4 colour Casimirs. These arise in 4-point box graphs through the general fully symmetric tensors, [57],

$$d_F^{abcd} = \frac{1}{6} \text{Tr} \left(T^a T^{(b} T^c T^d) \right) \ , \ d_A^{abcd} = \frac{1}{6} \text{Tr} \left(T_A^a T_A^{(b} T_A^c T_A^d) \right) \tag{B.1}$$

where T^a are the group generators and the subscripts F and A indicate the fundamental and adjoint representations respectively. These can be related to the structure constants f^{abc} and the fully symmetric $SU(N_c)$ tensor d^{abc} via the $SU(N_c)$ relation

$$T^a T^b = \frac{1}{2N_c} \delta^{ab} + \frac{1}{2} d^{abc} T^c + \frac{i}{2} f^{abc} T^c . \tag{B.2}$$

When there is a contracted tensor product of generators we use

$$T_{IJ}^a T_{KL}^a = \frac{1}{2} \left[\delta_{IL} \delta_{KJ} - \frac{1}{N_c} \delta_{IJ} \delta_{KL} \right] . \tag{B.3}$$

In studying 4-point identity one has more than one colour tensor that can appear in the Green's functions contributing to (4.2). This is in contrast to the 3-point case where f^{abc} is the only structure that appears a low loop order. Therefore for (4.2) we have to have a basis which spans the colour space. If we define the tensors

$$f_4^{abcd} \equiv f^{abe} f^{cde} \ , \ d_4^{abcd} \equiv d^{abe} d^{cde} \tag{B.4}$$

then the second object is not independent of d_F^{abcd} or d_A^{abcd} since for instance

$$f_4^{abcd} = \frac{2}{N_c} \left[\delta^{ac} \delta^{bd} - \delta^{ad} \delta^{bc} \right] + d_4^{abcd} - d_4^{adbc} . \tag{B.5}$$

using results from [11, 66]. In [35] the mapping from the non-fully symmetric tensor d_4^{abcd} was constructed with for example

$$\begin{aligned}
d_4^{abcd} &= -\frac{1}{3} \left[f_4^{abcd} - \frac{2}{N_c} \left[\delta^{ac} \delta^{bd} - \delta^{ad} \delta^{bc} \right] \right] + \frac{2}{3} \left[f_4^{acbd} - \frac{2}{N_c} \left[\delta^{ab} \delta^{cd} - \delta^{ad} \delta^{bc} \right] \right] \\
&+ \frac{4}{N_c} \left[d_A^{acbd} - \frac{2}{3} \left[\delta^{ab} \delta^{cd} + \delta^{ac} \delta^{bd} + \delta^{ad} \delta^{bc} \right] \right]
\end{aligned}
\tag{B.6}$$

for purely gluonic or ghost boxes and

$$\begin{aligned}
d_4^{abcd} &= -\frac{1}{3} \left[f_4^{abcd} - \frac{2}{N_c} \left[\delta^{ac} \delta^{bd} - \delta^{ad} \delta^{bc} \right] \right] + \frac{2}{3} \left[f_4^{acbd} - \frac{2}{N_c} \left[\delta^{ab} \delta^{cd} - \delta^{ad} \delta^{bc} \right] \right] \\
&+ 8 \left[d_F^{acbd} - \frac{1}{12N_c} \left[\delta^{ab} \delta^{cd} + \delta^{ac} \delta^{bd} + \delta^{ad} \delta^{bc} \right] \right]
\end{aligned}
\tag{B.7}$$

for boxes involving quarks only. The use of d_F^{abcd} and d_A^{abcd} is more natural rather than d_4^{abcd} given the fully symmetric nature of the 4-point identity.

C Gluon vertex function examples.

The full arbitrary gauge expression of the 3-gluon vertex function at the symmetric point is given by

$$\begin{aligned}
-i \Gamma_{\mu\nu\sigma}^{ggg}(p, q, r)|_{x=y=1} &= [\eta_{\mu\nu}q_\sigma - \eta_{\mu\nu}p_\sigma + 2\eta_{\mu\sigma}p_\nu + \eta_{\mu\sigma}q_\nu - \eta_{\nu\sigma}p_\mu - 2\eta_{\nu\sigma}q_\mu] g \\
&+ \left[\left[\left[-\frac{4}{3}T_F N_f + \frac{2}{3}C_A + \frac{3}{4}\xi C_A \right] \frac{1}{\epsilon} - 2T_F N_f + \frac{4}{3}C_A - \frac{32}{81}\pi^2 T_F N_f \right. \right. \\
&\quad + \frac{1}{81}\pi^2 C_A - \frac{3}{2}\xi C_A + \frac{5}{54}\xi\pi^2 C_A + \frac{1}{2}\xi^2 C_A + \frac{1}{27}\xi^2\pi^2 C_A \\
&\quad + \frac{1}{24}\xi^3 C_A + \frac{16}{27}\psi'(\frac{1}{3})T_F N_f - \frac{1}{54}\psi'(\frac{1}{3})C_A - \frac{5}{36}\psi'(\frac{1}{3})\xi C_A \\
&\quad \left. \left. - \frac{1}{18}\psi'(\frac{1}{3})\xi^2 C_A \right] \eta_{\mu\nu}p_\sigma \right. \\
&+ \left[\left[\left[\frac{4}{3}T_F N_f - \frac{2}{3}C_A - \frac{3}{4}\xi C_A \right] \frac{1}{\epsilon} + 2T_F N_f - \frac{4}{3}C_A \right. \right. \\
&\quad + \frac{32}{81}\pi^2 T_F N_f - \frac{1}{81}\pi^2 C_A + \frac{3}{2}\xi C_A - \frac{5}{54}\xi\pi^2 C_A - \frac{1}{2}\xi^2 C_A \\
&\quad - \frac{1}{27}\xi^2\pi^2 C_A - \frac{1}{24}\xi^3 C_A - \frac{16}{27}\psi'(\frac{1}{3})T_F N_f + \frac{1}{54}\psi'(\frac{1}{3})C_A \\
&\quad \left. \left. + \frac{5}{36}\psi'(\frac{1}{3})\xi C_A + \frac{1}{18}\psi'(\frac{1}{3})\xi^2 C_A \right] \eta_{\mu\nu}q_\sigma \right. \\
&+ \left[\left[\left[\frac{8}{3}T_F N_f - \frac{4}{3}C_A - \frac{3}{2}\xi C_A \right] \frac{1}{\epsilon} + 4T_F N_f - \frac{8}{3}C_A \right. \right. \\
&\quad + \frac{64}{81}\pi^2 T_F N_f - \frac{2}{81}\pi^2 C_A + 3\xi C_A - \frac{5}{27}\xi\pi^2 C_A - \xi^2 C_A \\
&\quad - \frac{2}{27}\xi^2\pi^2 C_A - \frac{1}{12}\xi^3 C_A - \frac{32}{27}\psi'(\frac{1}{3})T_F N_f + \frac{1}{27}\psi'(\frac{1}{3})C_A \\
&\quad \left. \left. + \frac{5}{18}\psi'(\frac{1}{3})\xi C_A + \frac{1}{9}\psi'(\frac{1}{3})\xi^2 C_A \right] \eta_{\mu\sigma}p_\nu \right. \\
&+ \left[\left[\left[\frac{4}{3}T_F N_f - \frac{2}{3}C_A - \frac{3}{4}\xi C_A \right] \frac{1}{\epsilon} + 2T_F N_f - \frac{4}{3}C_A \right. \right. \\
&\quad + \frac{32}{81}\pi^2 T_F N_f - \frac{1}{81}\pi^2 C_A + \frac{3}{2}\xi C_A - \frac{5}{54}\xi\pi^2 C_A - \frac{1}{2}\xi^2 C_A \\
&\quad - \frac{1}{27}\xi^2\pi^2 C_A - \frac{1}{24}\xi^3 C_A - \frac{16}{27}\psi'(\frac{1}{3})T_F N_f + \frac{1}{54}\psi'(\frac{1}{3})C_A \\
&\quad \left. \left. + \frac{5}{36}\psi'(\frac{1}{3})\xi C_A + \frac{1}{18}\psi'(\frac{1}{3})\xi^2 C_A \right] \eta_{\mu\sigma}q_\nu \right. \\
&+ \left[\left[\left[-\frac{4}{3}T_F N_f + \frac{2}{3}C_A + \frac{3}{4}\xi C_A \right] \frac{1}{\epsilon} - 2T_F N_f + \frac{4}{3}C_A \right. \right. \\
&\quad - \frac{32}{81}\pi^2 T_F N_f + \frac{1}{81}\pi^2 C_A - \frac{3}{2}\xi C_A + \frac{5}{54}\xi\pi^2 C_A + \frac{1}{2}\xi^2 C_A \\
&\quad + \frac{1}{27}\xi^2\pi^2 C_A + \frac{1}{24}\xi^3 C_A + \frac{16}{27}\psi'(\frac{1}{3})T_F N_f - \frac{1}{54}\psi'(\frac{1}{3})C_A \\
&\quad \left. \left. - \frac{5}{36}\psi'(\frac{1}{3})\xi C_A - \frac{1}{18}\psi'(\frac{1}{3})\xi^2 C_A \right] \eta_{\nu\sigma}p_\mu \right. \\
&+ \left[\left[\left[-\frac{8}{3}T_F N_f + \frac{4}{3}C_A + \frac{3}{2}\xi C_A \right] \frac{1}{\epsilon} - 4T_F N_f + \frac{8}{3}C_A \right. \right.
\end{aligned}$$

$$\begin{aligned}
& -\frac{64}{81}\pi^2 T_F N_f + \frac{2}{81}\pi^2 C_A - 3\xi C_A + \frac{5}{27}\xi\pi^2 C_A + \xi^2 C_A \\
& + \frac{2}{27}\xi^2\pi^2 C_A + \frac{1}{12}\xi^3 C_A + \frac{32}{27}\psi'(\frac{1}{3})T_F N_f - \frac{1}{27}\psi'(\frac{1}{3})C_A \\
& - \frac{5}{18}\psi'(\frac{1}{3})\xi C_A - \frac{1}{9}\psi'(\frac{1}{3})\xi^2 C_A \Big] \eta_{\nu\sigma} q_\mu \\
& + \left[\frac{16}{27}T_F N_f - \frac{8}{27}C_A + \frac{128}{243}\pi^2 T_F N_f - \frac{64}{243}\pi^2 C_A + \xi C_A \right. \\
& - \frac{2}{27}\xi\pi^2 C_A + \frac{1}{12}\xi^2 C_A + \frac{1}{27}\xi^2\pi^2 C_A + \frac{1}{9}\xi^3 C_A \\
& + \frac{2}{81}\xi^3\pi^2 C_A - \frac{64}{81}\psi'(\frac{1}{3})T_F N_f + \frac{32}{81}\psi'(\frac{1}{3})C_A + \frac{1}{9}\psi'(\frac{1}{3})\xi C_A \\
& \left. - \frac{1}{18}\psi'(\frac{1}{3})\xi^2 C_A - \frac{1}{27}\psi'(\frac{1}{3})\xi^3 C_A \right] \frac{p_\mu p_\nu p_\sigma}{\mu^2} \\
& + \left[-\frac{28}{27}T_F N_f + \frac{14}{27}C_A + \frac{64}{243}\pi^2 T_F N_f - \frac{32}{243}\pi^2 C_A \right. \\
& + \frac{3}{2}\xi C_A + \frac{1}{27}\xi\pi^2 C_A - \frac{7}{12}\xi^2 C_A - \frac{1}{9}\xi^2\pi^2 C_A \\
& - \frac{7}{36}\xi^3 C_A - \frac{2}{81}\xi^3\pi^2 C_A - \frac{32}{81}\psi'(\frac{1}{3})T_F N_f + \frac{16}{81}\psi'(\frac{1}{3})C_A \\
& \left. - \frac{1}{18}\psi'(\frac{1}{3})\xi C_A + \frac{1}{6}\psi'(\frac{1}{3})\xi^2 C_A + \frac{1}{27}\psi'(\frac{1}{3})\xi^3 C_A \right] \frac{p_\mu p_\nu q_\sigma}{\mu^2} \\
& + \left[\frac{8}{27}T_F N_f - \frac{4}{27}C_A + \frac{64}{243}\pi^2 T_F N_f - \frac{32}{243}\pi^2 C_A \right. \\
& + \frac{1}{2}\xi C_A - \frac{1}{27}\xi\pi^2 C_A + \frac{1}{24}\xi^2 C_A + \frac{1}{54}\xi^2\pi^2 C_A \\
& + \frac{1}{18}\xi^3 C_A + \frac{1}{81}\xi^3\pi^2 C_A - \frac{32}{81}\psi'(\frac{1}{3})T_F N_f + \frac{16}{81}\psi'(\frac{1}{3})C_A \\
& \left. + \frac{1}{18}\psi'(\frac{1}{3})\xi C_A - \frac{1}{36}\psi'(\frac{1}{3})\xi^2 C_A - \frac{1}{54}\psi'(\frac{1}{3})\xi^3 C_A \right] \frac{p_\mu p_\sigma q_\nu}{\mu^2} \\
& + \left[-\frac{8}{27}T_F N_f + \frac{4}{27}C_A - \frac{64}{243}\pi^2 T_F N_f + \frac{32}{243}\pi^2 C_A \right. \\
& - \frac{1}{2}\xi C_A + \frac{1}{27}\xi\pi^2 C_A - \frac{1}{24}\xi^2 C_A - \frac{1}{54}\xi^2\pi^2 C_A \\
& - \frac{1}{18}\xi^3 C_A - \frac{1}{81}\xi^3\pi^2 C_A + \frac{32}{81}\psi'(\frac{1}{3})T_F N_f - \frac{16}{81}\psi'(\frac{1}{3})C_A \\
& \left. - \frac{1}{18}\psi'(\frac{1}{3})\xi C_A + \frac{1}{36}\psi'(\frac{1}{3})\xi^2 C_A + \frac{1}{54}\psi'(\frac{1}{3})\xi^3 C_A \right] \frac{p_\mu p_\sigma q_\nu}{\mu^2} \\
& + \left[\frac{44}{27}T_F N_f - \frac{22}{27}C_A + \frac{64}{243}\pi^2 T_F N_f - \frac{32}{243}\pi^2 C_A \right. \\
& - \frac{1}{2}\xi C_A - \frac{1}{9}\xi\pi^2 C_A + \frac{2}{3}\xi^2 C_A + \frac{4}{27}\xi^2\pi^2 C_A \\
& + \frac{11}{36}\xi^3 C_A + \frac{4}{81}\xi^3\pi^2 C_A - \frac{32}{81}\psi'(\frac{1}{3})T_F N_f + \frac{16}{81}\psi'(\frac{1}{3})C_A \\
& \left. + \frac{1}{6}\psi'(\frac{1}{3})\xi C_A - \frac{2}{9}\psi'(\frac{1}{3})\xi^2 C_A - \frac{2}{27}\psi'(\frac{1}{3})\xi^3 C_A \right] \frac{p_\nu p_\sigma q_\mu}{\mu^2} \\
& + \left[-\frac{44}{27}T_F N_f + \frac{22}{27}C_A - \frac{64}{243}\pi^2 T_F N_f + \frac{32}{243}\pi^2 C_A \right.
\end{aligned}$$

$$\begin{aligned}
& + \frac{1}{2}\xi C_A + \frac{1}{9}\xi\pi^2 C_A - \frac{2}{3}\xi^2 C_A - \frac{4}{27}\xi^2\pi^2 C_A \\
& - \frac{11}{36}\xi^3 C_A - \frac{4}{81}\xi^3\pi^2 C_A + \frac{32}{81}\psi'(\frac{1}{3})T_F N_f - \frac{16}{81}\psi'(\frac{1}{3})C_A \\
& - \frac{1}{6}\psi'(\frac{1}{3})\xi C_A + \frac{2}{9}\psi'(\frac{1}{3})\xi^2 C_A + \frac{2}{27}\psi'(\frac{1}{3})\xi^3 C_A \left] \frac{p_\nu q_\mu q_\sigma}{\mu^2} \right. \\
& + \left[\frac{28}{27}T_F N_f - \frac{14}{27}C_A - \frac{64}{243}\pi^2 T_F N_f + \frac{32}{243}\pi^2 C_A \right. \\
& - \frac{3}{2}\xi C_A - \frac{1}{27}\xi\pi^2 C_A + \frac{7}{12}\xi^2 C_A + \frac{1}{9}\xi^2\pi^2 C_A \\
& + \frac{7}{36}\xi^3 C_A + \frac{2}{81}\xi^3\pi^2 C_A + \frac{32}{81}\psi'(\frac{1}{3})T_F N_f - \frac{16}{81}\psi'(\frac{1}{3})C_A \\
& + \left. \frac{1}{18}\psi'(\frac{1}{3})\xi C_A - \frac{1}{6}\psi'(\frac{1}{3})\xi^2 C_A - \frac{1}{27}\psi'(\frac{1}{3})\xi^3 C_A \right] \frac{p_\sigma q_\mu q_\nu}{\mu^2} \\
& + \left[-\frac{16}{27}T_F N_f + \frac{8}{27}C_A - \frac{128}{243}\pi^2 T_F N_f + \frac{64}{243}\pi^2 C_A \right. \\
& - \xi C_A + \frac{2}{27}\xi\pi^2 C_A - \frac{1}{12}\xi^2 C_A - \frac{1}{27}\xi^2\pi^2 C_A \\
& - \frac{1}{9}\xi^3 C_A - \frac{2}{81}\xi^3\pi^2 C_A + \frac{64}{81}\psi'(\frac{1}{3})T_F N_f - \frac{32}{81}\psi'(\frac{1}{3})C_A \\
& - \left. \frac{1}{9}\psi'(\frac{1}{3})\xi C_A + \frac{1}{18}\psi'(\frac{1}{3})\xi^2 C_A + \frac{1}{27}\psi'(\frac{1}{3})\xi^3 C_A \right] \frac{q_\mu q_\nu q_\sigma}{\mu^2} \Big] g^3 \\
& + O(g^5) \tag{C.1}
\end{aligned}$$

in terms of the full tensor basis where we note again that we have used the compact notation $\xi = 1 - \alpha$. Also for assistance at the 3-point symmetric point $x = y = 1$ we have

$$\Phi_1(1, 1) = \frac{4\pi^2}{9} - \frac{2}{3}\psi'(\frac{1}{3}) \tag{C.2}$$

which is related to the Clausen function since $\Delta_G(1, 1) = -3$ leading to a complex value for $\rho(1, 1)$ and an imaginary one for $\lambda(1, 1)$.

For the 4-point identity we record the contraction of the symmetric point quartic gluon Green's function with one external momentum to illustrate several subtle points. The Landau gauge expression restricted to $SU(N_c)$ is

$$\begin{aligned}
\Gamma_{\mu\nu\sigma\rho}^{gggg\,abcd}(p, q, r, s) s^\rho \Big| & = \left[f_4^{abcd}\eta_{\mu\nu}s_\sigma - 2f_4^{abcd}\eta_{\mu\sigma}s_\nu + f_4^{abcd}\eta_{\nu\sigma}s_\mu \right. \\
& \left. - 2f_4^{acbd}\eta_{\mu\nu}s_\sigma + f_4^{acbd}\eta_{\mu\sigma}s_\nu + f_4^{acbd}\eta_{\nu\sigma}s_\mu \right] \frac{g^2}{\mu^2} \\
& + \frac{2}{3}[N_f - N_c] \left[f_4^{abcd}\eta_{\mu\nu}s_\sigma - 2f_4^{abcd}\eta_{\mu\sigma}s_\nu + f_4^{abcd}\eta_{\nu\sigma}s_\mu \right. \\
& \left. - 2f_4^{acbd}\eta_{\mu\nu}s_\sigma + f_4^{acbd}\eta_{\mu\sigma}s_\nu + f_4^{acbd}\eta_{\nu\sigma}s_\mu \right] \frac{g^4}{\mu^2\epsilon} \\
& + \left[\left[\frac{8401}{1280}N_c \ln(\frac{4}{3}) - \frac{59}{192}N_c - \frac{269}{15360}N_c\tilde{\Phi}_1(\frac{9}{16}) - \frac{515}{1024}N_c\tilde{\Phi}_1(\frac{3}{4}) \right. \right. \\
& \left. \left. - \frac{5}{4}N_f \ln(\frac{4}{3}) + \frac{3}{16}N_f\tilde{\Phi}_1(\frac{3}{4}) \right] \eta_{\mu\nu}p_\sigma \right. \\
& \left. + \left[\frac{7387}{5120}N_c \ln(\frac{4}{3}) - \frac{5}{16}N_c - \frac{6031}{122880}N_c\tilde{\Phi}_1(\frac{9}{16}) - \frac{341}{4096}N_c\tilde{\Phi}_1(\frac{3}{4}) \right. \right.
\end{aligned}$$

$$\begin{aligned}
& + \left[\frac{1}{12} N_f - \frac{5}{16} N_f \ln\left(\frac{4}{3}\right) + \frac{3}{64} N_f \tilde{\Phi}_1\left(\frac{3}{4}\right) \right] \eta_{\mu\nu} q_\sigma \\
& + \left[\frac{13}{18} N_c + \frac{15839}{3072} N_c \ln\left(\frac{4}{3}\right) - \frac{1169}{24576} N_c \tilde{\Phi}_1\left(\frac{9}{16}\right) - \frac{1415}{4096} N_c \tilde{\Phi}_1\left(\frac{3}{4}\right) \right. \\
& \quad \left. + \frac{37}{36} N_f - \frac{53}{48} N_f \ln\left(\frac{4}{3}\right) - \frac{15}{64} N_f \tilde{\Phi}_1\left(\frac{3}{4}\right) \right] \eta_{\mu\nu} s_\sigma \\
& + \left[\frac{40991}{5120} N_c \ln\left(\frac{4}{3}\right) - \frac{119}{192} N_c - \frac{8183}{122880} N_c \tilde{\Phi}_1\left(\frac{9}{16}\right) - \frac{2401}{4096} N_c \tilde{\Phi}_1\left(\frac{3}{4}\right) \right. \\
& \quad \left. + \frac{1}{12} N_f - \frac{25}{16} N_f \ln\left(\frac{4}{3}\right) + \frac{15}{64} N_f \tilde{\Phi}_1\left(\frac{3}{4}\right) \right] \eta_{\mu\sigma} q_\nu \\
& + \left[\frac{1169}{40960} N_c \tilde{\Phi}_1\left(\frac{9}{16}\right) - \frac{1189}{576} N_c - \frac{35417}{15360} N_c \ln\left(\frac{4}{3}\right) + \frac{429}{4096} N_c \tilde{\Phi}_1\left(\frac{3}{4}\right) \right. \\
& \quad \left. - \frac{71}{36} N_f + \frac{31}{48} N_f \ln\left(\frac{4}{3}\right) + \frac{45}{64} N_f \tilde{\Phi}_1\left(\frac{3}{4}\right) \right] \eta_{\mu\sigma} s_\nu \\
& + \left[\frac{59}{192} N_c - \frac{8401}{1280} N_c \ln\left(\frac{4}{3}\right) + \frac{269}{15360} N_c \tilde{\Phi}_1\left(\frac{9}{16}\right) + \frac{515}{1024} N_c \tilde{\Phi}_1\left(\frac{3}{4}\right) \right. \\
& \quad \left. + \frac{5}{4} N_f \ln\left(\frac{4}{3}\right) - \frac{3}{16} N_f \tilde{\Phi}_1\left(\frac{3}{4}\right) \right] \eta_{\nu\sigma} p_\mu \\
& + \left[\frac{1719}{4096} N_c \tilde{\Phi}_1\left(\frac{3}{4}\right) - \frac{1}{192} N_c - \frac{26217}{5120} N_c \ln\left(\frac{4}{3}\right) - \frac{1293}{40960} N_c \tilde{\Phi}_1\left(\frac{9}{16}\right) \right. \\
& \quad \left. + \frac{1}{12} N_f + \frac{15}{16} N_f \ln\left(\frac{4}{3}\right) - \frac{9}{64} N_f \tilde{\Phi}_1\left(\frac{3}{4}\right) \right] \eta_{\nu\sigma} q_\mu \\
& + \left[\frac{593}{576} N_c - \frac{21617}{15360} N_c \ln\left(\frac{4}{3}\right) - \frac{1231}{40960} N_c \tilde{\Phi}_1\left(\frac{9}{16}\right) + \frac{645}{4096} N_c \tilde{\Phi}_1\left(\frac{3}{4}\right) \right. \\
& \quad \left. + \frac{37}{36} N_f + \frac{7}{48} N_f \ln\left(\frac{4}{3}\right) - \frac{27}{64} N_f \tilde{\Phi}_1\left(\frac{3}{4}\right) \right] \eta_{\nu\sigma} s_\mu \left] f_4^{abcd} \frac{g^4}{\mu^2} \right. \\
& + \left[\left[\frac{15455}{32768} N_c \tilde{\Phi}_1\left(\frac{3}{4}\right) - \frac{785273}{204800} N_c \ln\left(\frac{4}{3}\right) - \frac{25491}{819200} N_c \tilde{\Phi}_1\left(\frac{9}{16}\right) + \frac{11}{32} N_f \right. \right. \\
& \quad \left. \left. - \frac{2991}{10240} N_c + \frac{131}{128} N_f \ln\left(\frac{4}{3}\right) - \frac{117}{512} N_f \tilde{\Phi}_1\left(\frac{3}{4}\right) \right] p_\mu p_\nu q_\sigma \right. \\
& + \left[\frac{13457}{204800} N_c \ln\left(\frac{4}{3}\right) - \frac{281281}{819200} N_c \tilde{\Phi}_1\left(\frac{9}{16}\right) + \frac{7513}{32768} N_c \tilde{\Phi}_1\left(\frac{3}{4}\right) \right. \\
& \quad \left. - \frac{4881}{10240} N_c - \frac{3}{32} N_f + \frac{5}{128} N_f \ln\left(\frac{4}{3}\right) + \frac{189}{512} N_f \tilde{\Phi}_1\left(\frac{3}{4}\right) \right] p_\mu p_\nu s_\sigma \\
& + \left[\frac{1415083}{204800} N_c \ln\left(\frac{4}{3}\right) - \frac{3977}{30720} N_c - \frac{41439}{819200} N_c \tilde{\Phi}_1\left(\frac{9}{16}\right) - \frac{1}{32} N_f \right. \\
& \quad \left. - \frac{16669}{32768} N_c \tilde{\Phi}_1\left(\frac{3}{4}\right) - \frac{169}{128} N_f \ln\left(\frac{4}{3}\right) + \frac{63}{512} N_f \tilde{\Phi}_1\left(\frac{3}{4}\right) \right] p_\mu p_\sigma q_\nu \\
& + \left[\frac{189947}{819200} N_c \tilde{\Phi}_1\left(\frac{9}{16}\right) - \frac{13673}{10240} N_c - \frac{534959}{204800} N_c \ln\left(\frac{4}{3}\right) - \frac{3}{32} N_f \right. \\
& \quad \left. - \frac{9415}{32768} N_c \tilde{\Phi}_1\left(\frac{3}{4}\right) + \frac{5}{128} N_f \ln\left(\frac{4}{3}\right) + \frac{189}{512} N_f \tilde{\Phi}_1\left(\frac{3}{4}\right) \right] p_\mu p_\sigma s_\nu \\
& + \left[\frac{11}{32} N_f - \frac{2991}{10240} N_c - \frac{785273}{204800} N_c \ln\left(\frac{4}{3}\right) - \frac{25491}{819200} N_c \tilde{\Phi}_1\left(\frac{9}{16}\right) \right.
\end{aligned}$$

$$\begin{aligned}
& + \left[\frac{15455}{32768} N_c \tilde{\Phi}_1\left(\frac{3}{4}\right) + \frac{131}{128} N_f \ln\left(\frac{4}{3}\right) - \frac{117}{512} N_f \tilde{\Phi}_1\left(\frac{3}{4}\right) \right] p_\mu q_\nu q_\sigma \\
& + \left[\frac{14951}{4096} N_c \ln\left(\frac{4}{3}\right) - \frac{1297}{3072} N_c - \frac{2843}{16384} N_c \tilde{\Phi}_1\left(\frac{9}{16}\right) - \frac{1}{16} N_f \right. \\
& \quad \left. - \frac{3225}{16384} N_c \tilde{\Phi}_1\left(\frac{3}{4}\right) - \frac{41}{64} N_f \ln\left(\frac{4}{3}\right) + \frac{63}{256} N_f \tilde{\Phi}_1\left(\frac{3}{4}\right) \right] p_\mu q_\nu s_\sigma \\
& + \left[\frac{11}{16} N_f - \frac{8887}{5120} N_c - \frac{113341}{102400} N_c \ln\left(\frac{4}{3}\right) - \frac{6897}{409600} N_c \tilde{\Phi}_1\left(\frac{9}{16}\right) \right. \\
& \quad \left. + \frac{1803}{16384} N_c \tilde{\Phi}_1\left(\frac{3}{4}\right) + \frac{19}{64} N_f \ln\left(\frac{4}{3}\right) + \frac{27}{256} N_f \tilde{\Phi}_1\left(\frac{3}{4}\right) \right] p_\mu q_\sigma s_\nu \\
& + \left[\frac{5}{128} N_f \ln\left(\frac{4}{3}\right) - \frac{10441}{10240} N_c - \frac{459423}{204800} N_c \ln\left(\frac{4}{3}\right) - \frac{64941}{819200} N_c \tilde{\Phi}_1\left(\frac{9}{16}\right) \right. \\
& \quad \left. - \frac{4727}{32768} N_c \tilde{\Phi}_1\left(\frac{3}{4}\right) - \frac{3}{32} N_f + \frac{189}{512} N_f \tilde{\Phi}_1\left(\frac{3}{4}\right) \right] p_\mu s_\nu s_\sigma \\
& + \left[\frac{11}{32} N_f - \frac{2991}{10240} N_c - \frac{785273}{204800} N_c \ln\left(\frac{4}{3}\right) - \frac{25491}{819200} N_c \tilde{\Phi}_1\left(\frac{9}{16}\right) \right. \\
& \quad \left. + \frac{15455}{32768} N_c \tilde{\Phi}_1\left(\frac{3}{4}\right) + \frac{131}{128} N_f \ln\left(\frac{4}{3}\right) - \frac{117}{512} N_f \tilde{\Phi}_1\left(\frac{3}{4}\right) \right] p_\nu p_\sigma q_\mu \\
& + \left[\frac{13457}{204800} N_c \ln\left(\frac{4}{3}\right) - \frac{4881}{10240} N_c - \frac{281281}{819200} N_c \tilde{\Phi}_1\left(\frac{9}{16}\right) - \frac{3}{32} N_f \right. \\
& \quad \left. + \frac{7513}{32768} N_c \tilde{\Phi}_1\left(\frac{3}{4}\right) + \frac{5}{128} N_f \ln\left(\frac{4}{3}\right) + \frac{189}{512} N_f \tilde{\Phi}_1\left(\frac{3}{4}\right) \right] p_\nu p_\sigma s_\mu \\
& + \left[\frac{11}{32} N_f - \frac{2991}{10240} N_c - \frac{785273}{204800} N_c \ln\left(\frac{4}{3}\right) - \frac{25491}{819200} N_c \tilde{\Phi}_1\left(\frac{9}{16}\right) \right. \\
& \quad \left. + \frac{15455}{32768} N_c \tilde{\Phi}_1\left(\frac{3}{4}\right) + \frac{131}{128} N_f \ln\left(\frac{4}{3}\right) - \frac{117}{512} N_f \tilde{\Phi}_1\left(\frac{3}{4}\right) \right] p_\nu q_\mu q_\sigma \\
& + \left[\frac{2143}{5120} N_c - \frac{393031}{102400} N_c \ln\left(\frac{4}{3}\right) - \frac{19077}{409600} N_c \tilde{\Phi}_1\left(\frac{9}{16}\right) - \frac{7}{16} N_f \right. \\
& \quad \left. + \frac{4513}{16384} N_c \tilde{\Phi}_1\left(\frac{3}{4}\right) + \frac{49}{64} N_f \ln\left(\frac{4}{3}\right) + \frac{9}{256} N_f \tilde{\Phi}_1\left(\frac{3}{4}\right) \right] p_\nu q_\mu s_\sigma \\
& + \left[\frac{11}{16} N_f - \frac{6079}{5120} N_c + \frac{7123}{102400} N_c \ln\left(\frac{4}{3}\right) - \frac{134309}{409600} N_c \tilde{\Phi}_1\left(\frac{9}{16}\right) \right. \\
& \quad \left. + \frac{6971}{16384} N_c \tilde{\Phi}_1\left(\frac{3}{4}\right) + \frac{19}{64} N_f \ln\left(\frac{4}{3}\right) + \frac{27}{256} N_f \tilde{\Phi}_1\left(\frac{3}{4}\right) \right] p_\nu q_\sigma s_\mu \\
& + \left[\frac{13457}{204800} N_c \ln\left(\frac{4}{3}\right) - \frac{4881}{10240} N_c - \frac{281281}{819200} N_c \tilde{\Phi}_1\left(\frac{9}{16}\right) - \frac{3}{32} N_f \right. \\
& \quad \left. + \frac{7513}{32768} N_c \tilde{\Phi}_1\left(\frac{3}{4}\right) + \frac{5}{128} N_f \ln\left(\frac{4}{3}\right) + \frac{189}{512} N_f \tilde{\Phi}_1\left(\frac{3}{4}\right) \right] p_\nu s_\mu s_\sigma \\
& + \left[\frac{1415083}{204800} N_c \ln\left(\frac{4}{3}\right) - \frac{3977}{30720} N_c - \frac{41439}{819200} N_c \tilde{\Phi}_1\left(\frac{9}{16}\right) - \frac{1}{32} N_f \right. \\
& \quad \left. - \frac{16669}{32768} N_c \tilde{\Phi}_1\left(\frac{3}{4}\right) - \frac{169}{128} N_f \ln\left(\frac{4}{3}\right) + \frac{63}{512} N_f \tilde{\Phi}_1\left(\frac{3}{4}\right) \right] p_\sigma q_\mu q_\nu \\
& + \left[\frac{111}{1024} N_c - \frac{21871}{4096} N_c \ln\left(\frac{4}{3}\right) + \frac{3565}{16384} N_c \tilde{\Phi}_1\left(\frac{9}{16}\right) - \frac{7}{16} N_f \right.
\end{aligned}$$

$$\begin{aligned}
& + \left[\frac{1217}{16384} N_c \tilde{\Phi}_1\left(\frac{3}{4}\right) + \frac{49}{64} N_f \ln\left(\frac{4}{3}\right) + \frac{9}{256} N_f \tilde{\Phi}_1\left(\frac{3}{4}\right) \right] p_\sigma q_\mu s_\nu \\
& + \left[\frac{68099}{20480} N_c \ln\left(\frac{4}{3}\right) - \frac{565}{3072} N_c - \frac{18057}{81920} N_c \tilde{\Phi}_1\left(\frac{9}{16}\right) - \frac{1}{16} N_f \right. \\
& \quad \left. - \frac{1353}{16384} N_c \tilde{\Phi}_1\left(\frac{3}{4}\right) - \frac{41}{64} N_f \ln\left(\frac{4}{3}\right) + \frac{63}{256} N_f \tilde{\Phi}_1\left(\frac{3}{4}\right) \right] p_\sigma q_\nu s_\mu \\
& + \left[\frac{2825}{32768} N_c \tilde{\Phi}_1\left(\frac{3}{4}\right) - \frac{8113}{10240} N_c - \frac{62079}{204800} N_c \ln\left(\frac{4}{3}\right) - \frac{3}{32} N_f \right. \\
& \quad \left. - \frac{26393}{819200} N_c \tilde{\Phi}_1\left(\frac{9}{16}\right) + \frac{5}{128} N_f \ln\left(\frac{4}{3}\right) + \frac{189}{512} N_f \tilde{\Phi}_1\left(\frac{3}{4}\right) \right] p_\sigma s_\mu s_\nu \\
& \left[\frac{21}{32} N_f - \frac{21923}{30720} N_c - \frac{155463}{204800} N_c \ln\left(\frac{4}{3}\right) - \frac{92421}{819200} N_c \tilde{\Phi}_1\left(\frac{9}{16}\right) \right. \\
& \quad \left. + \frac{14241}{32768} N_c \tilde{\Phi}_1\left(\frac{3}{4}\right) + \frac{93}{128} N_f \ln\left(\frac{4}{3}\right) - \frac{171}{512} N_f \tilde{\Phi}_1\left(\frac{3}{4}\right) \right] q_\mu q_\nu q_\sigma \\
& + \left[+ \frac{8263}{7680} N_c + \frac{230763}{51200} N_c \ln\left(\frac{4}{3}\right) - \frac{3679}{204800} N_c \tilde{\Phi}_1\left(\frac{9}{16}\right) - \frac{3}{8} N_f \right. \\
& \quad \left. - \frac{2141}{8192} N_c \tilde{\Phi}_1\left(\frac{3}{4}\right) - \frac{19}{32} N_f \ln\left(\frac{4}{3}\right) - \frac{27}{128} N_f \tilde{\Phi}_1\left(\frac{3}{4}\right) \right] q_\mu q_\nu s_\sigma \\
& + \left[\frac{9}{8} N_f - \frac{3361}{2560} N_c - \frac{272993}{51200} N_c \ln\left(\frac{4}{3}\right) + \frac{25447}{102400} N_c \tilde{\Phi}_1\left(\frac{9}{16}\right) \right. \\
& \quad \left. + \frac{3823}{8192} N_c \tilde{\Phi}_1\left(\frac{3}{4}\right) + \frac{41}{32} N_f \ln\left(\frac{4}{3}\right) - \frac{63}{128} N_f \tilde{\Phi}_1\left(\frac{3}{4}\right) \right] q_\mu q_\sigma s_\nu \\
& + \left[\frac{25621}{409600} N_c \tilde{\Phi}_1\left(\frac{9}{16}\right) - \frac{129}{5120} N_c - \frac{499987}{102400} N_c \ln\left(\frac{4}{3}\right) - \frac{7}{16} N_f \right. \\
& \quad \left. - \frac{2299}{16384} N_c \tilde{\Phi}_1\left(\frac{3}{4}\right) + \frac{49}{64} N_f \ln\left(\frac{4}{3}\right) + \frac{9}{256} N_f \tilde{\Phi}_1\left(\frac{3}{4}\right) \right] q_\mu s_\nu s_\sigma \\
& + \left[\frac{2387}{7680} N_c + \frac{47437}{51200} N_c \ln\left(\frac{4}{3}\right) - \frac{1103}{6400} N_c \tilde{\Phi}_1\left(\frac{9}{16}\right) + \frac{3}{8} N_f \right. \\
& \quad \left. + \frac{2957}{8192} N_c \tilde{\Phi}_1\left(\frac{3}{4}\right) + \frac{11}{32} N_f \ln\left(\frac{4}{3}\right) - \frac{45}{128} N_f \tilde{\Phi}_1\left(\frac{3}{4}\right) \right] q_\nu q_\sigma s_\mu \\
& + \left[\frac{123847}{20480} N_c \ln\left(\frac{4}{3}\right) - \frac{1009}{3072} N_c - \frac{23061}{81920} N_c \tilde{\Phi}_1\left(\frac{9}{16}\right) - \frac{1}{16} N_f \right. \\
& \quad \left. - \frac{2965}{16384} N_c \tilde{\Phi}_1\left(\frac{3}{4}\right) - \frac{41}{64} N_f \ln\left(\frac{4}{3}\right) + \frac{63}{256} N_f \tilde{\Phi}_1\left(\frac{3}{4}\right) \right] q_\nu s_\mu s_\sigma \\
& + \left[\frac{16143}{102400} N_c \ln\left(\frac{4}{3}\right) - \frac{8379}{5120} N_c - \frac{70369}{409600} N_c \tilde{\Phi}_1\left(\frac{9}{16}\right) + \frac{11}{16} N_f \right. \\
& \quad \left. + \frac{1111}{16384} N_c \tilde{\Phi}_1\left(\frac{3}{4}\right) + \frac{19}{64} N_f \ln\left(\frac{4}{3}\right) + \frac{27}{256} N_f \tilde{\Phi}_1\left(\frac{3}{4}\right) \right] q_\sigma s_\mu s_\nu \\
& + \left[\frac{31497}{204800} N_c \ln\left(\frac{4}{3}\right) - \frac{9481}{10240} N_c - \frac{153401}{819200} N_c \tilde{\Phi}_1\left(\frac{9}{16}\right) + \frac{5}{128} N_f \ln\left(\frac{4}{3}\right) \right. \\
& \quad \left. - \frac{3}{32} N_f - \frac{4207}{32768} N_c \tilde{\Phi}_1\left(\frac{3}{4}\right) + \frac{189}{512} N_f \tilde{\Phi}_1\left(\frac{3}{4}\right) \right] s_\mu s_\nu s_\sigma \left] f_4^{abcd} \frac{g^4}{\mu^4} \right. \\
& + \left[\left[\frac{119}{192} N_c - \frac{40991}{5120} N_c \ln\left(\frac{4}{3}\right) + \frac{8183}{122880} N_c \tilde{\Phi}_1\left(\frac{9}{16}\right) - \frac{1}{12} N_f \right. \right.
\end{aligned}$$

$$\begin{aligned}
& + \left[\frac{2401}{4096} N_c \tilde{\Phi}_1\left(\frac{3}{4}\right) + \frac{25}{16} N_f \ln\left(\frac{4}{3}\right) - \frac{15}{64} N_f \tilde{\Phi}_1\left(\frac{3}{4}\right) \right] \eta_{\mu\nu} p_\sigma \\
& + \left[\frac{119}{192} N_c - \frac{40991}{5120} N_c \ln\left(\frac{4}{3}\right) + \frac{8183}{122880} N_c \tilde{\Phi}_1\left(\frac{9}{16}\right) - \frac{1}{12} N_f \right. \\
& \quad \left. + \frac{2401}{4096} N_c \tilde{\Phi}_1\left(\frac{3}{4}\right) + \frac{25}{16} N_f \ln\left(\frac{4}{3}\right) - \frac{15}{64} N_f \tilde{\Phi}_1\left(\frac{3}{4}\right) \right] \eta_{\mu\nu} q_\sigma \\
& + \left[\frac{1169}{12288} N_c \tilde{\Phi}_1\left(\frac{9}{16}\right) - \frac{13}{9} N_c - \frac{15839}{1536} N_c \ln\left(\frac{4}{3}\right) - \frac{37}{18} N_f \right. \\
& \quad \left. + \frac{1415}{2048} N_c \tilde{\Phi}_1\left(\frac{3}{4}\right) + \frac{53}{24} N_f \ln\left(\frac{4}{3}\right) + \frac{15}{32} N_f \tilde{\Phi}_1\left(\frac{3}{4}\right) \right] \eta_{\mu\nu} s_\sigma \\
& + \left[\frac{1}{192} N_c + \frac{26217}{5120} N_c \ln\left(\frac{4}{3}\right) + \frac{1293}{40960} N_c \tilde{\Phi}_1\left(\frac{9}{16}\right) - \frac{1}{12} N_f \right. \\
& \quad \left. - \frac{1719}{4096} N_c \tilde{\Phi}_1\left(\frac{3}{4}\right) - \frac{15}{16} N_f \ln\left(\frac{4}{3}\right) + \frac{9}{64} N_f \tilde{\Phi}_1\left(\frac{3}{4}\right) \right] \eta_{\mu\sigma} p_\nu \\
& + \left[\frac{5}{16} N_c - \frac{7387}{5120} N_c \ln\left(\frac{4}{3}\right) + \frac{6031}{122880} N_c \tilde{\Phi}_1\left(\frac{9}{16}\right) - \frac{1}{12} N_f \right. \\
& \quad \left. + \frac{341}{4096} N_c \tilde{\Phi}_1\left(\frac{3}{4}\right) + \frac{5}{16} N_f \ln\left(\frac{4}{3}\right) - \frac{3}{64} N_f \tilde{\Phi}_1\left(\frac{3}{4}\right) \right] \eta_{\mu\sigma} q_\nu \\
& + \left[\frac{149}{144} N_c + \frac{28517}{7680} N_c \ln\left(\frac{4}{3}\right) + \frac{31}{20480} N_c \tilde{\Phi}_1\left(\frac{9}{16}\right) + \frac{17}{18} N_f \right. \\
& \quad \left. - \frac{537}{2048} N_c \tilde{\Phi}_1\left(\frac{3}{4}\right) - \frac{19}{24} N_f \ln\left(\frac{4}{3}\right) - \frac{9}{32} N_f \tilde{\Phi}_1\left(\frac{3}{4}\right) \right] \eta_{\mu\sigma} s_\nu \\
& + \left[\frac{5}{16} N_c - \frac{7387}{5120} N_c \ln\left(\frac{4}{3}\right) + \frac{6031}{122880} N_c \tilde{\Phi}_1\left(\frac{9}{16}\right) - \frac{1}{12} N_f \right. \\
& \quad \left. + \frac{341}{4096} N_c \tilde{\Phi}_1\left(\frac{3}{4}\right) + \frac{5}{16} N_f \ln\left(\frac{4}{3}\right) - \frac{3}{64} N_f \tilde{\Phi}_1\left(\frac{3}{4}\right) \right] \eta_{\nu\sigma} p_\mu \\
& + \left[\frac{1}{192} N_c + \frac{26217}{5120} N_c \ln\left(\frac{4}{3}\right) + \frac{1293}{40960} N_c \tilde{\Phi}_1\left(\frac{9}{16}\right) - \frac{1}{12} N_f \right. \\
& \quad \left. - \frac{1719}{4096} N_c \tilde{\Phi}_1\left(\frac{3}{4}\right) - \frac{15}{16} N_f \ln\left(\frac{4}{3}\right) + \frac{9}{64} N_f \tilde{\Phi}_1\left(\frac{3}{4}\right) \right] \eta_{\nu\sigma} q_\mu \\
& + \left[\frac{149}{144} N_c + \frac{28517}{7680} N_c \ln\left(\frac{4}{3}\right) + \frac{31}{20480} N_c \tilde{\Phi}_1\left(\frac{9}{16}\right) + \frac{17}{18} N_f \right. \\
& \quad \left. - \frac{537}{2048} N_c \tilde{\Phi}_1\left(\frac{3}{4}\right) - \frac{19}{24} N_f \ln\left(\frac{4}{3}\right) - \frac{9}{32} N_f \tilde{\Phi}_1\left(\frac{3}{4}\right) \right] \eta_{\nu\sigma} s_\mu \Big] f_4^{abcd} \frac{g^4}{\mu^2} \\
& + \left[+ \left[\frac{21923}{30720} N_c + \frac{155463}{204800} N_c \ln\left(\frac{4}{3}\right) + \frac{92421}{819200} N_c \tilde{\Phi}_1\left(\frac{9}{16}\right) - \frac{21}{32} N_f \right. \right. \\
& \quad \left. \left. - \frac{14241}{32768} N_c \tilde{\Phi}_1\left(\frac{3}{4}\right) - \frac{93}{128} N_f \ln\left(\frac{4}{3}\right) + \frac{171}{512} N_f \tilde{\Phi}_1\left(\frac{3}{4}\right) \right] p_\mu p_\nu p_\sigma \right. \\
& + \left[\frac{1295}{3072} N_c - \frac{62981}{20480} N_c \ln\left(\frac{4}{3}\right) + \frac{6693}{81920} N_c \tilde{\Phi}_1\left(\frac{9}{16}\right) - \frac{5}{16} N_f \right. \\
& \quad \left. + \frac{607}{16384} N_c \tilde{\Phi}_1\left(\frac{3}{4}\right) + \frac{19}{64} N_f \ln\left(\frac{4}{3}\right) + \frac{27}{256} N_f \tilde{\Phi}_1\left(\frac{3}{4}\right) \right] p_\mu p_\nu q_\sigma \\
& + \left[\frac{295997}{819200} N_c \tilde{\Phi}_1\left(\frac{9}{16}\right) - \frac{18409}{30720} N_c - \frac{936509}{204800} N_c \ln\left(\frac{4}{3}\right) + \frac{15}{32} N_f \right.
\end{aligned}$$

$$\begin{aligned}
& + \left[\frac{1051}{32768} N_c \tilde{\Phi}_1\left(\frac{3}{4}\right) + \frac{71}{128} N_f \ln\left(\frac{4}{3}\right) - \frac{81}{512} N_f \tilde{\Phi}_1\left(\frac{3}{4}\right) \right] p_\mu p_\nu s_\sigma \\
& + \left[\frac{1295}{3072} N_c - \frac{62981}{20480} N_c \ln\left(\frac{4}{3}\right) + \frac{6693}{81920} N_c \tilde{\Phi}_1\left(\frac{9}{16}\right) - \frac{5}{16} N_f \right. \\
& \quad \left. + \frac{607}{16384} N_c \tilde{\Phi}_1\left(\frac{3}{4}\right) + \frac{19}{64} N_f \ln\left(\frac{4}{3}\right) + \frac{27}{256} N_f \tilde{\Phi}_1\left(\frac{3}{4}\right) \right] p_\mu p_\sigma q_\nu \\
& + \left[\frac{31471}{30720} N_c + \frac{345211}{204800} N_c \ln\left(\frac{4}{3}\right) - \frac{48763}{819200} N_c \tilde{\Phi}_1\left(\frac{9}{16}\right) - \frac{9}{32} N_f \right. \\
& \quad \left. - \frac{2413}{32768} N_c \tilde{\Phi}_1\left(\frac{3}{4}\right) - \frac{49}{128} N_f \ln\left(\frac{4}{3}\right) - \frac{9}{512} N_f \tilde{\Phi}_1\left(\frac{3}{4}\right) \right] p_\mu p_\sigma s_\nu \\
& + \left[\frac{1295}{3072} N_c - \frac{62981}{20480} N_c \ln\left(\frac{4}{3}\right) + \frac{6693}{81920} N_c \tilde{\Phi}_1\left(\frac{9}{16}\right) - \frac{5}{16} N_f \right. \\
& \quad \left. + \frac{607}{16384} N_c \tilde{\Phi}_1\left(\frac{3}{4}\right) + \frac{19}{64} N_f \ln\left(\frac{4}{3}\right) + \frac{27}{256} N_f \tilde{\Phi}_1\left(\frac{3}{4}\right) \right] p_\mu q_\nu q_\sigma \\
& + \left[\frac{1297}{1536} N_c - \frac{14951}{2048} N_c \ln\left(\frac{4}{3}\right) + \frac{2843}{8192} N_c \tilde{\Phi}_1\left(\frac{9}{16}\right) + \frac{1}{8} N_f \right. \\
& \quad \left. + \frac{3225}{8192} N_c \tilde{\Phi}_1\left(\frac{3}{4}\right) + \frac{41}{32} N_f \ln\left(\frac{4}{3}\right) - \frac{63}{128} N_f \tilde{\Phi}_1\left(\frac{3}{4}\right) \right] p_\mu q_\nu s_\sigma \\
& + \left[\frac{14743}{7680} N_c - \frac{113577}{51200} N_c \ln\left(\frac{4}{3}\right) + \frac{48591}{204800} N_c \tilde{\Phi}_1\left(\frac{9}{16}\right) - \frac{5}{8} N_f \right. \\
& \quad \left. - \frac{225}{8192} N_c \tilde{\Phi}_1\left(\frac{3}{4}\right) + \frac{11}{32} N_f \ln\left(\frac{4}{3}\right) - \frac{45}{128} N_f \tilde{\Phi}_1\left(\frac{3}{4}\right) \right] p_\mu q_\sigma s_\nu \\
& + \left[\frac{41413}{30720} N_c - \frac{779047}{204800} N_c \ln\left(\frac{4}{3}\right) + \frac{295551}{819200} N_c \tilde{\Phi}_1\left(\frac{9}{16}\right) + \frac{5}{32} N_f \right. \\
& \quad \left. + \frac{10657}{32768} N_c \tilde{\Phi}_1\left(\frac{3}{4}\right) + \frac{77}{128} N_f \ln\left(\frac{4}{3}\right) - \frac{315}{512} N_f \tilde{\Phi}_1\left(\frac{3}{4}\right) \right] p_\mu s_\nu s_\sigma \\
& + \left[\frac{2991}{5120} N_c + \frac{785273}{102400} N_c \ln\left(\frac{4}{3}\right) + \frac{25491}{409600} N_c \tilde{\Phi}_1\left(\frac{9}{16}\right) - \frac{11}{16} N_f \right. \\
& \quad \left. - \frac{15455}{16384} N_c \tilde{\Phi}_1\left(\frac{3}{4}\right) - \frac{131}{64} N_f \ln\left(\frac{4}{3}\right) + \frac{117}{256} N_f \tilde{\Phi}_1\left(\frac{3}{4}\right) \right] p_\nu p_\sigma q_\mu \\
& + \left[\frac{3665}{2048} N_c + \frac{215703}{40960} N_c \ln\left(\frac{4}{3}\right) + \frac{15541}{163840} N_c \tilde{\Phi}_1\left(\frac{9}{16}\right) - \frac{33}{32} N_f \right. \\
& \quad \left. - \frac{22805}{32768} N_c \tilde{\Phi}_1\left(\frac{3}{4}\right) - \frac{169}{128} N_f \ln\left(\frac{4}{3}\right) + \frac{63}{512} N_f \tilde{\Phi}_1\left(\frac{3}{4}\right) \right] p_\nu p_\sigma s_\mu \\
& + \left[\frac{2991}{5120} N_c + \frac{785273}{102400} N_c \ln\left(\frac{4}{3}\right) + \frac{25491}{409600} N_c \tilde{\Phi}_1\left(\frac{9}{16}\right) - \frac{11}{16} N_f \right. \\
& \quad \left. - \frac{15455}{16384} N_c \tilde{\Phi}_1\left(\frac{3}{4}\right) - \frac{131}{64} N_f \ln\left(\frac{4}{3}\right) + \frac{117}{256} N_f \tilde{\Phi}_1\left(\frac{3}{4}\right) \right] p_\nu q_\mu q_\sigma \\
& + \left[\frac{393031}{51200} N_c \ln\left(\frac{4}{3}\right) - \frac{2143}{2560} N_c + \frac{19077}{204800} N_c \tilde{\Phi}_1\left(\frac{9}{16}\right) + \frac{7}{8} N_f \right. \\
& \quad \left. - \frac{4513}{8192} N_c \tilde{\Phi}_1\left(\frac{3}{4}\right) - \frac{49}{32} N_f \ln\left(\frac{4}{3}\right) - \frac{9}{128} N_f \tilde{\Phi}_1\left(\frac{3}{4}\right) \right] p_\nu q_\mu s_\sigma \\
& + \left[\frac{1381}{1280} N_c + \frac{134913}{25600} N_c \ln\left(\frac{4}{3}\right) + \frac{353}{3200} N_c \tilde{\Phi}_1\left(\frac{9}{16}\right) - \frac{1}{4} N_f \right.
\end{aligned}$$

$$\begin{aligned}
& - \frac{2047}{4096} N_c \tilde{\Phi}_1\left(\frac{3}{4}\right) - \frac{17}{16} N_f \ln\left(\frac{4}{3}\right) - \frac{9}{64} N_f \tilde{\Phi}_1\left(\frac{3}{4}\right) \Big] p_\nu q_\sigma s_\mu \\
& + \left[\frac{5139}{10240} N_c + \frac{986517}{204800} N_c \ln\left(\frac{4}{3}\right) + \frac{230039}{819200} N_c \tilde{\Phi}_1\left(\frac{9}{16}\right) + \frac{17}{32} N_f \right. \\
& \quad \left. - \frac{2915}{32768} N_c \tilde{\Phi}_1\left(\frac{3}{4}\right) - \frac{103}{128} N_f \ln\left(\frac{4}{3}\right) - \frac{207}{512} N_f \tilde{\Phi}_1\left(\frac{3}{4}\right) \right] p_\nu s_\mu s_\sigma \\
& + \left[\frac{1295}{3072} N_c - \frac{62981}{20480} N_c \ln\left(\frac{4}{3}\right) + \frac{6693}{81920} N_c \tilde{\Phi}_1\left(\frac{9}{16}\right) - \frac{5}{16} N_f \right. \\
& \quad \left. + \frac{607}{16384} N_c \tilde{\Phi}_1\left(\frac{3}{4}\right) + \frac{19}{64} N_f \ln\left(\frac{4}{3}\right) + \frac{27}{256} N_f \tilde{\Phi}_1\left(\frac{3}{4}\right) \right] p_\sigma q_\mu q_\nu \\
& + \left[\frac{1381}{1280} N_c + \frac{134913}{25600} N_c \ln\left(\frac{4}{3}\right) + \frac{353}{3200} N_c \tilde{\Phi}_1\left(\frac{9}{16}\right) - \frac{1}{4} N_f \right. \\
& \quad \left. - \frac{2047}{4096} N_c \tilde{\Phi}_1\left(\frac{3}{4}\right) - \frac{17}{16} N_f \ln\left(\frac{4}{3}\right) - \frac{9}{64} N_f \tilde{\Phi}_1\left(\frac{3}{4}\right) \right] p_\sigma q_\mu s_\nu \\
& + \left[\frac{14743}{7680} N_c - \frac{113577}{51200} N_c \ln\left(\frac{4}{3}\right) + \frac{48591}{204800} N_c \tilde{\Phi}_1\left(\frac{9}{16}\right) - \frac{5}{8} N_f \right. \\
& \quad \left. - \frac{225}{8192} N_c \tilde{\Phi}_1\left(\frac{3}{4}\right) + \frac{11}{32} N_f \ln\left(\frac{4}{3}\right) - \frac{45}{128} N_f \tilde{\Phi}_1\left(\frac{3}{4}\right) \right] p_\sigma q_\nu s_\mu \\
& + \left[\frac{24871}{10240} N_c + \frac{29793}{204800} N_c \ln\left(\frac{4}{3}\right) + \frac{167131}{819200} N_c \tilde{\Phi}_1\left(\frac{9}{16}\right) - \frac{19}{32} N_f \right. \\
& \quad \left. - \frac{5047}{32768} N_c \tilde{\Phi}_1\left(\frac{3}{4}\right) - \frac{43}{128} N_f \ln\left(\frac{4}{3}\right) - \frac{243}{512} N_f \tilde{\Phi}_1\left(\frac{3}{4}\right) \right] p_\sigma s_\mu s_\nu \\
& + \left[\frac{21923}{30720} N_c + \frac{155463}{204800} N_c \ln\left(\frac{4}{3}\right) + \frac{92421}{819200} N_c \tilde{\Phi}_1\left(\frac{9}{16}\right) - \frac{21}{32} N_f \right. \\
& \quad \left. - \frac{14241}{32768} N_c \tilde{\Phi}_1\left(\frac{3}{4}\right) - \frac{93}{128} N_f \ln\left(\frac{4}{3}\right) + \frac{171}{512} N_f \tilde{\Phi}_1\left(\frac{3}{4}\right) \right] q_\mu q_\nu q_\sigma \\
& + \left[\frac{295997}{819200} N_c \tilde{\Phi}_1\left(\frac{9}{16}\right) - \frac{18409}{30720} N_c - \frac{936509}{204800} N_c \ln\left(\frac{4}{3}\right) + \frac{15}{32} N_f \right. \\
& \quad \left. + \frac{1051}{32768} N_c \tilde{\Phi}_1\left(\frac{3}{4}\right) + \frac{71}{128} N_f \ln\left(\frac{4}{3}\right) - \frac{81}{512} N_f \tilde{\Phi}_1\left(\frac{3}{4}\right) \right] q_\mu q_\nu s_\sigma \\
& + \left[\frac{3665}{2048} N_c + \frac{215703}{40960} N_c \ln\left(\frac{4}{3}\right) + \frac{15541}{163840} N_c \tilde{\Phi}_1\left(\frac{9}{16}\right) - \frac{33}{32} N_f \right. \\
& \quad \left. - \frac{22805}{32768} N_c \tilde{\Phi}_1\left(\frac{3}{4}\right) - \frac{169}{128} N_f \ln\left(\frac{4}{3}\right) + \frac{63}{512} N_f \tilde{\Phi}_1\left(\frac{3}{4}\right) \right] q_\mu q_\sigma s_\nu \\
& + \left[\frac{5139}{10240} N_c + \frac{986517}{204800} N_c \ln\left(\frac{4}{3}\right) + \frac{230039}{819200} N_c \tilde{\Phi}_1\left(\frac{9}{16}\right) + \frac{17}{32} N_f \right. \\
& \quad \left. - \frac{2915}{32768} N_c \tilde{\Phi}_1\left(\frac{3}{4}\right) - \frac{103}{128} N_f \ln\left(\frac{4}{3}\right) - \frac{207}{512} N_f \tilde{\Phi}_1\left(\frac{3}{4}\right) \right] q_\mu s_\nu s_\sigma \\
& + \left[\frac{31471}{30720} N_c + \frac{345211}{204800} N_c \ln\left(\frac{4}{3}\right) - \frac{48763}{819200} N_c \tilde{\Phi}_1\left(\frac{9}{16}\right) - \frac{9}{32} N_f \right. \\
& \quad \left. - \frac{2413}{32768} N_c \tilde{\Phi}_1\left(\frac{3}{4}\right) - \frac{49}{128} N_f \ln\left(\frac{4}{3}\right) - \frac{9}{512} N_f \tilde{\Phi}_1\left(\frac{3}{4}\right) \right] q_\nu q_\sigma s_\mu \\
& + \left[\frac{41413}{30720} N_c - \frac{779047}{204800} N_c \ln\left(\frac{4}{3}\right) + \frac{295551}{819200} N_c \tilde{\Phi}_1\left(\frac{9}{16}\right) + \frac{5}{32} N_f \right.
\end{aligned}$$

$$\begin{aligned}
& + \left[\frac{10657}{32768} N_c \tilde{\Phi}_1\left(\frac{3}{4}\right) + \frac{77}{128} N_f \ln\left(\frac{4}{3}\right) - \frac{315}{512} N_f \tilde{\Phi}_1\left(\frac{3}{4}\right) \right] q_\nu s_\mu s_\sigma \\
& + \left[+ \frac{24871}{10240} N_c + \frac{29793}{204800} N_c \ln\left(\frac{4}{3}\right) + \frac{167131}{819200} N_c \tilde{\Phi}_1\left(\frac{9}{16}\right) - \frac{19}{32} N_f \right. \\
& \quad \left. - \frac{5047}{32768} N_c \tilde{\Phi}_1\left(\frac{3}{4}\right) - \frac{43}{128} N_f \ln\left(\frac{4}{3}\right) - \frac{243}{512} N_f \tilde{\Phi}_1\left(\frac{3}{4}\right) \right] q_\sigma s_\mu s_\nu \\
& + \left[\frac{9481}{5120} N_c - \frac{31497}{102400} N_c \ln\left(\frac{4}{3}\right) + \frac{153401}{409600} N_c \tilde{\Phi}_1\left(\frac{9}{16}\right) - \frac{5}{64} N_f \ln\left(\frac{4}{3}\right) \right. \\
& \quad \left. + \frac{3}{16} N_f + \frac{4207}{16384} N_c \tilde{\Phi}_1\left(\frac{3}{4}\right) - \frac{189}{256} N_f \tilde{\Phi}_1\left(\frac{3}{4}\right) \right] s_\mu s_\nu s_\sigma \left] f_4^{abcd} \frac{g^4}{\mu^4} \right. \\
& + \left[\left[\frac{29}{16} \ln\left(\frac{4}{3}\right) - \frac{1}{8} - \frac{7}{8} \tilde{\Phi}_1\left(\frac{9}{16}\right) + \frac{69}{64} \tilde{\Phi}_1\left(\frac{3}{4}\right) \right] \eta_{\mu\nu} p_\sigma \right. \\
& + \left[-\frac{1}{8} + \frac{29}{16} \ln\left(\frac{4}{3}\right) - \frac{7}{8} \tilde{\Phi}_1\left(\frac{9}{16}\right) + \frac{69}{64} \tilde{\Phi}_1\left(\frac{3}{4}\right) \right] \eta_{\mu\nu} q_\sigma \\
& + \left[\frac{1}{4} + \frac{37}{80} \ln\left(\frac{4}{3}\right) + \frac{1001}{1280} \tilde{\Phi}_1\left(\frac{9}{16}\right) - \frac{105}{64} \tilde{\Phi}_1\left(\frac{3}{4}\right) \right] \eta_{\mu\nu} s_\sigma \\
& + \left[\frac{1}{8} - \frac{29}{16} \ln\left(\frac{4}{3}\right) + \frac{7}{8} \tilde{\Phi}_1\left(\frac{9}{16}\right) - \frac{69}{64} \tilde{\Phi}_1\left(\frac{3}{4}\right) \right] \eta_{\mu\sigma} q_\nu \\
& + \left[\frac{3}{8} - \frac{27}{20} \ln\left(\frac{4}{3}\right) + \frac{2121}{1280} \tilde{\Phi}_1\left(\frac{9}{16}\right) - \frac{87}{32} \tilde{\Phi}_1\left(\frac{3}{4}\right) \right] \eta_{\mu\sigma} s_\nu \\
& + \left[\frac{1}{8} - \frac{29}{16} \ln\left(\frac{4}{3}\right) + \frac{7}{8} \tilde{\Phi}_1\left(\frac{9}{16}\right) - \frac{69}{64} \tilde{\Phi}_1\left(\frac{3}{4}\right) \right] \eta_{\nu\sigma} p_\mu \\
& + \left[\frac{3}{8} - \frac{27}{20} \ln\left(\frac{4}{3}\right) + \frac{2121}{1280} \tilde{\Phi}_1\left(\frac{9}{16}\right) - \frac{87}{32} \tilde{\Phi}_1\left(\frac{3}{4}\right) \right] \eta_{\nu\sigma} s_\mu \left] d_A^{abcd} \frac{g^4}{\mu^2} \right. \\
& + \left[\left[\frac{267}{2560} + \frac{49953}{25600} \ln\left(\frac{4}{3}\right) - \frac{9621}{409600} \tilde{\Phi}_1\left(\frac{9}{16}\right) + \frac{1707}{4096} \tilde{\Phi}_1\left(\frac{3}{4}\right) \right] p_\mu p_\nu q_\sigma \right. \\
& + \left[\frac{45}{512} - \frac{1161}{1024} \ln\left(\frac{4}{3}\right) + \frac{897}{16384} \tilde{\Phi}_1\left(\frac{9}{16}\right) - \frac{5235}{4096} \tilde{\Phi}_1\left(\frac{3}{4}\right) \right] p_\mu p_\nu s_\sigma \\
& + \left[\frac{659}{2560} - \frac{68079}{25600} \ln\left(\frac{4}{3}\right) + \frac{564003}{409600} \tilde{\Phi}_1\left(\frac{9}{16}\right) - \frac{6357}{4096} \tilde{\Phi}_1\left(\frac{3}{4}\right) \right] p_\mu p_\sigma q_\nu \\
& + \left[\frac{2913}{2560} - \frac{45693}{25600} \ln\left(\frac{4}{3}\right) + \frac{1342401}{409600} \tilde{\Phi}_1\left(\frac{9}{16}\right) - \frac{16095}{4096} \tilde{\Phi}_1\left(\frac{3}{4}\right) \right] p_\mu p_\sigma s_\nu \\
& + \left[\frac{659}{2560} - \frac{68079}{25600} \ln\left(\frac{4}{3}\right) + \frac{564003}{409600} \tilde{\Phi}_1\left(\frac{9}{16}\right) - \frac{6357}{4096} \tilde{\Phi}_1\left(\frac{3}{4}\right) \right] p_\mu q_\nu q_\sigma \\
& + \left[\frac{301}{1280} - \frac{29901}{12800} \ln\left(\frac{4}{3}\right) + \frac{189957}{204800} \tilde{\Phi}_1\left(\frac{9}{16}\right) - \frac{2871}{2048} \tilde{\Phi}_1\left(\frac{3}{4}\right) \right] p_\mu q_\nu s_\sigma \\
& + \left[\frac{141}{1280} - \frac{18651}{12800} \ln\left(\frac{4}{3}\right) + \frac{103257}{204800} \tilde{\Phi}_1\left(\frac{9}{16}\right) - \frac{2925}{2048} \tilde{\Phi}_1\left(\frac{3}{4}\right) \right] p_\mu q_\sigma s_\nu \\
& + \left[\frac{1113}{2560} - \frac{72693}{25600} \ln\left(\frac{4}{3}\right) + \frac{697401}{409600} \tilde{\Phi}_1\left(\frac{9}{16}\right) - \frac{10311}{4096} \tilde{\Phi}_1\left(\frac{3}{4}\right) \right] p_\mu s_\nu s_\sigma \\
& + \left[\frac{267}{2560} + \frac{49953}{25600} \ln\left(\frac{4}{3}\right) - \frac{9621}{409600} \tilde{\Phi}_1\left(\frac{9}{16}\right) + \frac{1707}{4096} \tilde{\Phi}_1\left(\frac{3}{4}\right) \right] p_\nu p_\sigma q_\mu \\
& + \left[\frac{45}{512} - \frac{1161}{1024} \ln\left(\frac{4}{3}\right) + \frac{897}{16384} \tilde{\Phi}_1\left(\frac{9}{16}\right) - \frac{5235}{4096} \tilde{\Phi}_1\left(\frac{3}{4}\right) \right] p_\nu p_\sigma s_\mu
\end{aligned}$$

$$\begin{aligned}
& + \left[\frac{267}{2560} + \frac{49953}{25600} \ln\left(\frac{4}{3}\right) - \frac{9621}{409600} \tilde{\Phi}_1\left(\frac{9}{16}\right) + \frac{1707}{4096} \tilde{\Phi}_1\left(\frac{3}{4}\right) \right] p_\nu q_\mu q_\sigma \\
& + \left[\frac{2505}{2048} \tilde{\Phi}_1\left(\frac{3}{4}\right) - \frac{1203}{1280} - \frac{10317}{12800} \ln\left(\frac{4}{3}\right) - \frac{556731}{204800} \tilde{\Phi}_1\left(\frac{9}{16}\right) \right] p_\nu q_\mu s_\sigma \\
& + \left[\frac{1449}{1280} + \frac{20781}{12800} \ln\left(\frac{4}{3}\right) + \frac{563133}{204800} \tilde{\Phi}_1\left(\frac{9}{16}\right) - \frac{4269}{2048} \tilde{\Phi}_1\left(\frac{3}{4}\right) \right] p_\nu q_\sigma s_\mu \\
& + \left[\frac{45}{512} - \frac{1161}{1024} \ln\left(\frac{4}{3}\right) + \frac{897}{16384} \tilde{\Phi}_1\left(\frac{9}{16}\right) - \frac{5235}{4096} \tilde{\Phi}_1\left(\frac{3}{4}\right) \right] p_\nu s_\mu s_\sigma \\
& + \left[\frac{267}{2560} + \frac{49953}{25600} \ln\left(\frac{4}{3}\right) - \frac{9621}{409600} \tilde{\Phi}_1\left(\frac{9}{16}\right) + \frac{1707}{4096} \tilde{\Phi}_1\left(\frac{3}{4}\right) \right] p_\sigma q_\mu q_\nu \\
& + \left[\frac{1449}{1280} + \frac{20781}{12800} \ln\left(\frac{4}{3}\right) + \frac{563133}{204800} \tilde{\Phi}_1\left(\frac{9}{16}\right) - \frac{4269}{2048} \tilde{\Phi}_1\left(\frac{3}{4}\right) \right] p_\sigma q_\mu s_\nu \\
& + \left[\frac{141}{1280} - \frac{18651}{12800} \ln\left(\frac{4}{3}\right) + \frac{103257}{204800} \tilde{\Phi}_1\left(\frac{9}{16}\right) - \frac{2925}{2048} \tilde{\Phi}_1\left(\frac{3}{4}\right) \right] p_\sigma q_\nu s_\mu \\
& + \left[\frac{405}{512} - \frac{81}{1024} \ln\left(\frac{4}{3}\right) + \frac{26697}{16384} \tilde{\Phi}_1\left(\frac{9}{16}\right) - \frac{11019}{4096} \tilde{\Phi}_1\left(\frac{3}{4}\right) \right] p_\sigma s_\mu s_\nu \\
& + \left[\frac{45}{512} - \frac{1161}{1024} \ln\left(\frac{4}{3}\right) + \frac{897}{16384} \tilde{\Phi}_1\left(\frac{9}{16}\right) - \frac{5235}{4096} \tilde{\Phi}_1\left(\frac{3}{4}\right) \right] q_\mu q_\nu s_\sigma \\
& + \left[\frac{45}{512} - \frac{1161}{1024} \ln\left(\frac{4}{3}\right) + \frac{897}{16384} \tilde{\Phi}_1\left(\frac{9}{16}\right) - \frac{5235}{4096} \tilde{\Phi}_1\left(\frac{3}{4}\right) \right] q_\mu q_\sigma s_\nu \\
& + \left[\frac{45}{512} - \frac{1161}{1024} \ln\left(\frac{4}{3}\right) + \frac{897}{16384} \tilde{\Phi}_1\left(\frac{9}{16}\right) - \frac{5235}{4096} \tilde{\Phi}_1\left(\frac{3}{4}\right) \right] q_\mu s_\nu s_\sigma \\
& + \left[\frac{2913}{2560} - \frac{45693}{25600} \ln\left(\frac{4}{3}\right) + \frac{1342401}{409600} \tilde{\Phi}_1\left(\frac{9}{16}\right) - \frac{16095}{4096} \tilde{\Phi}_1\left(\frac{3}{4}\right) \right] q_\nu q_\sigma s_\mu \\
& + \left[\frac{1113}{2560} - \frac{72693}{25600} \ln\left(\frac{4}{3}\right) + \frac{697401}{409600} \tilde{\Phi}_1\left(\frac{9}{16}\right) - \frac{10311}{4096} \tilde{\Phi}_1\left(\frac{3}{4}\right) \right] q_\nu s_\mu s_\sigma \\
& + \left[\frac{405}{512} - \frac{81}{1024} \ln\left(\frac{4}{3}\right) + \frac{26697}{16384} \tilde{\Phi}_1\left(\frac{9}{16}\right) - \frac{11019}{4096} \tilde{\Phi}_1\left(\frac{3}{4}\right) \right] q_\sigma s_\mu s_\nu \\
& + \left[\frac{1323}{1280} - \frac{14463}{12800} \ln\left(\frac{4}{3}\right) + \frac{503691}{204800} \tilde{\Phi}_1\left(\frac{9}{16}\right) \right. \\
& \quad \left. - \frac{7989}{2048} \tilde{\Phi}_1\left(\frac{3}{4}\right) \right] s_\mu s_\nu s_\sigma \Big] d_A^{abcd} \frac{g^4}{\mu^4} \tag{C.3}
\end{aligned}$$

where we have set

$$\tilde{\Phi}_1\left(\frac{3}{4}\right) = \Phi_1\left(\frac{3}{4}, \frac{3}{4}\right) \quad , \quad \tilde{\Phi}_1\left(\frac{9}{16}\right) = \Phi_1\left(\frac{9}{16}, \frac{9}{16}\right) \tag{C.4}$$

for shorthand. In [35] the non-contracted expression included the quartic colour group Casimir in the fundamental representation d_F^{abcd} of (B.1) in addition to the adjoint one. When the full expression for $\Gamma_{\mu\nu\sigma\rho}^{ggggabcd}(p, q, r, s)$, which contains d_F^{abcd} , is contracted with s^ρ to produce (C.3) it transpires that all the d_F^{abcd} terms cancel. This is not unexpected since there are no other places in the identity (4.2) for such a Casimir to arise at one loop. The places where d_F^{abcd} can potentially appear are in the various orientations of $\Gamma_{\nu\sigma\lambda}^{c\bar{c}ggabcd}(p, q, r, s)$ and at one loop there are no box graphs involving quarks. However $\Gamma_{\mu\nu\sigma\rho}^{ggggabcd}(p, q, r, s)$ does depend on N_f through the reorganization of the group theory associated with the purely quark boxes.

While the expressions for each orientation of $\Gamma_{\mu\nu\sigma}^{c\bar{c}ggabcd}(p, q, r, s)$ is similar we provide that for

the case of A for purposes of the discussion. In the Landau gauge we have

$$\begin{aligned}
\Gamma_{A\mu\nu\sigma}^{c\bar{c}ggabcd}(p, q, r, s) \Big| = & \left[\left[\frac{2821}{25600} \ln\left(\frac{4}{3}\right) - \frac{63}{1280} + \frac{33}{25600} \tilde{\Phi}_1\left(\frac{9}{16}\right) + \frac{101}{4096} \tilde{\Phi}_1\left(\frac{3}{4}\right) \eta_{\mu\nu} p_\sigma \right] \right. \\
& + \left[\frac{16217}{204800} \tilde{\Phi}_1\left(\frac{9}{16}\right) - \frac{239}{1280} - \frac{181}{12800} \ln\left(\frac{4}{3}\right) - \frac{263}{2048} \tilde{\Phi}_1\left(\frac{3}{4}\right) \right] \eta_{\mu\nu} q_\sigma \\
& + \left[\frac{1}{640} - \frac{339}{25600} \ln\left(\frac{4}{3}\right) - \frac{9901}{204800} \tilde{\Phi}_1\left(\frac{9}{16}\right) - \frac{287}{4096} \tilde{\Phi}_1\left(\frac{3}{4}\right) \right] \eta_{\mu\nu} s_\sigma \\
& + \left[\frac{9761}{102400} \tilde{\Phi}_1\left(\frac{9}{16}\right) - \frac{109}{1280} - \frac{10767}{25600} \ln\left(\frac{4}{3}\right) - \frac{663}{4096} \tilde{\Phi}_1\left(\frac{3}{4}\right) \right] \eta_{\mu\sigma} p_\nu \\
& + \left[\frac{259}{512} \ln\left(\frac{4}{3}\right) - \frac{11}{256} + \frac{121}{8192} \tilde{\Phi}_1\left(\frac{9}{16}\right) - \frac{247}{2048} \tilde{\Phi}_1\left(\frac{3}{4}\right) \right] \eta_{\mu\sigma} q_\nu \\
& + \left[\frac{2537}{25600} \ln\left(\frac{4}{3}\right) - \frac{29}{320} + \frac{12933}{204800} \tilde{\Phi}_1\left(\frac{9}{16}\right) + \frac{341}{4096} \tilde{\Phi}_1\left(\frac{3}{4}\right) \right] \eta_{\mu\sigma} s_\nu \\
& + \left[\frac{263}{3840} - \frac{15661}{76800} \ln\left(\frac{4}{3}\right) - \frac{3503}{76800} \tilde{\Phi}_1\left(\frac{9}{16}\right) + \frac{337}{4096} \tilde{\Phi}_1\left(\frac{3}{4}\right) \right] \eta_{\nu\sigma} p_\mu \\
& + \left[\frac{183}{1280} - \frac{5343}{12800} \ln\left(\frac{4}{3}\right) - \frac{18849}{204800} \tilde{\Phi}_1\left(\frac{9}{16}\right) + \frac{387}{2048} \tilde{\Phi}_1\left(\frac{3}{4}\right) \right] \eta_{\nu\sigma} q_\mu \\
& + \left[\frac{1}{16} - \frac{199}{1024} \ln\left(\frac{4}{3}\right) - \frac{367}{8192} \tilde{\Phi}_1\left(\frac{9}{16}\right) + \frac{237}{4096} \tilde{\Phi}_1\left(\frac{3}{4}\right) \right] \eta_{\nu\sigma} s_\mu \Big] N_c f_4^{abcd} \frac{g^4}{\mu^2} \\
& + \left[\left[\frac{18211}{204800} \tilde{\Phi}_1\left(\frac{9}{16}\right) - \frac{1609}{30720} - \frac{183663}{204800} \ln\left(\frac{4}{3}\right) - \frac{3983}{32768} \tilde{\Phi}_1\left(\frac{3}{4}\right) \right] p_\mu p_\nu p_\sigma \right. \\
& + \left[\frac{35329}{819200} \tilde{\Phi}_1\left(\frac{9}{16}\right) - \frac{4151}{15360} - \frac{931}{1600} \ln\left(\frac{4}{3}\right) - \frac{129}{4096} \tilde{\Phi}_1\left(\frac{3}{4}\right) \right] p_\mu p_\nu q_\sigma \\
& - \left[\frac{121}{30720} + \frac{35241}{204800} \ln\left(\frac{4}{3}\right) + \frac{86097}{819200} \tilde{\Phi}_1\left(\frac{9}{16}\right) + \frac{1249}{32768} \tilde{\Phi}_1\left(\frac{3}{4}\right) \right] p_\mu p_\nu s_\sigma \\
& + \left[\frac{1037}{46080} + \frac{12517}{38400} \ln\left(\frac{4}{3}\right) - \frac{5777}{819200} \tilde{\Phi}_1\left(\frac{9}{16}\right) - \frac{433}{4096} \tilde{\Phi}_1\left(\frac{3}{4}\right) \right] p_\mu p_\sigma q_\nu \\
& + \left[\frac{12231}{204800} \ln\left(\frac{4}{3}\right) - \frac{1741}{30720} + \frac{66957}{819200} \tilde{\Phi}_1\left(\frac{9}{16}\right) + \frac{1695}{32768} \tilde{\Phi}_1\left(\frac{3}{4}\right) \right] p_\mu p_\sigma s_\nu \\
& + \left[\frac{30401}{307200} \ln\left(\frac{4}{3}\right) - \frac{269}{9216} - \frac{3757}{51200} \tilde{\Phi}_1\left(\frac{9}{16}\right) + \frac{1259}{16384} \tilde{\Phi}_1\left(\frac{3}{4}\right) \right] p_\mu q_\nu q_\sigma \\
& + \left[\frac{37}{360} + \frac{113231}{307200} \ln\left(\frac{4}{3}\right) - \frac{16307}{819200} \tilde{\Phi}_1\left(\frac{9}{16}\right) - \frac{111}{16384} \tilde{\Phi}_1\left(\frac{3}{4}\right) \right] p_\mu q_\nu s_\sigma \\
& + \left[\frac{12689}{102400} \ln\left(\frac{4}{3}\right) - \frac{389}{1536} - \frac{53129}{819200} \tilde{\Phi}_1\left(\frac{9}{16}\right) + \frac{1589}{16384} \tilde{\Phi}_1\left(\frac{3}{4}\right) \right] p_\mu q_\sigma s_\nu \\
& + \left[\frac{497}{30720} - \frac{53433}{204800} \ln\left(\frac{4}{3}\right) + \frac{5941}{204800} \tilde{\Phi}_1\left(\frac{9}{16}\right) - \frac{409}{32768} \tilde{\Phi}_1\left(\frac{3}{4}\right) \right] p_\mu s_\nu s_\sigma \\
& + \left[\frac{1287}{5120} - \frac{7233}{51200} \ln\left(\frac{4}{3}\right) + \frac{3771}{819200} \tilde{\Phi}_1\left(\frac{9}{16}\right) - \frac{855}{8192} \tilde{\Phi}_1\left(\frac{3}{4}\right) \right] p_\nu p_\sigma q_\mu \\
& + \left[\frac{4959}{32768} \tilde{\Phi}_1\left(\frac{3}{4}\right) - \frac{11}{2048} - \frac{331353}{204800} \ln\left(\frac{4}{3}\right) - \frac{22671}{819200} \tilde{\Phi}_1\left(\frac{9}{16}\right) \right] p_\nu p_\sigma s_\mu \\
& + \left[\frac{1395}{16384} \tilde{\Phi}_1\left(\frac{3}{4}\right) - \frac{117}{5120} - \frac{40701}{102400} \ln\left(\frac{4}{3}\right) - \frac{10971}{204800} \tilde{\Phi}_1\left(\frac{9}{16}\right) \right] p_\nu q_\mu q_\sigma \\
& + \left[\frac{333}{2560} + \frac{3459}{20480} \ln\left(\frac{4}{3}\right) + \frac{1473}{163840} \tilde{\Phi}_1\left(\frac{9}{16}\right) - \frac{261}{16384} \tilde{\Phi}_1\left(\frac{3}{4}\right) \right] p_\nu q_\mu s_\sigma
\end{aligned}$$

$$\begin{aligned}
& + \left[\frac{3369}{16384} \tilde{\Phi}_1\left(\frac{3}{4}\right) - \frac{583}{2560} - \frac{133707}{102400} \ln\left(\frac{4}{3}\right) - \frac{44733}{819200} \tilde{\Phi}_1\left(\frac{9}{16}\right) \right] p_\nu q_\sigma s_\mu \\
& + \left[\frac{3663}{32768} \tilde{\Phi}_1\left(\frac{3}{4}\right) - \frac{1501}{10240} - \frac{132177}{204800} \ln\left(\frac{4}{3}\right) - \frac{36711}{204800} \tilde{\Phi}_1\left(\frac{9}{16}\right) \right] p_\nu s_\mu s_\sigma \\
& + \left[\frac{617}{5120} + \frac{6339}{102400} \ln\left(\frac{4}{3}\right) - \frac{20817}{409600} \tilde{\Phi}_1\left(\frac{9}{16}\right) - \frac{117}{16384} \tilde{\Phi}_1\left(\frac{3}{4}\right) \right] p_\sigma q_\mu q_\nu \\
& + \left[\frac{123}{1280} + \frac{16947}{102400} \ln\left(\frac{4}{3}\right) - \frac{4497}{819200} \tilde{\Phi}_1\left(\frac{9}{16}\right) - \frac{1161}{16384} \tilde{\Phi}_1\left(\frac{3}{4}\right) \right] p_\sigma q_\mu s_\nu \\
& + \left[\frac{583}{7680} - \frac{61603}{102400} \ln\left(\frac{4}{3}\right) - \frac{11997}{819200} \tilde{\Phi}_1\left(\frac{9}{16}\right) + \frac{849}{16384} \tilde{\Phi}_1\left(\frac{3}{4}\right) \right] p_\sigma q_\nu s_\mu \\
& + \left[\frac{59}{10240} - \frac{58089}{204800} \ln\left(\frac{4}{3}\right) + \frac{12543}{204800} \tilde{\Phi}_1\left(\frac{9}{16}\right) - \frac{777}{32768} \tilde{\Phi}_1\left(\frac{3}{4}\right) \right] p_\sigma s_\mu s_\nu \\
& + \left[\frac{279}{2048} \tilde{\Phi}_1\left(\frac{3}{4}\right) - \frac{367}{5120} - \frac{1239}{5120} \ln\left(\frac{4}{3}\right) - \frac{15453}{163840} \tilde{\Phi}_1\left(\frac{9}{16}\right) \right] q_\mu q_\nu q_\sigma \\
& + \left[\frac{973}{2560} - \frac{14511}{102400} \ln\left(\frac{4}{3}\right) + \frac{39831}{819200} \tilde{\Phi}_1\left(\frac{9}{16}\right) + \frac{117}{16384} \tilde{\Phi}_1\left(\frac{3}{4}\right) \right] q_\mu q_\nu s_\sigma \\
& + \left[\frac{2925}{16384} \tilde{\Phi}_1\left(\frac{3}{4}\right) - \frac{453}{1280} - \frac{36063}{102400} \ln\left(\frac{4}{3}\right) - \frac{17427}{819200} \tilde{\Phi}_1\left(\frac{9}{16}\right) \right] q_\mu q_\sigma s_\nu \\
& + \left[\frac{249}{1280} - \frac{28809}{25600} \ln\left(\frac{4}{3}\right) + \frac{14457}{102400} \tilde{\Phi}_1\left(\frac{9}{16}\right) - \frac{81}{4096} \tilde{\Phi}_1\left(\frac{3}{4}\right) \right] q_\mu s_\nu s_\sigma \\
& + \left[\frac{55181}{102400} \ln\left(\frac{4}{3}\right) - \frac{61}{3840} - \frac{103071}{819200} \tilde{\Phi}_1\left(\frac{9}{16}\right) + \frac{1545}{16384} \tilde{\Phi}_1\left(\frac{3}{4}\right) \right] q_\nu q_\sigma s_\mu \\
& + \left[\frac{63871}{51200} \ln\left(\frac{4}{3}\right) - \frac{551}{7680} - \frac{5547}{51200} \tilde{\Phi}_1\left(\frac{9}{16}\right) - \frac{225}{8192} \tilde{\Phi}_1\left(\frac{3}{4}\right) \right] q_\nu s_\mu s_\sigma \\
& + \left[\frac{7413}{10240} \ln\left(\frac{4}{3}\right) - \frac{1039}{2560} - \frac{3549}{20480} \tilde{\Phi}_1\left(\frac{9}{16}\right) + \frac{921}{8192} \tilde{\Phi}_1\left(\frac{3}{4}\right) \right] q_\sigma s_\mu s_\nu \\
& + \left[\frac{70173}{204800} \ln\left(\frac{4}{3}\right) - \frac{299}{2048} - \frac{11091}{204800} \tilde{\Phi}_1\left(\frac{9}{16}\right) \right. \\
& \quad \left. - \frac{579}{32768} \tilde{\Phi}_1\left(\frac{3}{4}\right) \right] s_\mu s_\nu s_\sigma \left] N_c f_4^{abcd} \frac{g^4}{\mu^4} \right. \\
& + \left[\left[\frac{16497}{204800} \tilde{\Phi}_1\left(\frac{9}{16}\right) - \frac{27}{640} - \frac{23717}{25600} \ln\left(\frac{4}{3}\right) - \frac{169}{4096} \tilde{\Phi}_1\left(\frac{3}{4}\right) \right] \eta_{\mu\nu} p_\sigma \right. \\
& + \left[\frac{11}{256} - \frac{259}{512} \ln\left(\frac{4}{3}\right) - \frac{121}{8192} \tilde{\Phi}_1\left(\frac{9}{16}\right) + \frac{247}{2048} \tilde{\Phi}_1\left(\frac{3}{4}\right) \right] \eta_{\mu\nu} q_\sigma \\
& + \left[\frac{2477}{51200} \tilde{\Phi}_1\left(\frac{9}{16}\right) - \frac{61}{1280} - \frac{10413}{25600} \ln\left(\frac{4}{3}\right) + \frac{835}{4096} \tilde{\Phi}_1\left(\frac{3}{4}\right) \right] \eta_{\mu\nu} s_\sigma \\
& + \left[\frac{11}{80} + \frac{3183}{25600} \ln\left(\frac{4}{3}\right) - \frac{15953}{204800} \tilde{\Phi}_1\left(\frac{9}{16}\right) + \frac{627}{4096} \tilde{\Phi}_1\left(\frac{3}{4}\right) \right] \eta_{\mu\sigma} p_\nu \\
& + \left[\frac{239}{1280} + \frac{181}{12800} \ln\left(\frac{4}{3}\right) - \frac{16217}{204800} \tilde{\Phi}_1\left(\frac{9}{16}\right) + \frac{263}{2048} \tilde{\Phi}_1\left(\frac{3}{4}\right) \right] \eta_{\mu\sigma} q_\nu \\
& + \left[\frac{241}{1280} + \frac{23}{25600} \ln\left(\frac{4}{3}\right) - \frac{13059}{102400} \tilde{\Phi}_1\left(\frac{9}{16}\right) + \frac{239}{4096} \tilde{\Phi}_1\left(\frac{3}{4}\right) \right] \eta_{\mu\sigma} s_\nu \\
& + \left[\frac{16397}{76800} \ln\left(\frac{4}{3}\right) - \frac{143}{1920} + \frac{28523}{614400} \tilde{\Phi}_1\left(\frac{9}{16}\right) - \frac{437}{4096} \tilde{\Phi}_1\left(\frac{3}{4}\right) \right] \eta_{\nu\sigma} p_\mu
\end{aligned}$$

$$\begin{aligned}
& + \left[\frac{5343}{12800} \ln\left(\frac{4}{3}\right) - \frac{183}{1280} + \frac{18849}{204800} \tilde{\Phi}_1\left(\frac{9}{16}\right) - \frac{387}{2048} \tilde{\Phi}_1\left(\frac{3}{4}\right) \right] \eta_{\nu\sigma} q_\mu \\
& + \left[\frac{5711}{25600} \ln\left(\frac{4}{3}\right) - \frac{103}{1280} + \frac{4837}{102400} \tilde{\Phi}_1\left(\frac{9}{16}\right) \right. \\
& \quad \left. - \frac{537}{4096} \tilde{\Phi}_1\left(\frac{3}{4}\right) \right] \eta_{\nu\sigma} s_\mu \left] N_c f_4^{abcd} \frac{g^4}{\mu^2} \right. \\
& + \left[\left[\frac{517}{6144} - \frac{101217}{204800} \ln\left(\frac{4}{3}\right) - \frac{7211}{204800} \tilde{\Phi}_1\left(\frac{9}{16}\right) + \frac{4543}{32768} \tilde{\Phi}_1\left(\frac{3}{4}\right) \right] p_\mu p_\nu p_\sigma \right. \\
& + \left[\frac{1079}{7680} + \frac{3937}{51200} \ln\left(\frac{4}{3}\right) - \frac{1169}{51200} \tilde{\Phi}_1\left(\frac{9}{16}\right) + \frac{321}{8192} \tilde{\Phi}_1\left(\frac{3}{4}\right) \right] p_\mu p_\nu q_\sigma \\
& + \left[\frac{22113}{204800} \tilde{\Phi}_1\left(\frac{9}{16}\right) - \frac{3469}{30720} - \frac{103419}{204800} \ln\left(\frac{4}{3}\right) + \frac{7973}{32768} \tilde{\Phi}_1\left(\frac{3}{4}\right) \right] p_\mu p_\nu s_\sigma \\
& + \left[\frac{6679}{23040} + \frac{16139}{30720} \ln\left(\frac{4}{3}\right) - \frac{3103}{40960} \tilde{\Phi}_1\left(\frac{9}{16}\right) + \frac{469}{8192} \tilde{\Phi}_1\left(\frac{3}{4}\right) \right] p_\mu p_\sigma q_\nu \\
& + \left[\frac{13307}{30720} - \frac{66747}{204800} \ln\left(\frac{4}{3}\right) - \frac{12423}{102400} \tilde{\Phi}_1\left(\frac{9}{16}\right) + \frac{1605}{32768} \tilde{\Phi}_1\left(\frac{3}{4}\right) \right] p_\mu p_\sigma s_\nu \\
& + \left[\frac{979}{23040} + \frac{104741}{307200} \ln\left(\frac{4}{3}\right) + \frac{17153}{819200} \tilde{\Phi}_1\left(\frac{9}{16}\right) - \frac{973}{16384} \tilde{\Phi}_1\left(\frac{3}{4}\right) \right] p_\mu q_\nu q_\sigma \\
& + \left[\frac{10571}{163840} \tilde{\Phi}_1\left(\frac{9}{16}\right) - \frac{67}{1152} - \frac{8303}{61440} \ln\left(\frac{4}{3}\right) + \frac{363}{16384} \tilde{\Phi}_1\left(\frac{3}{4}\right) \right] p_\mu q_\nu s_\sigma \\
& + \left[\frac{307}{960} - \frac{17341}{102400} \ln\left(\frac{4}{3}\right) + \frac{73291}{819200} \tilde{\Phi}_1\left(\frac{9}{16}\right) - \frac{745}{16384} \tilde{\Phi}_1\left(\frac{3}{4}\right) \right] p_\mu q_\sigma s_\nu \\
& + \left[\frac{1253}{30720} + \frac{44853}{204800} \ln\left(\frac{4}{3}\right) + \frac{17101}{819200} \tilde{\Phi}_1\left(\frac{9}{16}\right) + \frac{1421}{32768} \tilde{\Phi}_1\left(\frac{3}{4}\right) \right] p_\mu s_\nu s_\sigma \\
& + \left[\frac{1221}{25600} \ln\left(\frac{4}{3}\right) - \frac{21}{256} - \frac{1503}{102400} \tilde{\Phi}_1\left(\frac{9}{16}\right) + \frac{189}{4096} \tilde{\Phi}_1\left(\frac{3}{4}\right) \right] p_\nu p_\sigma q_\mu \\
& + \left[\frac{497}{10240} + \frac{179397}{204800} \ln\left(\frac{4}{3}\right) - \frac{20259}{204800} \tilde{\Phi}_1\left(\frac{9}{16}\right) + \frac{1125}{32768} \tilde{\Phi}_1\left(\frac{3}{4}\right) \right] p_\nu p_\sigma s_\mu \\
& + \left[\frac{123}{640} + \frac{31119}{102400} \ln\left(\frac{4}{3}\right) + \frac{35631}{819200} \tilde{\Phi}_1\left(\frac{9}{16}\right) - \frac{2349}{16384} \tilde{\Phi}_1\left(\frac{3}{4}\right) \right] p_\nu q_\mu q_\sigma \\
& + \left[\frac{22701}{819200} \tilde{\Phi}_1\left(\frac{9}{16}\right) - \frac{33}{128} - \frac{21891}{102400} \ln\left(\frac{4}{3}\right) + \frac{1737}{16384} \tilde{\Phi}_1\left(\frac{3}{4}\right) \right] p_\nu q_\mu s_\sigma \\
& + \left[\frac{257}{2560} + \frac{147903}{102400} \ln\left(\frac{4}{3}\right) - \frac{55443}{819200} \tilde{\Phi}_1\left(\frac{9}{16}\right) - \frac{1653}{16384} \tilde{\Phi}_1\left(\frac{3}{4}\right) \right] p_\nu q_\sigma s_\mu \\
& + \left[\frac{127}{2048} - \frac{16563}{204800} \ln\left(\frac{4}{3}\right) + \frac{123759}{819200} \tilde{\Phi}_1\left(\frac{9}{16}\right) + \frac{405}{32768} \tilde{\Phi}_1\left(\frac{3}{4}\right) \right] p_\nu s_\mu s_\sigma \\
& + \left[\frac{25}{512} - \frac{15921}{102400} \ln\left(\frac{4}{3}\right) + \frac{33381}{819200} \tilde{\Phi}_1\left(\frac{9}{16}\right) - \frac{837}{16384} \tilde{\Phi}_1\left(\frac{3}{4}\right) \right] p_\sigma q_\mu q_\nu \\
& + \left[\frac{153}{512} - \frac{47727}{102400} \ln\left(\frac{4}{3}\right) + \frac{65847}{819200} \tilde{\Phi}_1\left(\frac{9}{16}\right) - \frac{459}{16384} \tilde{\Phi}_1\left(\frac{3}{4}\right) \right] p_\sigma q_\mu s_\nu \\
& + \left[\frac{1001}{3840} + \frac{172967}{102400} \ln\left(\frac{4}{3}\right) - \frac{24957}{819200} \tilde{\Phi}_1\left(\frac{9}{16}\right) - \frac{2661}{16384} \tilde{\Phi}_1\left(\frac{3}{4}\right) \right] p_\sigma q_\nu s_\mu \\
& + \left[\frac{4463}{10240} - \frac{105339}{204800} \ln\left(\frac{4}{3}\right) - \frac{50583}{819200} \tilde{\Phi}_1\left(\frac{9}{16}\right) - \frac{3}{32768} \tilde{\Phi}_1\left(\frac{3}{4}\right) \right] p_\sigma s_\mu s_\nu
\end{aligned}$$

$$\begin{aligned}
& + \left[\frac{367}{5120} + \frac{1239}{5120} \ln\left(\frac{4}{3}\right) + \frac{15453}{163840} \tilde{\Phi}_1\left(\frac{9}{16}\right) - \frac{279}{2048} \tilde{\Phi}_1\left(\frac{3}{4}\right) \right] q_\mu q_\nu q_\sigma \\
& + \left[\frac{29919}{409600} \tilde{\Phi}_1\left(\frac{9}{16}\right) - \frac{289}{1024} - \frac{11283}{102400} \ln\left(\frac{4}{3}\right) + \frac{693}{16384} \tilde{\Phi}_1\left(\frac{3}{4}\right) \right] q_\mu q_\nu s_\sigma \\
& + \left[\frac{2313}{5120} + \frac{10269}{102400} \ln\left(\frac{4}{3}\right) + \frac{14637}{102400} \tilde{\Phi}_1\left(\frac{9}{16}\right) - \frac{2115}{16384} \tilde{\Phi}_1\left(\frac{3}{4}\right) \right] q_\mu q_\sigma s_\nu \\
& + \left[\frac{44721}{51200} \ln\left(\frac{4}{3}\right) - \frac{99}{1024} - \frac{15987}{819200} \tilde{\Phi}_1\left(\frac{9}{16}\right) + \frac{567}{8192} \tilde{\Phi}_1\left(\frac{3}{4}\right) \right] q_\mu s_\nu s_\sigma \\
& + \left[\frac{857}{15360} + \frac{79961}{102400} \ln\left(\frac{4}{3}\right) - \frac{12903}{409600} \tilde{\Phi}_1\left(\frac{9}{16}\right) - \frac{687}{16384} \tilde{\Phi}_1\left(\frac{3}{4}\right) \right] q_\nu q_\sigma s_\mu \\
& + \left[\frac{331}{3072} - \frac{3779}{12800} \ln\left(\frac{4}{3}\right) + \frac{98727}{819200} \tilde{\Phi}_1\left(\frac{9}{16}\right) + \frac{99}{4096} \tilde{\Phi}_1\left(\frac{3}{4}\right) \right] q_\nu s_\mu s_\sigma \\
& + \left[\frac{2599}{5120} - \frac{15573}{25600} \ln\left(\frac{4}{3}\right) + \frac{102777}{819200} \tilde{\Phi}_1\left(\frac{9}{16}\right) - \frac{15}{2048} \tilde{\Phi}_1\left(\frac{3}{4}\right) \right] q_\sigma s_\mu s_\nu \\
& + \left[\frac{2243}{10240} - \frac{1773}{8192} \ln\left(\frac{4}{3}\right) + \frac{6729}{81920} \tilde{\Phi}_1\left(\frac{9}{16}\right) \right. \\
& \quad \left. + \frac{1995}{32768} \tilde{\Phi}_1\left(\frac{3}{4}\right) \right] s_\mu s_\nu s_\sigma \left] N_c f_4^{abcd} \frac{g^4}{\mu^4} \right. \\
& + \left[\left[\frac{81}{640} + \frac{6909}{6400} \ln\left(\frac{4}{3}\right) + \frac{13437}{102400} \tilde{\Phi}_1\left(\frac{9}{16}\right) - \frac{285}{1024} \tilde{\Phi}_1\left(\frac{3}{4}\right) \right] \eta_{\mu\nu} p_\sigma \right. \\
& + \left[\frac{1437}{1600} \ln\left(\frac{4}{3}\right) - \frac{21}{80} - \frac{2967}{12800} \tilde{\Phi}_1\left(\frac{9}{16}\right) + \frac{57}{256} \tilde{\Phi}_1\left(\frac{3}{4}\right) \right] \eta_{\mu\nu} q_\sigma \\
& + \left[\frac{87}{640} + \frac{423}{6400} \ln\left(\frac{4}{3}\right) - \frac{39261}{102400} \tilde{\Phi}_1\left(\frac{9}{16}\right) + \frac{321}{1024} \tilde{\Phi}_1\left(\frac{3}{4}\right) \right] \eta_{\mu\nu} s_\sigma \\
& + \left[\frac{249}{640} + \frac{1161}{6400} \ln\left(\frac{4}{3}\right) + \frac{37173}{102400} \tilde{\Phi}_1\left(\frac{9}{16}\right) - \frac{513}{1024} \tilde{\Phi}_1\left(\frac{3}{4}\right) \right] \eta_{\mu\sigma} p_\nu \\
& + \left[\frac{21}{80} - \frac{1437}{1600} \ln\left(\frac{4}{3}\right) + \frac{2967}{12800} \tilde{\Phi}_1\left(\frac{9}{16}\right) - \frac{57}{256} \tilde{\Phi}_1\left(\frac{3}{4}\right) \right] \eta_{\mu\sigma} q_\nu \\
& + \left[\frac{51}{128} - \frac{213}{256} \ln\left(\frac{4}{3}\right) - \frac{621}{4096} \tilde{\Phi}_1\left(\frac{9}{16}\right) + \frac{93}{1024} \tilde{\Phi}_1\left(\frac{3}{4}\right) \right] \eta_{\mu\sigma} s_\nu \\
& + \left[\frac{1057}{6400} \ln\left(\frac{4}{3}\right) - \frac{7}{640} + \frac{79301}{102400} \tilde{\Phi}_1\left(\frac{9}{16}\right) - \frac{1161}{1024} \tilde{\Phi}_1\left(\frac{3}{4}\right) \right] \eta_{\nu\sigma} p_\mu \\
& + \left[\frac{3171}{6400} \ln\left(\frac{4}{3}\right) - \frac{21}{640} + \frac{237903}{102400} \tilde{\Phi}_1\left(\frac{9}{16}\right) - \frac{3483}{1024} \tilde{\Phi}_1\left(\frac{3}{4}\right) \right] \eta_{\nu\sigma} s_\mu \left] d_A^{abcd} \frac{g^4}{\mu^2} \right. \\
& + \left[\left[\frac{2119}{2560} + \frac{123771}{51200} \ln\left(\frac{4}{3}\right) + \frac{6603}{3200} \tilde{\Phi}_1\left(\frac{9}{16}\right) - \frac{23493}{8192} \tilde{\Phi}_1\left(\frac{3}{4}\right) \right] p_\mu p_\nu p_\sigma \right. \\
& + \left[\frac{1}{256} + \frac{93951}{51200} \ln\left(\frac{4}{3}\right) + \frac{345189}{409600} \tilde{\Phi}_1\left(\frac{9}{16}\right) - \frac{8469}{8192} \tilde{\Phi}_1\left(\frac{3}{4}\right) \right] p_\mu p_\nu q_\sigma \\
& + \left[\frac{307}{2560} + \frac{1563}{25600} \ln\left(\frac{4}{3}\right) - \frac{256041}{409600} \tilde{\Phi}_1\left(\frac{9}{16}\right) + \frac{717}{4096} \tilde{\Phi}_1\left(\frac{3}{4}\right) \right] p_\mu p_\nu s_\sigma \\
& + \left[\frac{989}{1920} - \frac{553}{2048} \ln\left(\frac{4}{3}\right) + \frac{87279}{81920} \tilde{\Phi}_1\left(\frac{9}{16}\right) - \frac{11181}{8192} \tilde{\Phi}_1\left(\frac{3}{4}\right) \right] p_\mu p_\sigma q_\nu \\
& + \left[\frac{461}{512} - \frac{3351}{25600} \ln\left(\frac{4}{3}\right) + \frac{289197}{409600} \tilde{\Phi}_1\left(\frac{9}{16}\right) - \frac{3537}{4096} \tilde{\Phi}_1\left(\frac{3}{4}\right) \right] p_\mu p_\sigma s_\nu
\end{aligned}$$

$$\begin{aligned}
& + \left[\frac{211}{3840} + \frac{15263}{51200} \ln\left(\frac{4}{3}\right) + \frac{536397}{409600} \tilde{\Phi}_1\left(\frac{9}{16}\right) - \frac{13845}{8192} \tilde{\Phi}_1\left(\frac{3}{4}\right) \right] p_\mu q_\nu q_\sigma \\
& + \left[\frac{709}{3840} - \frac{15791}{25600} \ln\left(\frac{4}{3}\right) - \frac{14397}{102400} \tilde{\Phi}_1\left(\frac{9}{16}\right) - \frac{135}{4096} \tilde{\Phi}_1\left(\frac{3}{4}\right) \right] p_\mu q_\nu s_\sigma \\
& + \left[\frac{31}{160} - \frac{333}{5120} \ln\left(\frac{4}{3}\right) + \frac{3459}{40960} \tilde{\Phi}_1\left(\frac{9}{16}\right) - \frac{1725}{4096} \tilde{\Phi}_1\left(\frac{3}{4}\right) \right] p_\mu q_\sigma s_\nu \\
& + \left[\frac{643}{2560} - \frac{1587}{6400} \ln\left(\frac{4}{3}\right) - \frac{58839}{409600} \tilde{\Phi}_1\left(\frac{9}{16}\right) - \frac{159}{2048} \tilde{\Phi}_1\left(\frac{3}{4}\right) \right] p_\mu s_\nu s_\sigma \\
& + \left[\frac{297}{640} + \frac{64863}{51200} \ln\left(\frac{4}{3}\right) + \frac{245187}{409600} \tilde{\Phi}_1\left(\frac{9}{16}\right) - \frac{5805}{8192} \tilde{\Phi}_1\left(\frac{3}{4}\right) \right] p_\nu p_\sigma q_\mu \\
& + \left[\frac{1209}{2560} + \frac{11277}{5120} \ln\left(\frac{4}{3}\right) + \frac{336609}{81920} \tilde{\Phi}_1\left(\frac{9}{16}\right) - \frac{22761}{4096} \tilde{\Phi}_1\left(\frac{3}{4}\right) \right] p_\nu p_\sigma s_\mu \\
& + \left[\frac{297}{640} + \frac{64863}{51200} \ln\left(\frac{4}{3}\right) + \frac{245187}{409600} \tilde{\Phi}_1\left(\frac{9}{16}\right) - \frac{5805}{8192} \tilde{\Phi}_1\left(\frac{3}{4}\right) \right] p_\nu q_\mu q_\sigma \\
& + \left[\frac{3861}{4096} \tilde{\Phi}_1\left(\frac{3}{4}\right) - \frac{81}{640} - \frac{2259}{5120} \ln\left(\frac{4}{3}\right) - \frac{12213}{8192} \tilde{\Phi}_1\left(\frac{9}{16}\right) \right] p_\nu q_\mu s_\sigma \\
& + \left[\frac{429}{1280} + \frac{39519}{25600} \ln\left(\frac{4}{3}\right) + \frac{268803}{102400} \tilde{\Phi}_1\left(\frac{9}{16}\right) - \frac{12537}{4096} \tilde{\Phi}_1\left(\frac{3}{4}\right) \right] p_\nu q_\sigma s_\mu \\
& + \left[\frac{201}{2560} + \frac{2727}{6400} \ln\left(\frac{4}{3}\right) + \frac{313659}{409600} \tilde{\Phi}_1\left(\frac{9}{16}\right) - \frac{2781}{2048} \tilde{\Phi}_1\left(\frac{3}{4}\right) \right] p_\nu s_\mu s_\sigma \\
& + \left[\frac{297}{640} + \frac{64863}{51200} \ln\left(\frac{4}{3}\right) + \frac{245187}{409600} \tilde{\Phi}_1\left(\frac{9}{16}\right) - \frac{5805}{8192} \tilde{\Phi}_1\left(\frac{3}{4}\right) \right] p_\sigma q_\mu q_\nu \\
& + \left[\frac{117}{128} + \frac{18639}{25600} \ln\left(\frac{4}{3}\right) + \frac{148221}{204800} \tilde{\Phi}_1\left(\frac{9}{16}\right) - \frac{1701}{4096} \tilde{\Phi}_1\left(\frac{3}{4}\right) \right] p_\sigma q_\mu s_\nu \\
& + \left[\frac{47}{160} + \frac{15807}{25600} \ln\left(\frac{4}{3}\right) + \frac{389583}{204800} \tilde{\Phi}_1\left(\frac{9}{16}\right) - \frac{11133}{4096} \tilde{\Phi}_1\left(\frac{3}{4}\right) \right] p_\sigma q_\nu s_\mu \\
& + \left[\frac{303}{512} + \frac{4401}{3200} \ln\left(\frac{4}{3}\right) + \frac{757449}{409600} \tilde{\Phi}_1\left(\frac{9}{16}\right) - \frac{5013}{2048} \tilde{\Phi}_1\left(\frac{3}{4}\right) \right] p_\sigma s_\mu s_\nu \\
& + \left[\frac{207}{640} - \frac{2007}{2048} \ln\left(\frac{4}{3}\right) - \frac{111879}{81920} \tilde{\Phi}_1\left(\frac{9}{16}\right) + \frac{10125}{8192} \tilde{\Phi}_1\left(\frac{3}{4}\right) \right] q_\mu q_\nu s_\sigma \\
& + \left[\frac{207}{640} - \frac{2007}{2048} \ln\left(\frac{4}{3}\right) - \frac{111879}{81920} \tilde{\Phi}_1\left(\frac{9}{16}\right) + \frac{10125}{8192} \tilde{\Phi}_1\left(\frac{3}{4}\right) \right] q_\mu q_\sigma s_\nu \\
& + \left[\frac{207}{640} - \frac{2007}{2048} \ln\left(\frac{4}{3}\right) - \frac{111879}{81920} \tilde{\Phi}_1\left(\frac{9}{16}\right) + \frac{10125}{8192} \tilde{\Phi}_1\left(\frac{3}{4}\right) \right] q_\mu s_\nu s_\sigma \\
& + \left[\frac{211}{1280} + \frac{45789}{51200} \ln\left(\frac{4}{3}\right) + \frac{1609191}{409600} \tilde{\Phi}_1\left(\frac{9}{16}\right) - \frac{41535}{8192} \tilde{\Phi}_1\left(\frac{3}{4}\right) \right] q_\nu q_\sigma s_\mu \\
& + \left[\frac{59}{256} - \frac{44571}{51200} \ln\left(\frac{4}{3}\right) + \frac{386631}{409600} \tilde{\Phi}_1\left(\frac{9}{16}\right) - \frac{10935}{8192} \tilde{\Phi}_1\left(\frac{3}{4}\right) \right] q_\nu s_\mu s_\sigma \\
& + \left[\frac{33}{128} + \frac{8037}{10240} \ln\left(\frac{4}{3}\right) + \frac{132633}{81920} \tilde{\Phi}_1\left(\frac{9}{16}\right) - \frac{20475}{8192} \tilde{\Phi}_1\left(\frac{3}{4}\right) \right] q_\sigma s_\mu s_\nu \\
& + \left[\frac{1101}{2560} + \frac{12087}{51200} \ln\left(\frac{4}{3}\right) + \frac{191439}{204800} \tilde{\Phi}_1\left(\frac{9}{16}\right) \right. \\
& \quad \left. - \frac{12033}{8192} \tilde{\Phi}_1\left(\frac{3}{4}\right) \right] s_\mu s_\nu s_\sigma \Big] d_A^{abcd} \frac{g^4}{\mu^4} \tag{C.5}
\end{aligned}$$

also for $SU(N_c)$. Unlike $\Gamma_{\mu\nu\sigma\rho}^{ggg\,abcd}(p, q, r, s)$ there are no quark contributions.

References.

- [1] J.C. Taylor, Nucl. Phys. **B33** (1971), 436.
- [2] A. Slavnov, Theor. Math. Phys. **10** (1972), 99.
- [3] G. 't Hooft, Nucl. Phys. **B33** (1971), 173.
- [4] S. Weinberg, Phys. Phys. **D8** (1973), 3497;
- [5] G. 't Hooft & M.J.G. Veltman, Nucl. Phys. **B50** (1972), 318.
- [6] S.D. Joglekar & B.W. Lee, Annals Phys. **97** (1976), 160.
- [7] W. Celmaster & R.J. Gonsalves, Phys. Rev. Lett. **42** (1979), 1435.
- [8] W. Celmaster & R.J. Gonsalves, Phys. Rev. **D20** (1979), 1420.
- [9] J.S. Ball & T.W. Chiu, Phys. Rev. **D22** (1980), 2550; Phys. Rev. **D23** (1981), 3085(E).
- [10] S.K. Kim & M. Baker, Nucl. Phys. **B164** (1980), 152.
- [11] P. Pascual & R. Tarrach, Nucl. Phys. **B174** (1980), 123; Nucl. Phys. **B181** (1981), 546.
- [12] R. Alkofer & L. von Smekal, Phys. Rept. **353** (2001), 281.
- [13] J.M. Pawłowski, Annals Phys. **322** (2007), 2831.
- [14] C.S. Fischer, A. Maas & J.M. Pawłowski, Annals Phys. **324** (2009), 2408.
- [15] M.Q. Huber, arXiv:1808.05227 [hep-ph].
- [16] D. Binosi, D. Ibañez & J. Papavassiliou, Phys. Rev. **D87** (2013), 125026.
- [17] G. Eichmann, R. Williams, R. Alkofer & M. Vujanovic, Phys. Rev. **D89** (2014), 105014.
- [18] A.C. Aguilar, D. Binosi, D. Ibañez & J. Papavassiliou, Phys. Rev. **D90** (2014), 065027.
- [19] A.L. Blum, R. Alkofer, M.Q. Huber & A. Windisch, EPJ Web Conf. **137** (2017), 03001.
- [20] M. Vujanovic & T. Mendes, Phys. Rev. **D99** (2019), 034501.
- [21] A.C. Aguilar, M.N. Ferreira, C.T. Figueiredo & J. Papavassiliou, Phys. Rev. **D99** (2019), 094010.
- [22] C. Kellermann & C.S. Fischer, Phys. Rev. **D78** (2008), 025015.
- [23] C. Kellermann & C.S. Fischer, arXiv:0905.2506 [hep-ph].
- [24] V. Mader & R. Alkofer, Proc. Sci., ConfinementX (2012), 063.
- [25] D. Binosi, D. Ibañez & J. Papavassiliou, JHEP **1409** (2014), 059.
- [26] A.K. Cyrol, M.Q. Huber & L. von Smekal, Eur. Phys. J. **C75** (2015), 102.
- [27] M.Q. Huber, Eur. Phys. J. **C77** (2017), 733.
- [28] B.E. Lautrup, *Of ghoulies and ghosties: an introduction to QCD*, (1977), NBI-HE-76-14.
- [29] P. Cvitanović, Nucl. Phys. **B130** (1977), 114.

- [30] P. Cvitanovic, *Field theory* (1983), RX-1012 (NORDITA).
- [31] D. Kreimer, M. Sars & W. van Suijlekom, *Annals Phys.* **336** (2013), 180.
- [32] H. Kissler & D. Kreimer, *Phys. Lett.* **B764** (2017), 318.
- [33] H. Kißler, *Computational and diagrammatic techniques for perturbative Quantum Electrodynamics*, Ph.D. thesis (2017),
<http://www2.mathematik.hu-berlin.de/~kreimer/wp-content/uploads/KisslerDiss.pdf>.
- [34] O. Piguet & S.P. Sorella, *Lect. Notes Phys.* **M128** (1995), 1.
- [35] J.A. Gracey, *Phys. Rev.* **D90** (2014), 025011.
- [36] J.A. Gracey, *Phys. Rev.* **D95** (2017), 065013.
- [37] D. Kreimer, *Annals Phys.* **321** (2006), 2757.
- [38] D. Kreimer & W.D. van Suijlekom, *Nucl. Phys.* **B820** (2009), 682.
- [39] D. Kreimer & K. Yeats, *Elect. J. Combin.* **20** (2013), P41.
- [40] M. Sars, *Parametric representation of Feynman amplitudes in gauge theories*, Ph.D. thesis (2015),
<http://www2.mathematik.hu-berlin.de/~kreimer/wp-content/uploads/SarsThesisNeu.pdf>.
- [41] H. Kißler, *PoS LL2018* (2018), 032.
- [42] P. Cvitanović, P.G. Lauwers & P.N. Scharbach, *Nucl. Phys.* **B186** (1981), 165.
- [43] A.I. Davydychev, P. Osland & O.V. Tarasov, *Phys. Rev.* **D54** (1996), 4087; *Phys. Rev.* **D59** (1999), 109901(E).
- [44] M. Binger & S.J. Brodsky, *Phys. Rev.* **D74** (2006), 054016.
- [45] N. Ahmadinia & C. Schubert, *Nucl. Phys.* **B869** (2013), 417.
- [46] J.A. Gracey, *Phys. Rev.* **D90** (2014), 025014.
- [47] A.I. Davydychev, *J. Phys.* **A25** (1992), 5587.
- [48] S. Laporta, *Int. J. Mod. Phys.* **A15** (2000), 5087.
- [49] C. Studerus, *Comput. Phys. Commun.* **181** (2010), 1293.
- [50] A. von Manteuffel & C. Studerus, arXiv:1201.4330 [hep-ph].
- [51] G. 't Hooft & M.J.G. Veltman, *Nucl. Phys.* **B153** (1979), 365.
- [52] N.I. Usyukina & A.I. Davydychev, *Phys. Lett.* **B332** (1994), 159.
- [53] J.A.M. Vermaseren, math-ph/0010025.
- [54] M. Tentyukov & J.A.M. Vermaseren, *Comput. Phys. Commun.* **181** (2010), 1419.
- [55] P. Nogueira, *J. Comput. Phys.* **105** (1993), 279.
- [56] J. Ablinger, J. Blümlein & C. Schneider, *J. Math. Phys.* **52** (2011), 102301.

- [57] T. van Ritbergen, A.N. Schellekens & J.A.M. Vermaseren, *Int. J. Mod. Phys.* **A14** (1999), 41.
- [58] A. Denner, U. Nierste & R. Scharf, *Nucl. Phys.* **B367** (1991), 637.
- [59] N.I. Usyukina & A.I. Davydychev, *Phys. Lett.* **B298** (1993), 363.
- [60] G. Curci & R. Ferrari, *Nuovo Cim.* **A32** (1976), 151.
- [61] G. 't Hooft, *Nucl. Phys.* **B190** (1981), 455.
- [62] A.S. Kronfeld, G. Schierholz & U.J. Wiese, *Nucl. Phys.* **B293** (1987), 461.
- [63] A.S. Kronfeld, M.L. Laursen, G. Schierholz & U.J. Wiese, *Phys. Lett.* **B198** (1987), 516.
- [64] J.C. Collins & J.A.M. Vermaseren, arXiv:1606.01177 [cs.OH].
- [65] A.C. Hearn, *Reduce: a user oriented interactive system for algebraic simplification* (1967), C670826-1, SITP-282.
- [66] A.J. Macfarlane, A. Sudbery & P.H. Weisz, *Commun. Math. Phys.* **11** (1968), 77.